

Review for “Spatial and temporal CCN variations in convection-permitting aerosol microphysics simulations in an idealised marine tropical domain”

Paper summary and recommendation:

This paper disentangles the contribution of different processes to the overall CCN variability detected over a domain the size of a conventional general circulation model (GCM) grid box for the case of a convective tropical marine boundary layer. The study is performed in a simplified idealised setup. Feedback pathways between aerosol concentrations and the environment via radiative or cloud microphysical interactions are ignored. Thereby, an attribution of different processes to CCN variability due to spatial and temporal variability of size and number of the 3 mixed-modes contributing to the CCN budget (Aitken, accumulation and coarse mode) is obtained. The authors show that CCN concentrations may vary up to a factor 3-8 throughout the simulation domain. Understanding the origins of this variability is an important step towards estimating the potential biases of aerosol-cloud interaction estimates obtained by GCMs, which do not resolve this variability. I therefore recommend this article for publication in Atmos. Chem. Phys. following minor revisions.

We thank the reviewer for their review and note they recognise the paper's value in providing information to explore potential biases in aerosol-cloud interaction estimates from lower spatial resolution GCMs.

Our replies to each of the reviewers' comments are provided below (coloured red) and, where changes to the manuscript have been made, these are highlighted in the track-changes version of the document provided.

Minor Comments – general:

- I believe that your aerosol concentrations are spun up from an entirely clean (i.e. $Naero=0.0\text{ cm}^{-3}$) atmosphere. Please state this explicitly in the manuscript. I agree with the authors that this gives you the opportunity to disentangle the individual processes. However, this may be at least partially responsible for the high variability in CCN (800%) obtained after 12h of simulation following the period of intensive updrafts. If that is the case, context should be provided for the interpretation of this estimate. If you initialised a homogeneous profile of e.g. accumulation mode aerosol, would you still obtain such a high degree of variability of CCN following the intense updraft period? Please comment.



Yes, that's correct – the aerosol concentrations were initialized to zero at the start of the simulation. In the revised manuscript, we have added a sentence to state this explicitly (lines 12-13, page 5). We also agree that the period of intensive updrafts at around 4-7h of simulation is a likely causing an unusually high degree of variability. We do already note the unusual nature of this period in the Abstract (page 1, line 17) and have added “with intense wind-speed conditions” to further suggest the connection between those conditions and increased sea-spray emission.

- The phrase “strongly convective” period (or conditions) seems to refer to different things throughout the manuscript. Sometimes the phrase seems to be used to refer to the time period of intensive updrafts and strong horizontal winds and sometimes to periods of intense rain fall. Please define this term and use it consistently throughout the manuscript.

We have clarified use of this phrase in the manuscript (page 1, line 30; page 5, lines 30-31; page 7, lines 5-6; page 8, lines 10-11). Mostly, we refer to the “strongly convective period” as meaning the period when the dynamical conditions (updrafts and horizontal wind speeds) are intense.

- It has been shown (e.g. Textor et al, 2006: “Analysis and quantification of the diversities of aerosol life cycles within AeroCom”) that different assumptions made in modeling the sea salt flux may yield vastly different estimates of sea salt emission fluxes. How sensitive do the authors think their results are to their implemented SS emission parameterisation? Please comment.

The simulations apply the Gong et al. (2003) sea-spray source function, which includes the behavior of the Monahan et al. (1986) parameterisation, with additional parameter to control emission of ultra-fine sea spray particles. The parameterisation was used by many of the global models in phase 1 of the AeroCom intercomparison, as analysed by Textor et al. (2006). As we also explain in our responses to the other reviewer, in Figure 5 of the recent paper by Salter et al., (2015), several different sea-spray source functions are presented in terms of their emission flux against wind speed, with the Gong being in the mid-range of the different parameterisations. We therefore believe our results are not sensitive to the particular sea-spray emission parameterisations and would be robust if a different emissions scheme were used.

Gong, S. L.: A parameterization of sea-salt aerosol source function for sub- and super-micron particles, Global Biogeochem. Cycles., 14, 1097-1103, 2003.

Monahan, E. C., Spiel, D. E., and Davidson, K. L.: A model of marine aerosol generation via whitecaps and wave disruption. Oceanic Whitecaps. Edited by EC Monahan and G MacNiochaill, pp 167-193, D Reidel, Norwell, Mass, 1986.

Salter, M. E., Zieger, P., Acosta Navarro, J. C., Grythe, H., Kirkevåg, A., Rosati, B., Riipinen, I., and Nilsson, E. D.: An empirically derived inorganic sea spray source function incorporating sea surface temperature, Atmos. Chem. Phys., 15, 11047-11066, doi:10.5194/acp-15-11047-2015, 2015.

Textor, C., Schulz, M., Guibert, S., Kinne, S., Balkanski, Y., Bauer, S., Berntsen, T., Berglen, T., Boucher, O., Chin, M., Dentener, F., Diehl, T., Easter, R., Feichter, H., Fillmore, D., Ghan, S., Ginoux, P., Gong, S., Grini, A., Hendricks, J., Horowitz, L., Huang, P., Isaksen, I., Iversen, I., Kloster, S., Koch, D., Kirkevåg, A., Kristjansson, J. E., Krol, M., Lauer, A., Lamarque, J. F., Liu, X., Montanaro, V., Myhre, G., Penner, J., Pitari, G., Reddy, S., Seland, Ø., Stier, P., Takemura, T., and Tie, X.: Analysis and quantification of the diversities of aerosol life cycles within AeroCom, Atmos. Chem. Phys., 6, 1777-1813, doi:10.5194/acp-6-1777-2006, 2006.

Minor Comments – specific:

- P3L10: Please include reference Zubler et al (2011):“Simulation of dimming and brightening in Europe from 1958 to 2001 using a regional climate model”, JGR, doi:10.1029/2010JD015396.

Done

- P3L10-L12: Two recent studies have investigated the impact of resolution on aerosol variability and aerosol-cloud interactions in regional climate models down to the kilometre scale for boundary layer clouds. These references should be added:

◦ Possner et al (2016): “The resolution dependence of cloud effects and ship-induced aerosol cloud interactions in marine stratocumulus”, JGR, doi:10.1002/2015JD024685.

◦ Weigum et al (2016): “Effect of aerosol subgrid variability on aerosol optical depth and cloud condensation nuclei: implications for global aerosol modelling”, ACP, doi:10.5194/acp-16-13619-2016.

Thanks -- we added citations to these references in the manuscript.

- P3L18: Please clarify complexity of aerosol treatment here, as there have been numerous studies investigating the sensitivity of marine deep and shallow convection to simplified aerosol treatments.

We are not sure what the reviewer refers to here. In the final paragraph of this section we do refer to the simulations applying an aerosol microphysics, and the particular type of aerosol dynamics scheme is clearly described in section 2.1, which follows immediately from this section. We therefore feel the level of detail given in this Introduction part of the manuscript is sufficient.

- P3L23: Please rephrase “to well characterize”.

By “well characterize” we mean that the model will represent the dominant sources of CCN variability and therefore simulated CCN variations would be expected to be realistic. We therefore feel the word “well” is appropriate here. However, on reflection, perhaps that word does not need to be stated explicitly. We deleted it and also removed the 2nd instance of “influences” later in the sentence to improve the wording.

- P3L25: How do the authors determine the “realistic” level of variability? Please add references here.

We cite Yang et al. (2011) as a study that includes a similar level of model complexity.

Yang, Q., W. I. Gustafson Jr., Fast, J. D., Wang, H., Easter, R. C., Morrison, H., Lee, Y.-N., Chapman, E. G., Spak, S. N., and Mena-Carrasco, M. A.: Assessing regional scale predictions of aerosols, marine stratocumulus, and their interactions during VOCALS-REx using WRF-Chem, Atmos. Chem. Phys., 11, 11951-11975, doi:10.5194/acp-11-11951-2011, 2011.

- P4L30: Please rephrase “only a short demonstration simulation is here carried out”.

Done

- P4L31: Please rephrase “carried on”.

Done

- P5L11: Please rephrase “becomes precipitating”, “becoming more intense”.

Done

- P5L22: Please rephrase “associated cold pooling”.

Done

- P6L24: By which criterion do you define your simulation to have fully spun up? Please clarify.

As discussed earlier in the manuscript, the model is spinning up over the simulation, including the period of convective instability at ~6h. Whilst we do not have specific criteria, we consider our focus on the last 12 hours of the simulation to be after the initial spin-up of the dynamics and primary aerosol (sea spray) in the model. We acknowledge that the secondary sulphate particles may still be spinning up, and we do discuss this clearly within the existing manuscript text.



- P7L20: The correspondence between patterns in highest particle concentrations and smaller particle sizes in Fig. 3 is not obvious to me in this particular figure. Please elaborate, or remove comment.

As this is not a key element of the study we decided to remove this comment.

- P7L31ff: The second half of the day is not only characterised by calmer wind conditions, but also by intense precipitation between 12 – 18 h. I believe that it should be mentioned here.

Yes – we agree. We now refer to this at this point as the reviewer suggest.

• P8L31: “adjusts to the very strong sea-salt emission and wet removal”. However precipitation only really intensifies much later than 8h after initialisation. Please comment on the role of wet removal during this period.

Even if the precipitation rate is less intense than later in the simulation, it is in average equal to 10 mm/h over the 5-8h period. So, the wet removal process becomes effective at this period of precipitation onset. We clarified this in the manuscript.

• P9L31 – P10L1: Remove sentence “The relative decrease in ...”. You already stated that it is linear. *Done*

• P10L30: “... sea-salt aerosol are transported vertically by turbulent diffusion”, I would have thought that the convective updrafts would also contribute? Please comment, or adapt text.

You are right. We clarified the manuscript.

• P11L9: Please rephrase “wind speeds condition”.

Done

• P11L21ff: The authors state that CCN variations can be as large as factor 8. This number is obtained 12h after the simulation (Fig. 8). At this time the winds subside and precipitation builds up. So, how well does it characterise the CCN variability obtained during the period of intense updrafts? It may be helpful to include a box diagram for 6h after initialisation in Fig. 8.

We explain already that the processes mean we consider the CCN variability to be well characterized in the simulations. As above, this strongly convectively unstable period is not so representative of typical conditions and we therefore feel additional box diagram is not needed.

Furthermore the authors state that the CCN variability is large whilst the accumulation mode variability is smaller. This is confusing as I would assume most CCN to stem from the accumulation mode (see Fig 7.).  *Please clarify.*

• Fig 1: For illustrative purposes the authors may consider adding a line of adiabatic parcel ascent. *We added a line representing the adiabatic parcel ascent and its specific levels (LCL, CCL and LFC).*

• Fig 2: Please rephrase “mean total top cloud height” to “mean cloud top height”.

Done.

Please rephrase “rain accumulation” to “accumulated rain” or “accumulated precipitation”.

Done.

• Fig 4: For clarification it may help adding day and night markers for the sulfate chemistry.

As described in the section 2, there is no diurnal cycle in the model (page 4, line 30).

• Fig6 and Fig7: Does your aerosol scheme specify modal boundaries for the Aitken, accumulation and coarse mode? If so what are these? These could be added in the model description section.

The process of mode-merging is explained in Mann et al. (2010), and yes the scheme includes so-called “separation diameters” which determine at what point the particle size has grown large enough to be transferred to the adjacent larger mode. The values used are those as revised in Mann et al. (2012) to better capture size distributions simulated with the more complex sectional aerosol scheme. We feel the existing references are adequate here and think it is not necessary to re-state the values used explicitly.

Mann, G. W., Carslaw, K. S., Spracklen, D. V., Ridley, D. A., Manktelow, P. T., Chipperfield, M. P., Pickering, S. J., and Johnson, C. E.: Description and evaluation of GLOMAP-mode: a modal global aerosol microphysics model for the UKCA composition-climate model, Geosci. Model Dev., 3, 519-551, 2010.

Mann, G. W., Carslaw, K. S., Ridley, D. A., Spracklen, D. V., Pringle, K. J., Merikanto, J., Korhonen, H., Schwarz, J. P., Lee, L. A., Manktelow, P. T., Woodhouse, M. T., Schmidt, A., Breider, T. J., Emmerson, K. M., Reddington, C. L., Chipperfield, M. P., and Pickering, S. J.: Inter-comparison of modal and sectional aerosol microphysics representations within the same 3-D global chemical transport model, Atmos. Chem. Phys., 12, 4449-4476, 2012.

- Fig 7: What causes the large variability in radius for the accumulation mode particles up to 8h after initialisation? This is discussed in the text on P8L30ff, but I would have thought that the SS emission radius would be tighter constrained and that wet removal processes play a larger role later during the simulation (after 12h) as the RR peaks. Please clarify.

The large variability in radius of accumulation mode particles is caused by several processes, including those mentioned by the reviewer. The model size distribution responds to the different rapid changes during this high wind speed period that is generating strong sea-spray emissions. We therefore expect both emissions effects and removal effects to be influencing the behavior of the model. The different influences are complex and we feel our current qualitative discussion in the text is sufficient.

Review for: “Spatial and temporal CCN variations in convection permitting aerosol microphysics simulations in an idealised marine tropical domain”

Summary and recommendation:

This article employs a convection-permitting resolution model to assess the contribution of spatial and temporal variations in aerosol properties for the case of a convective tropical marine boundary layer to CCN variability across a domain the size of a GCM grid box. The model is setup in a simplified idealised configuration in which the radiation scheme was turned off and CCN concentrations do not feed through to the cloud microphysics. Subsequently, the current setup ignores feedbacks associated with aerosol-radiative and aerosol-cloud microphysical interactions that may impact the simulated aerosol field in the model. The authors find that the simulated CCN concentrations can vary significantly over the domain, more than a factor of 8 during strongly convective conditions. They assess the contribution of dynamical, chemical and microphysical processes to this high variability in CCN and attribute it to increased sea salt/DMS emissions when spatial and temporal wind speed fluctuations become resolved at this convection-permitting resolution, increasing peak wind-speeds. This is an interesting finding as current GCMs cannot explicitly resolve sub-grid scale variability in wind speeds. Such modelling frameworks are required to elicit the impact of spatial/temporal resolution in GCMs on the representation of aerosol-cloud interactions. Therefore, I recommend publication of this article ACP once the following revisions have been addressed:

We thank the reviewer for their constructive review and address each of the specific comments raised below with our responses coloured red, and, where changes to the manuscript have been made, these are highlighted in the track-changes version of the document provided.

General comments:

- The modelling framework developed is described as ground-breaking. One of the key advantages of the model is in the use of a unified modelling (UM) framework to investigate the dependence of parameters involved in aerosol-cloud interactions on model resolution. However, this strength has not been captivated upon in this study. There is a lack of evaluation of the impact of the increased resolution in the model on the parameters of interest. A comparison of the domain averaged parameter values presented in the study to the same parameters simulated by the GCM would be highly beneficial and greatly strengthen the conclusions presented. Does the observed sub-grid scale variability in CCN impact the average CCN concentration across the domain compared to a GCM? This comparison should be provided before publication in ACP.

In our Figures 8 and 9 we specifically assess the CCN variability in the model, presenting the full pdf of the distribution in the vertical and at different points of the simulation across varying wind speed conditions. We agree strongly that comparing this CCN variability against that found from a lower resolution simulation with the same GCM would be a valuable comparison to make. Indeed the capability to nest down from global simulations with parameterized convection to limited-area domains runs at convection permitting resolution will enable this to be quantified in future studies with this Unified Model (UM) framework. However, the simulations here are with an idealized configuration of the UM whereby the solar variations

across a daily cycle are de-activated. We therefore feel comparing CCN variability across different horizontal resolution would best be reserved for a future study with the nested UM.

- CCN represent the aerosol particles that can form cloud droplets under reasonable atmospheric supersaturations. Accordingly, CCN concentrations always refer to a specific supersaturation, for example, CCN (0.1%) or CCN (0.5%) and one should be careful when comparing CCN concentrations measured or simulated at different supersaturations. What supersaturation was used throughout the article for the CCN concentrations presented?

Yes, we should have specified that, as in Mann et al. (2012), CCN concentrations are calculated here as soluble particles with dry diameter larger than 50nm, which corresponds to a supersaturation of 0.35%, calculated by Kohler theory for a pure sulphuric acid solution droplet. The marine aerosol review article by O'Dowd et al. (1997) refers to this threshold size as a good representative for activating nuclei. The revised manuscript now gives this definition for CCN at first use in the results section, referring to the specific threshold size and supersaturation used in the calculations.

The variability in CCN concentrations reported in this idealised configuration has been shown to be strongly dependant on variability in wind speed across the domain. This is unsurprising considering the strong wind-speed dependence of the sea spray emission parameterisation employed. Accordingly more discussion is required as to the sensitivity of the results presented on the choice of sea spray emission parameterisation with regard to the following:

- As the findings presented are strongly linked to the simulated wind speed field across the domain some discussion is required as to how accurate the simulated wind field and convective perturbation is compared to the real world. Also, is the aerosol, thus, CCN variability simulated expected compared to observations? Please discuss in relation to the footprint of flux measurements performed to measure sea-salt emissions in the marine environment and associated variability observed from these measurement campaigns.

We consider the model wind speed field across the domain, as simulated by the atmospheric dynamics in the MetUM, to be, for this type of model, highly realistic since the convection is explicitly resolved (no convection parameterization is required). The reviewer refers to the temporal footprint of flux measurements used to measure sea-salt emission. As we discuss in the reply to their later comment, that's an interesting point in relation to the time-window for the flux measurements used in deriving and evaluating the sea-spray source function flux used in our study. We consider this to be part of the future analysis in terms of applying the nested UM framework to assess the CCN variability in simulations with different spatial resolution.

- Numerous sea-salt emission parameterisations exist, derived from a variety of in-situ measurement campaigns and laboratory experiments. How does the chosen parameterisations wind-speed dependence compare to the range of parameterisations in the literature, e.g. Fig. 5 Salter et al., 2015? How might a different parameterisation alter the high variability in CCN across the domain found?

As we explain in the text, sea-salt is emitted according to the Gong (2003) sea-spray emission parameterization, as applied in our global model simulations (e.g. Mann et al., 2010). The Gong parameterization is based on the Monahan et al. (1986) sea-spray source function with a parameterization to better capture emissions of ultra-fine sea-spray. We have set the theta parameter controlling these ultra-fine sea-sprays to 30 in these simulations, as applied in Gong (2003). As in our reply to Reviewer 1, the Gong-Monahan emissions flux lie within the mid-range of other parameterizations in the literature (see e.g. Figure 5 of Salter et al., 2015),

so, in our view, it is reasonable to expect our results to be robust, with this sea-spray emissions parameterization particularly designed to capture the emitted ultra-fine sea spray.

- The onset of wave breaking is important for sea spray aerosol formation. It is generally recognized that the whitecap fraction and therefore sea spray aerosol production is zero for wind speeds less than $\sim 3 \text{ m s}^{-1}$ (Blanchard, 1963; Monahan, 1971). The implication of this with respect to the findings requires discussion, for example, what is the contribution of the total CCN variability simulated between $0\text{-}3 \text{ m s}^{-1}$? At what wind speeds does the CCN concentration begin to increase sharply, is there a threshold value?

There is no threshold velocity in the sea-spray source function, but, since the Gong parameterization is based on Monahan et al. (1986), it applies the emissions flux to be proportional to the 10m wind speed to the power 3.41, so the increase is quite steep as wind speed increases. Similarly, at the low windspeeds range mentioned (0-3 m/s) emissions fluxes will be low, and the non-linear dependence of the sea-spray emissions is one reason why this additional CCN variability becomes higher at this higher spatial resolution. We point out in the Introduction (page 3 lines 6-8) and feel this is explored sufficiently with the current text.

- Discussion is required on the applicability of the chosen parameterisation of the resolution of the model (1Km) and time-step. Typically sea salt emission parameterisations are applicable to certain footprints, and parameterisations developed from in-situ observations are dependent on the memory of the wave field (a rising sea will result in a different emission profile than a falling sea). In addition parameterisations are developed using longer time windows for averaging for flux measurements compared to the model time-step employed. Is the sea spray source function being applied in the model at this temporal/spatial resolution in the way it was designed?

As we state in the manuscript (page 5, lines 4-5), emissions are calculated (and enacted) every timestep of the simulation, which is 30 seconds at this high spatial resolution. Although the reviewer is absolutely correct to point out that wave state of the sea surface affects emitted sea-spray (e.g. Grythe et al., 2014, ACP), in our simulations with the Gong (2003) parameterization, these affects are not included. To address the reviewer comments we added the following to the revised manuscript:

"Other influences such as changes in sea surface wave state will also influence sea spray emissions (e.g. Grythe et al., 2014), but these effects are not resolved in this study. The Gong-Monahan parameterization used here is based on sea spray flux measurements made over a longer time period than the model timestep (30s), and observing capabilities now include eddy covariance sea-spray flux measurements (e.g. Norris et al., 2012), we expect our approach will resolve the dominant sources of sea spray emissions flux variability."

Minor comments:

- Section 2: A figure of the modified sea-spray source function used in the study would be beneficial here, especially for experimentalists.

We feel it is sufficient to reference the Gong (2003) paper. It's an established parameterization and was recommended for models to use in the AeroCom phase 1 co-ordinated experiment.

- Section 2: For a modelling framework described as ground-breaking the model description is relatively sparse, for instance, how is hygroscopic growth parameterised in the model? This

will affect the evolution of the aerosol field across the domain. Please provide a more detailed description of the aerosol microphysics scheme.

The ground-breaking aspect of this study is the ability to use a new numerical framework that is based on a coupling between the UKCA detailed aerosol module and the MetUM model at very high scale.

Regarding the hygroscopic growth, this aerosol process is parameterized thanks to the ZSR method (Zadanovksii, 1948; Stokes and Robinson, 1966) using data from Jacobson et al. (1996) to calculate the binary electrolyte molalities. The complete description of the hygroscopic growth parameterization as well as the description of all the others aerosol processes of the model are described in details in Mann et al. (2010).

We modified the manuscript in order to inform the reader that a complete description of the different aerosol processes is provided in this paper.

- Section 2.2: It is widely known 1-moment cloud microphysics schemes introduce errors compared to 2 or 3 moment schemes. Some justification of this choice is required, was it due to computational restraints?

Yes, in this study a single-moment microphysics scheme is used as it is the only one currently available in the latest version of the Unified Model at that time. We clarified the description of the microphysics scheme in the manuscript.

- Section 3.2, line 8: “Aitken mode are almost exclusively secondary in nature”: Please reword, this is too strong, studies exist which show emission of sea spray in this size regime, e.g. Salter et al., 2015.

We clarified the manuscript.

- Section 4, line 25. “comprising two elements”: reword.

We clarified the manuscript.

- Fig.4: Why do the error bars in DMS & SO₂/H₂SO₄ not correspond? Some discussion on expected oxidation timescales required, why is there no offset between H₂SO₄ & DMS observed?

We explain in the text that the steps involved for the SO₂ and H₂SO₄ to be produced following oxidation in the atmosphere and we do not understand the reviewer’s point here. We feel the existing text is sufficient here to explain what is shown in the Figure.

- Recent studies have probed the dependence of aerosol processes on model resolution, for instance Weigum et al., 2016. This should be referenced.

We added this reference in the introduction section.

References:

Blanchard, D. C.: The electrification of the atmosphere by particles from bubbles in the sea, Prog. Oceanogr., 1, 171–202, 1963.

Monahan, E. C.: Oceanic whitecaps, *J. Phys. Oceanogr.*, 1, 139– 144, 1971.

Salter, M. E., Zieger, P., Acosta Navarro, J. C., Grythe, H., Kirkevåg, A., Rosati, B., Riipinen, I., and Nilsson, E. D.: An empirically derived inorganic sea spray source function incorporating sea surface temperature, *Atmos. Chem. Phys.*, 15, 11047-11066, doi:10.5194/acp-15-11047-2015, 2015.

Weigum et al.: Effect of aerosol subgrid variability on aerosol optical depth and cloud condensation nuclei: implications for global aerosol modelling, *ACP* doi:10.5194/acp-16-13619-2016.

Gong, S. L.: A parameterization of sea-salt aerosol source function for sub- and super-micron particles, *Global Biogeochem. Cycles.*, 14, 1097-1103, 2003.

Grythe H., Ström, J., Krejci, R., Quinn, P. and Stohl, A., A review of sea-spray aerosol source functions using a large global set of sea salt aerosol concentration measurements, *Atmos. Chem. Phys.*, 14, 1277–1297, 2014.

Jacobson, M. Z., Tabazadeh, A., and Turco, R. P.: Simulating equilibrium within aerosols and non-equilibrium between gases and aerosols, *J. Geophys. Res.*, 101(D4), 9079–9091, 1996.

Mann, G. W., Carslaw, K. S., Spracklen, D. V., Ridley, D. A., Manktelow, P. T., Chipperfield, M. P., Pickering, S. J., and Johnson, C. E.: Description and evaluation of GLOMAP-mode: a modal global aerosol microphysics model for the UKCA composition-climate model, *Geosci. Model Dev.*, 3, 519-551, 2010.

Mann, G. W., Carslaw, K. S., Ridley, D. A., Spracklen, D. V., Pringle, K. J., Merikanto, J., Korhonen, H., Schwarz, J. P., Lee, L. A., Manktelow, P. T., Woodhouse, M. T., Schmidt, A., Breider, T. J., Emmerson, K. M., Reddington, C. L., Chipperfield, M. P., and Pickering, S. J.: Intercomparison of modal and sectional aerosol microphysics representations within the same 3-D global chemical transport model, *Atmos. Chem. Phys.*, 12, 4449-4476, doi:10.5194/acp-12-4449-2012, 2012.

Monahan, E. C., Spiel, D. E., and Davidson, K. L.: A model of marine aerosol generation via whitecaps and wave disruption. *Oceanic Whitecaps*. Edited by EC Monahan and G MacNiochaill, pp 167-193, D Reidel, Norwell, Mass, 1986.

Norris, S. J., Brooks, I. M., Hill, M. K. Brooks, B. J., Smith, M. H., Sproson, D. A. J.: Eddy covariance measurements of the sea spray aerosol flux over the open ocean, *J. Geophys. Res.*, vol. 117, doi:10.1029/2011JD016549, 2012.

O'Dowd, C. D., Smith, M. H., Consterdine, I. E., and Lowe, J. A.: Marine aerosol, sea salt, and the marine sulphur cycle: a short review, *Atmos. Environ.*, 31, 73-80, 1997.

Salter, M. E., Zieger, P., Acosta Navarro, J. C., Grythe, H., Kirkevåg, A., Rosati, B., Riipinen, I., and Nilsson, E. D.: An empirically derived inorganic sea spray source function incorporating sea surface temperature, *Atmos. Chem. Phys.*, 15, 11047-11066, doi:10.5194/acp-15-11047-2015, 2015.

Stokes, R. H. and Robinson, R. A.: Interactions in aqueous non-electrolyte solutions. I. Solute-solvent equilibria, *J. Phys. Chem.*, 70, 2126–2130, 1966.

Zadanovskii, A. B.: New methods for calculating solubilities of electrolytes in multicomponent systems, *Zh. Fiz. Khim.*, 22, 1475–1485, 1948.

Spatial and temporal CCN variations in convection-permitting aerosol microphysics simulations in an idealised marine tropical domain

Céline Planche^{1,*}, Graham W. Mann^{1,2}, Kenneth S. Carslaw¹, Mohit Dalvi³, John H. Marsham^{1,2}, and

5 Paul R. Field^{1,3}

¹ School of Earth and Environment, University of Leeds, Leeds, United Kingdom

² National Centre for Atmospheric Science, United Kingdom

³ Met Office, Exeter, United Kingdom

*Now at: Université Clermont Auvergne, Laboratoire de Météorologie Physique, OPGC/CNRS UMR 6016, Clermont-10 Ferrand, France

Correspondence to: Céline Planche (C.Planche@opgc.univ-bpclermont.fr) and Graham Mann (G.W.Mann@leeds.ac.uk)

Abstract. A convection-permitting limited area model with periodic lateral boundary conditions and prognostic aerosol

microphysics is applied to investigate how concentrations of cloud condensation nuclei (CCN) in the marine boundary layer are affected by high resolution dynamical and thermodynamic fields. The high-resolution aerosol microphysics–dynamics

15 model, which resolves differential particle growth and aerosol composition across the particle size range, is applied on a domain designed to match approximately a single grid square of a climate model. We find that, during strongly convective conditions with intense wind-speed conditions, CCN concentrations vary by more than a factor of 8 across the domain (5th-

95th percentile range), and a factor of ~3 at more moderate wind-speed conditions. One reason for these large sub-climate-grid-scale variations in CCN is that emissions of sea-salt and DMS are much higher when spatial and temporal wind speed

20 fluctuations become resolved at this convection-permitting resolution (making peak wind speeds higher). By analysing how the model evolves during spin-up, we gain new insight into the way primary sea-salt and secondary sulphate particles contribute to the overall CCN variance in these realistic conditions, and find a marked difference in the variability of super-micron and sub-micron CCN. Whereas the super-micron CCN are highly variable, being dominated by strongly fluctuating emitted sea-spray, the sub-micron CCN tend to be steadier, being mainly produced on longer timescales following growth

25 after new particle formation in the free troposphere, with fluctuations inherently buffered by the fact that coagulation is faster at higher particle concentrations. We also find that sub-micron CCN are less variable in particle size, the accumulation mode mean size varying by ~20% (0.101 to 0.123 µm diameter) compared to ~35% (0.75 to 1.10 µm diameter) for coarse mode particles at this resolution. We explore how the CCN variability changes in the vertical, and at different points in the spin-up, showing how CCN concentrations are introduced both by the emissions close to the surface, and at higher altitudes

30 during strongly convective wind-speed conditions associated to the intense convective period. We also explore how the non-linear variation of sea-salt emissions with wind speed propagates into variations in sea-salt mass mixing ratio and CCN

concentrations, finding less variation in the latter two quantities due to the longer transport timescales inherent with finer CCN, which sediment more slowly. The complex mix of sources and diverse community of processes involved makes sub-grid parameterization of CCN variations difficult. However, the results presented here illustrate the limitations of predictions with large-scale models and the high-resolution aerosol-dynamics modelling system shows promise for future studies where
5 the aerosol variations will propagate through to modified cloud microphysical evolution.

Keywords. Aerosol particles, CCN variability, UKCA, GLOMAP-mode, sub-climate scale, idealised marine tropical case.

1 Introduction

Aerosol particles affect the Earth's climate system directly by scattering and absorbing short-wave and long-wave radiation and indirectly by influencing the albedo and lifetime of clouds (e.g. Lohmann and Feichter, 2005). Successive IPCC climate
10 assessment reports (e.g. Forster et al., 2007; Myhre et al., 2013) have identified the radiative forcing due to aerosol-climate interactions as having a high level of uncertainty that needs to be better constrained for improved prediction of anthropogenic climate change.

Atmospheric aerosols, whether natural or anthropogenic, originate from two different pathways: directly emitted “primary particles” (e.g. sea-spray, in marine environments) and secondary particles, which are formed by nucleation, often first
15 requiring oxidation of gaseous precursors such as dimethyl sulphide (DMS). In general, the primary particle population can be straightforwardly classified into natural (dust, sea-spray, primary biogenic) or anthropogenic (e.g. carbonaceous particles from fossil-fuel combustion sources). However, this classification is not possible for secondary particles because of the complex interactions and influences of gases with both natural and anthropogenic sources (such as sulphur dioxide) and the moderating influence of additional semi-volatile species such as ammonia and nitric acid. In the marine boundary layer
20 however, the dominant two sources of cloud condensation nuclei (CCN) are DMS and sea-spray (e.g. Raes et al., 1993; O'Dowd and de Leeuw, 2007; Boucher et al., 2013) and the relative simplicity of this particular compartment of the atmosphere allows the systematic assessment of how two types of natural particles: primary sea-spray and secondary sulphate particles from DMS, influence aerosol-cloud interactions. Carslaw et al. (2013) highlight the importance of quantifying such natural aerosols in order to accurately characterise the anthropogenic radiative forcing via aerosol-cloud
25 interactions.

Until recently, computational costs have tended to constrain most climate models participating in international climate assessment reports to treat aerosol-cloud interactions in a simplified way, with only the mass of several aerosol types transported. With this conventional approach, CCN (number) concentrations are derived from the transported masses based on an assumed size distribution for each type, often taken to be globally uniform (e.g. Jones et al., 2011). The need to
30 represent aerosol-cloud interactions more realistically has been a major motivation for the development of a new generation of composition-climate models with interactive aerosol microphysics. The models transport both particle number

concentrations and component masses (e.g. sulphate, black carbon) in multiple size classes (e.g. Mann et al., 2014), and allow to represent sources of primary and secondary CCN explicitly. For example, the UK's Earth System Model for CMIP6 (Coupled Model Intercomparison Project phase 6) includes the GLOMAP (Global Model of Aerosol Processes) aerosol microphysics module (Mann et al., 2010; 2012), which resolves differential particle growth and aerosol composition across 5 the particle size range including internal mixtures via the computationally efficient modal aerosol dynamics approach.

In order to understand how aerosols and clouds interact, it is important to assess how aerosol properties vary at finer spatial scales than are resolved in climate models, where both convective-dynamical and aerosol microphysical effects are likely to cause non-linear CCN variations. Whereas many modelling studies have assessed the main features of global variations in the aerosol particle size distribution (e.g. Ghan et al., 2001; Adams and Seinfeld, 2002; Spracklen et al., 2005) and several 10 have explored aerosol-cloud interactions in regional scale models (e.g. Bangert et al., 2011; [Zubler et al., 2011](#); Yang et al., 2012) only a few studies (Ekman et al., 2004; 2006; Wang et al., 2011; Archer-Nicholls et al., 2016; [Possner et al., 2016](#); [Weigum et al., 2016](#)) have explored the microphysical properties of aerosols, and their potential interactions with clouds, at resolutions of ~1km where convection is resolved.

It is known that deep convection can lead to transport of aerosols (e.g. Yin et al., 2012). In arid environments, cold-pool 15 outflows from convection can be a major source of dust uplift, which is missed by large-scale models that parameterise moist convection (Marsham et al., 2011; 2013; Pope et al., 2016). Similarly, it has been shown that over oceans such convectively generated flows can both increase gaseous DMS emission and transport, since the convection generates locally strong winds leading to high emissions that are then preferentially transported by the convection (Devine et al., 2006). There are, however, 20 few model studies of aerosols in ocean environments with deep convection (e.g. Cui et al., 2011) or shallow convection (e.g. Kaufman et al., 2005).

The main objective of the current study is to assess spatial and temporal variations in aerosol properties in a convection-permitting resolution model (grid-spacing ~1 km), in particular investigating the concentration range of different sized CCN, considering potential implications for aerosol-cloud interactions simulated by current composition-climate models. In order 25 to well-characterize the influence of both the dynamics and aerosol microphysic~~sal influences~~ on cloud-relevant aerosol properties, the GLOMAP aerosol microphysics scheme is applied at high resolution over an idealised three-dimensional tropical marine domain. The convection-permitting aerosol microphysics simulations represent a highly realistic representation of CCN variations ([e.g. Yang et al., 2011](#)), providing a ground-breaking research tool for investigating aerosol-cloud interactions. The model includes interactive emissions of DMS and sea-spray and an online tropospheric chemistry scheme, ensuring the simulations include a comprehensive treatment of the combined effects from dynamical, 30 chemical and aerosol-microphysics processes occurring in the marine boundary layer. The paper is organised as follows: after a description of the UKCA (UK Chemistry and Aerosol) model and its high resolution configuration in Section 2, simulation results are described in Section 3. Section 4 summarizes, concludes and discusses the findings.

2 Model description

2.1 The UK Chemistry and Aerosol model (UKCA)

The UKCA sub-model of the UK Met Office Unified Model (MetUM) is used (hereafter UM-UKCA), including the GLOMAP-mode aerosol microphysics scheme (Mann et al., 2010) which calculates the evolution of aerosol mass and number in several log-normal size modes. The scheme represents each size mode as an internal mixture, with several aerosol components able to be simulated including sulphate (SU), sea-salt (SS), dust (DU), black carbon (BC), and particulate organic matter (POM) (including primary and biogenic secondary POM). Any number of modes (with fixed standard deviation) and possible components can be tracked, but the simulations here apply the “standard” configuration used in UM-UKCA (e.g. as in Bellouin et al., 2013) with 4 components (SU, SS, BC, POM) in 5 modes (Table 1) and dust transported separately in the existing 6-bin MetUM scheme (Woodward, 2001). The aerosol processes are simulated in a size-resolved manner and include primary emissions, secondary particle formation by binary homogeneous nucleation of sulphuric acid and water, growth by coagulation, hygroscopic growth, ageing, condensation and cloud-processing and removal by dry deposition, nucleation scavenging, impaction scavenging and sedimentation. All the details about the description of the different aerosol processes and the size distributions in UKCA are available in Mann et al. (2010; 2012).

The standard tropospheric chemistry configuration of UM-UKCA is used (O'Connor et al., 2014) which includes $O_x\text{-}HO_x\text{-}NO_y$ chemistry with degradation of methane, ethane and propane. The implementation here also includes the extension for aerosol precursor chemistry (as in Bellouin et al., 2013) for the oxidation of sulphur precursors DMS and SO_2 , and produces secondary organic aerosols via gas-phase oxidation of a biogenic monoterpene tracer.

2.2 High-resolution configuration of UM-UKCA

The simulations are carried out with UM-UKCA applied in a high resolution limited area model with periodic lateral boundary conditions, specifically applying the Numerical Weather Prediction configuration of MetUM GA4.0 (Walters et al., 2014). MetUM GA4.0 provides tracer transport, boundary-layer mixing, large-scale cloud and precipitation, with UKCA simulating atmospheric chemistry and aerosol processes. The limited area domain is centred close to the equator (1.32° , 1.08°) and set to 240 km x 240 km with 1.5 km horizontal grid-spacing. At this resolution, much of the convective-scale dynamics is resolved, and the MetUM convection parameterization (Gregory and Rowntree, 1990) is not applied. Cloud microphysics is represented using a single moment scheme (Wilson and Ballard, 1999). Even if the representation of some microphysical processes may not be well captured compared to multi-moment microphysics schemes (Morrison et al., 2009), the operational Numerical Weather Prediction (NWP) models, such as the MetUM (Wilkinson et al., 2012; Planche et al., 2015), generally use single-moment microphysics schemes. In these idealised simulations the radiation scheme was switched off, with the model therefore evolving without a diurnal cycle introduced by the daily variation in solar insolation or in variations in long wave cooling. The prognostic aerosols analysed here therefore also do not affect clear sky interact radiatively transfer. The interactive We analyse CCN concentrations, defined as soluble particles with $D_p > 50$ nm



(supersaturation of 0.35%), the size taken as representative for activating nuclei in marine stratocumulus regions (e.g. O'Dowd et al., 1997). Note however that, as well as being radiatively non-interactive, the CCN variations simulated by the model also do not feed through to modified cloud physics, with the investigation here exploring only variations in aerosol properties. A 73-level vertical grid is used up to a model top of 80 km, with 50 levels in the troposphere, 21 of which span the lowest 2 km of the atmosphere. Only a short demonstration. The simulation analysed here is here carried out with just over 24 hours integration time from an initial time of 09:00 UTC on May 24, 2002. Emissions are calculated on the simulation timestep of 30 s with UKCA chemistry and aerosol processes integrated every 10 timesteps, i.e. every 5 min.

Emissions of DMS and sea spray are interactive in the model, with their flux into the atmosphere primarily driven by variations in the model wind speed (using the same approaches described in Bellouin et al., 2013). Anthropogenic emissions of SO₂ and BC/OC are taken from the corresponding relevant grid-cell of from the IPCC AR5 global emission data (Lamarque et al., 2010), with monoterpene and biomass BC/OC emissions from the GEIA¹ and GFEDv2² databases respectively, but sources from these sectors are not significant in this domain. At the initial time, the chemistry tracers and the aerosol precursor gas phase tracers are respectively set to 1 pptv and 0.001 pptv whereas the aerosol concentrations are spun up from an entirely clean environment.

The thermodynamic (temperature and humidity) and dynamic (horizontal wind) variables are initialised from a single model profile (Figure 1) taken from a global aqua-planet configuration of a MetUM operational run (where all land points are removed). The profiles are deliberately chosen to be strongly unstable so that the model will experience a sudden deep convective instability in the early phase of its evolution. The convective perturbation can clearly be seen in Figure 2, with deep convective clouds forming after a few hours, reaching up to a cloud top height of approximately 18 km (Figure 2a). The precipitation onset is system becomes precipitating after ~5 hours of simulation (Figure 2b), with the surface rain rate becoming more intensifies after 12 h of simulation and building up to reaches a maximum of approximately 80 mm h⁻¹ between 14 and 16 h of simulation. The mean horizontal surface wind speeds over the domain increase only slightly from 2 up to around 4 m s⁻¹ as the storm develops (Figure 2c), but variations within the domain are large with a maximum one standard deviation range of 3 to 9 m s⁻¹ and strong wind speeds occurring consistently between 6 h and 10 h of simulation (15:00 and 19:00 UTC). Between 3 and 6 h of integration (12:00 to 15:00 UTC), intense vertical wind speeds occur (Figure 2d) and those upward movements will transport DMS into the free troposphere where, after oxidation, it is known to cause new aerosol particle formation (e.g. Raes et al., 1993), with subsequent growth and re-entrainment into the boundary layer of the resulting secondary particles constituting a major source of marine CCN on the global scale (e.g. Korhonen et al., 2008). The sharp variations in horizontal wind speeds will also induce strong variations in the emission of sea-spray particles, since their source function has a cubic dependence on horizontal wind speed (e.g. Gong et al., 2002). Other influences such as changes in sea surface wave state will also influence sea spray emissions (e.g. Grythe et al., 2014), but these effects are not

¹ Global Emissions Inventory Activity: www.geiacenter.org

² Global Fire Emissions Database, Version2: www.globalfiredata.org

resolved in this study. The Gong-Monahan parameterization used here is based on sea spray flux measurements made over a longer time period than the model timestep (30s), and observing capabilities now include eddy covariance sea-spray flux measurements (e.g. Norris et al., 2012), we expect our approach will resolve the dominant sources of sea spray emissions flux variability. Figures 3a-c present the variation in aerosol particle concentrations across the domain at the time of maximum convective instability, i.e. intense updrafts and horizontal wind speeds, with squall lines and associated cold pooling clearly apparent, with very strong particle concentration gradients across the gust fronts, and the gravity currents inducing regions of greatly enhanced sea-spray emission. The strong convective event causes a rapid spin-up of the atmospheric composition in the model, giving an opportunity to assess the variation in aerosol properties across a range of wind speeds during the decay after the storm has subsided. In the next section, these high-resolution spatial variations in size-resolved aerosol properties are explored, examining how the different aerosol sources and processes represented in the simulations influence fluctuations in marine boundary layer CCN concentrations at this convection-permitting resolution.

3 Results

3.1 Gas-to-particle conversion

To aid interpretation and inference from the assessment of aerosol properties in subsequent sections, in this first part of the results we explore how the substantial emission of DMS during the intense storm period propagates through to simulated concentrations of its oxidised forms sulphur dioxide (SO_2) and sulphuric acid (H_2SO_4). Emissions of DMS vary strongly with wind speed and emissions fluxes will therefore be highest between 7 h and 9 h when the peak of the wind speed fluctuations is at maximum. The high emissions lead to a peak in the domain-mean DMS concentration with maximum of ~10 pptm after 9 h of simulations (i.e. at 18:00 UTC). DMS is oxidised by OH during the daytime and by NO_3 at night, both reactions producing SO_2 which, in the gas phase, goes on to form H_2SO_4 vapour following further reaction with OH. Figure 4 illustrates the timescales associated with these processes. The domain-averaged surface SO_2 and H_2SO_4 concentrations are peaking much later than DMS (22 h of simulation, 07:00 UTC, day +1) at respectively ~18 and 6.5×10^{-3} pptm. Given the photochemistry involved, the peak concentration at 07:00 UTC is surprising, but illustrates how atmospheric composition at the surface is strongly influenced by dynamical effects, not just atmospheric chemistry. That the model was still spinning up at this time is greatly beneficial as it helps identify which processes cause the CCN variations and allows to better understand the temporal signatures of the different processes involved. The gas phase H_2SO_4 produced from the emitted DMS is a prerequisite for effective new particle formation and also causes growth of existing particles following vapour condensation, both effects being important sources of marine cloud condensation nuclei (e.g. Korhonen et al., 2008). Although BC and POM are resolved in the model, and UKCA chemistry includes the oxidation of monoterpenes, their emission in this marine domain is negligible. Rather sea spray and DMS-derived sulphate particles are the only two significant particle sources in these simulations.

Hereafter, the analysis focuses on assessing separately the aerosol particles in the different size modes, investigating how the identified driver sources and processes are influencing simulated CCN variations at this convection permitting resolution. The analysis is restricted to the last 12 h of simulation with an emphasis on the results obtained after 18 h of integration, by which time the model has fully spun-up.Indeed, according to the extreme convective instability that induces intense updrafts
5 the spin-up time lasts approximately 6 h.

3.2 Properties of the aerosol fields

In this section, the focus is on quantifying variations in aerosol properties in the three different particle size ranges: Aitken, accumulation and coarse modes. The analysis begins (Figure 3) with instantaneous snapshots of surface aerosol particle concentration and size at two different times in the simulation. Figures 3a-c present a snapshot of spatial variability at 6 h of
10 integration, when ~~an dynamics~~ intense storm period was occurring. Figures 3d-i show the snapshot spatial variation at 18 h of integration, in more modest and representative wind speed conditions but with intense rain rates. The coarse mode consists entirely of sea-spray particles, so highest particle concentrations are expected to generally be indicating regions where simulated horizontal wind speeds are highest. However, during the initial storm period, and at this high spatial
15 resolution, there are also regions of intense localised precipitation (greater than 10 mm h⁻¹) and powerful vertical wind speeds, which will also strongly influence aerosol properties due to removal and transport effects. At 6 h of simulation, Figures 3a-c show that particle concentrations in the two largest modes (accumulation and coarse) are indeed extremely variable over the entire domain. For example, particle concentrations vary from 1 to 1,000 cm⁻³ for the accumulation mode and from 0.1 to 100 cm⁻³ for the coarse mode. Note however that this very high aerosol variability is unrealistically large, being mostly due to the model being initialised with a “warm bubble” to ensure model spin-up proceeds rapidly. However,
20 the period from 12 to 24 hours of integration can be considered to span representative range of wind speed conditions, and we focus on this 2nd half of the day in the rest of the results sections.

Despite the fact that particles in Aitken mode can be affected by the emission of sea spray (e.g., Salter et al., 2015), In this remote marine domain, particles in the Aitken mode are almost exclusively secondary in nature, being originally formed via nucleation in the free troposphere. Over the initial 12 hours, free troposphere concentrations of the driver gas for nucleation,
25 H₂SO₄ are not yet high enough to initiate significant particle formation, with low simulated concentrations of its precursor species SO₂ (see Figure 4) and timescales for oxidation and transport being relative long. After 18 h of simulations, the strongly convective episode has passed, and coarse mode particle concentrations (Figure 3f), although still quite variable,
have more moderate peak concentrations, lower by around a factor of 10 than during the intense storm period (Figures 3c, f).
Accumulation mode particle concentrations at 18 h (Figure 3e) are also much less variable than at 6 h, with highest
30 concentration in the same regions that coarse mode particle concentrations were highest, likely indicating where sea spray emissions are highest (horizontal wind speeds are strongest). Patches of low concentrations are also found where the precipitation is most intense, with the washout rate (impaction scavenging efficiency) tied to rainfall rates. In the Aitken

mode (Figure 3d), particle concentrations have become significant by 18 h, although still an order of magnitude lower than in the accumulation mode. Spatial variations in the size of the aerosol particles ~~are~~ is also highest for the coarse mode (Figure 3i), ~~with regions of highest particle concentration generally corresponding to smaller particles,~~ likely reflecting the nature of the sea spray source function. The general spatial patterns of size variation seen for the coarse mode are also seen for the 5 accumulation mode (Figure 3h) but the accumulation mode has additional regions of lower particle size where Aitken mode particle concentrations are highest (Figure 3d). This co-variation is expected, since the accumulation mode mean radius will be lower, on average, when there are a significant number of smaller particles being chemically cloud processed or mode-merged in from the Aitken mode. Over the domain, mean particle size variations are largest for the Aitken mode at 118% min-to-max ratio (geometric mean radius from 22 to 48 nm), compared to ~20% for the accumulation mode (101 to 123 nm) 10 and ~35% for the coarse mode (0.75 to 1.10 μm).

In Figure 5 we show Hovmöller diagrams to further explore the temporal evolution in surface concentrations of Aitken, accumulation and coarse mode particles during the last 12 h of integration (at $y = 150$ km). Highest particle concentrations from accumulation and coarse modes are apparent between 12 and 15 h of integrations, whereas Aitken mode particle concentrations evolve with quite different time-variation. The convective storm period in the first 12 hours causes very 15 strong wind speeds and the decay of the coarse mode particles concentrations over this second half of the day reflects the progression to calmer conditions, with consequently reduced sea spray emissions but also the intensification of the precipitation (Figure 2) increasing the scavenging process efficiency. By contrast, Aitken particle concentrations are steadily increasing to a maximum of around 1-2 particles per cm^3 after 22 h, matching that seen for SO_2 and gas phase H_2SO_4 (Figure 4), consistent with the timescales of the two oxidation steps required to convert enough of the emitted DMS into sulphuric 20 acid vapour to trigger new particle formation. For particles to reach Aitken sizes, growth by condensation and coagulation is also required, and since nucleation will mostly tend to occur in the free troposphere, any transition to a statically stable boundary layer during late evening would likely also be important, influencing particle entrainment and the timing of the increase in Aitken particle concentrations at the surface. In these idealised simulations however, the short wave and long 25 wave radiation schemes are switched off, there then being no solar-induced diurnal variations in boundary layer entrainment (but photochemical variations proceeding in the model based on local time).

Assessing how each of the size modes is spinning up reveals how temporal variations in marine CCN concentrations are actually reflecting the very different time-profiles of the two dominant CCN production pathways: primary emissions of sea-spray particles and entrainment of DMS-derived secondary particles formed in the free troposphere. The analysis illustrates the way a diverse community of processes (dynamical, chemical and microphysical) together determine CCN variations in 30 the marine boundary layer. Figure 5a shows an Aitken mode emerging after 17 h of integration which also explains the dip in accumulation mode size (contour lines), as a substantial number of smaller secondary particles is being “mode-merged in” from the Aitken mode at that time. For the coarse mode, as particle concentrations decrease, there is also a progression to smaller particles, which can be explained by that fact that, in the model, sedimentation (the dominant removal process for

this mode) removes both number and mass, enabling the simulation to reflect the fact that larger particles fall faster even when they are in the same mode.

A more quantitative analysis of the simulated aerosol properties is presented hereafter, with Figure 6 showing probability density functions (PDFs) of the geometric dry radius (a-c) and particle concentrations (d-f) for the Aitken, accumulation and coarse modes at different times in the 2nd twelve hours of the integration. The analysis shows that, for the accumulation and coarse modes, as seen in Figure 5, as time progresses, the particle size PDFs shift to smaller sizes, with the accumulation mode PDFs becoming much wider in the evening as the source of smaller particles from the Aitken mode becomes significant. By contrast, as Aitken mode concentrations increase, the particles are clearly also larger, reflecting that growth

processes are acting on the particles with this size-increase ceasing at about 18 h of integration, while particle concentrations continue to increase (likely due to entrainment). For the accumulation and coarse mode particles, this quantitative approach is consistent with sedimentation causing the shift in size distribution as the larger particles sediment out faster than the smaller ones. Figure 7 shows the temporal evolution of the mean and standard deviation of the geometric mean radius values and number concentration (over grid boxes in the domain) for Aitken, accumulation and coarse modes at the surface. The accumulation and coarse mode concentration and radius fields have largest spatial variations between 5 and 8 h as the model

adjusts to the very strong sea-salt emission and quite efficient wet removal induced by the precipitation onset during the peak convective activity, whereas Aitken mode concentrations, and their variations, stay approximately constant through that period. During the simulations, the mean radius and particle concentration values from the coarse mode are, on average, decreasing (Figures 7c, f), but the mean size variations show the opposite evolution, with greater variability in the calmer 2nd half of the day, reflecting the strengthening influence of sedimentation as sea-spray emissions decrease. For the accumulation mode, the mean particle size displays remarkably little variation over the domain between 9 and 14 h of simulation (as seen in Figure 6a), with the variation increasing as the source of secondary CCN from the Aitken mode becomes significant later in the day.

3.3 CCN spatial and temporal features

In this marine domain, sea-salt particles represent a major component of the CCN population (e.g. O'Dowd et al., 1997; O'Dowd and de Leeuw, 2007). Models parameterize sea-spray emission fluxes as a function of the 10 m wind speed (u_{10}), with some source functions linked directly to field measurements of the particle concentrations (e.g. Smith et al., 1993) while others (e.g. Monahan et al., 1986) reflect also the processes that form ocean whitecaps, and laboratory experiments on particle emissions. In the simulations presented here, the model uses the sea spray source function of Gong (2003) which applies the approach of Monahan et al. (1986), and its $u^{3.41}$ 10 m-wind-speed dependence, with a refined formulation with an additional parameter determining emission of ultra-fine sea-spray particles, as constrained by field measurements from O'Dowd et al. (1997).

In light of the inference of sea-spray emissions fluxes from measurements of particle concentrations, Figure 8 presents several snapshot variation box-plots for simulated sea-salt emission flux, sea-salt mass mixing ratio (mmr) and the CCN number concentration as a function of the u_{10} (called hereafter surface wind speed) at different integration times. At this convection-permitting resolution, the sea-salt emission fields are highly heterogeneous at each integration time with the 5 emission flux median highest at 12 h of integration then decreasing towards the end of the simulations, consistent with the mean wind speed evolution (Figure 2c). After their emission into the atmosphere, sea-salt aerosols are transported vertically by turbulence, with larger particles also being influenced by sedimentation. As expected, near the surface, the higher are the sea-salt emission fluxes, the higher are the sea-salt mmr, but, as we show below, the co-variation of the sea-salt mmr field with wind speed (Figure 8b) is fundamentally different than it is for sea-salt emission (Figure 8a). Sea-spray particles are 10 highly soluble and are, in most cases, directly emitted at sizes where they are effective CCN, but, as discussed earlier, in marine regions, the CCN population also has a substantial contribution from nucleated sulphate particles which have grown large enough to be CCN-active. Figure 8c shows the variation of CCN concentrations in this marine domain at different integration times and permits to explore how its variation compares to that seen for sea-spray mmr and emissions flux. By 15 sampling the four periods at 12, 15, 18 and 21 h of integration, it is possible to assess the spatial variability in sea-salt emissions, sea-salt concentrations, and CCN concentrations at a range of wind speed conditions; the earliest period 20 representing a strong convective period (i.e. intense wind speeds) when sea-spray would be dominant, and through the progression to calmer conditions later in the simulation. First, the relative change in the median between each period (12-15, 15-18 and 18-21 h) is assessed. As expected, the median sea-salt emission flux (Figure 8a) decreases linearly on the log-log plot over the period, reflecting the 3.41 exponent in the wind-speed-dependence for the sea-spray source function. The relative decrease in sea spray emissions between 12 h and 15 h is reflected also between 15 h and 18 h, and between 18 h and 21 h. By contrast, the median sea-salt mixing ratio (Figure 8b) decreases much more steeply over the 18-21 h period 25 than in the 12-15 h period, despite strong decreases in wind speed. This effect is likely a result of the timescale for the decay from the excited state acquired during the strong convection period (the strong turbulence and direct transport having lifted particles much higher) the atmosphere still “catching up”, with the adjustment to the new calmer conditions only being visible after 18 h of integration. The equivalent temporal decay for CCN concentrations is also curved (Figure 8c), but part 30 of the signal of steeper decline between 18 and 21 h (from the decreased sea-salt) is “straightened out” by the compensating emergence of the secondary nucleated particles making an important contribution to CCN in this later period (as we showed in Figure 7). In the calm conditions, wind speeds across the domain vary (5th to 95th percentile) from ~ 0.21 to 1.6 m s^{-1} , around a factor of 8, with the CCN concentration range from around 6 to 20 particles per cubic centimetre (a factor of 3). In contrast, during the strongly convective 12-15 h period (i.e. with intense wind speeds and moderate rain rates), the CCN variation is much larger, between 12 and 95 particles per cubic centimetre (a factor of 8).

Figure 9 presents the vertical variation of the simulated CCN concentration using an altitude PDF profile (a-PDF) for the same periods as mentioned above. As expected, on average, the CCN concentration drops-off with increasing altitude

reflecting a balance between turbulence and convection lifting the particles vertically and gravitational settling transporting larger particles back towards the surface. In the atmospheric surface layer (lowest 100 metres or so) the profile of mean CCN follows a power-law profile but the spatial CCN variance (standard deviation over grid boxes in the domain) decreases much less rapidly with altitude. As a consequence, the coefficient of variation increases with increasing altitude from approx. 11% at the surface to approx. 22.5% at 1.3 km height. The CCN concentration fields close to the surface are mainly influenced by the emissions whereas at higher altitudes they are mostly influenced by the transport. This explains why, after 12 h of simulation, the coefficient of variation is slightly higher than at the others times. Note that the emergence of the secondary nucleated particles is also visible in the CCN concentration vertical properties on the 18-21 h period.

4 Conclusions and Discussions

We have analysed spatial and temporal sea-spray and CCN variations in a convection-permitting model with interactive sea-spray emissions, sulphur chemistry and aerosol microphysics over an idealised marine tropical domain. In this marine atmosphere the two dominant CCN sources are both natural: ~~the cloud nuclei population comprising two elements~~ primary sea-spray particles and secondary sulphate particles. However, even in this relatively simple two-component CCN system, our analysis has revealed that there is a diverse community of processes: dynamical, chemical, and microphysical, that together combine to determine the number of particles which can activate to cloud droplets.

First, the dynamics strongly influences the sea-spray emissions since highest particle concentrations occur where wind speeds are highest, and there is a cubic wind speed dependence for sea-salt emission. The emitted sea-spray particles have a range of sizes, being directly emitted in both the accumulation (sub-micron) and coarse (super-micron) modes. After their emission into the atmosphere, sea-salt aerosols are transported vertically by turbulent diffusion and convective updrafts, with larger particles also being influenced by sedimentation. We show that the co-variation of sea-salt mass mixing ratio with wind speed is fundamentally different than that for sea-salt emission, with implications for derivations that treat the two synonymously. In particular, since sub-micron sea-spray has much longer atmospheric residence time (days) than super-micron sea-spray (hours), care must be taken when relating measured sea-spray concentrations to emissions. Intense localised precipitation during strong convection also impacts aerosol concentrations at the climate grid-scale with removal effects introducing strong variations (e.g. via the impaction scavenging process). The combination of these processes impacts the particle concentration properties, which become extremely variable in space (about a factor of 8 over the entire domain, one climate model grid square) and time.

Moreover, the emissions of DMS strongly vary spatially and temporally according to wind speeds conditions and become substantial during intense storm period (as in Devine et al., 2006). There is a requirement for gas phase species SO₂ and H₂SO₄ vapour to be sufficiently produced following oxidation of DMS before new sulphate particle formation in the free troposphere can occur, and the latter species also cause enhanced growth of existing particles following condensation. The combination of the two oxidation steps being required to convert emitted DMS into sulphuric acid vapour, with also the

timescales inherent in particle growth processes (e.g. coagulation and condensation), explain why here is a quite different time-variation for the Aitken mode particle concentrations. Provided the airmass has had sufficient time, a significant proportion of these small secondary particles grow large enough to be cloud processed or mode-merged from the Aitken mode to the accumulation mode. The effects of these processes is illuminated by assessing how each of the particle modes is 5 spinning up, revealing the way they influence spatial- and temporal CCN variations in the marine boundary layer.

Sea-spray particles are highly soluble and, in most cases, are directly emitted at sizes where they are already effective CCN. In contrast, a different component of the CCN population comprises nucleated sulphate particles which need more time to grow large enough to be CCN-active. The variations in the CCN concentrations are strong and can attain a factor of 8 in strongly convective conditions, mostly reflecting the properties of larger CCN. Smaller (sub-micron) CCN, from the 10 accumulation mode, tend to have less variation, which in part is due to their source having a significant contribution from the steady formation of secondary sulphate particles in the free troposphere. We have seen how dynamics and microphysical processes also affect CCN, in particular with a 2nd CCN peak at the top of the boundary layer during the strongly convective period before the secondary particles emerged. These effects combine to determine how the coefficient of variation in CCN concentration changes with altitude, our results suggesting an increase from around 10% at the surface to more than 20% at 15 the top of the marine boundary layer. Whereas CCN concentration fields close to the surface are mainly influenced by the emissions, at higher altitudes they are in general older, and inheriting influences propagated via transport.

We also examine spatial and temporal variations in aerosol particle size, finding that the geometric radius of the Aitken and coarse modes are particularly variable, which will introduce further variability in cloud droplet number concentrations and 20 cloud brightness. The different influences on the two CCN types (primary and secondary), and the diverse community of processes involved (microphysical, chemical and dynamical) makes sub-grid parameterization of the CCN variations difficult. This study provides valuable results on e.g. the impact of the local dynamics and aerosol sources on the CCN population and then on the aerosol-cloud interactions occurring at these fine spatial scales. Work to apply the UM-UKCA model for non-idealised case-studies with a nesting procedure to retain the larger scale influences has now been developed, 25 as is the capability to allow these aerosol variations to couple with a new cloud microphysics scheme in MetUM (Shipway and Hill, 2012).

Acknowledgement. This project was made possible through the financial support of the Leeds-Met Office Academic Partnership (ASCI project). The authors acknowledge use of the MONSooN system, a collaborative facility supplied under the Joint Weather and Climate Research Programme, which is a strategic partnership between the Met Office and the Natural 30 Environment Research Council. The lead author wishes to thank Douglas Parker for useful discussions. G. W. Mann is funded by the UK National Centre for Atmospheric Science, one of the UK Natural Environment Research Council (NERC) research centres. J. Marsham acknowledges funding from the SAMMBA project (NE/J009822/1).

References

Adams, P. J., and Seinfeld, J. H.: Predicting global aerosol size distributions in general circulation models, *J. Geophys. Res.*, 107, D19, 4370, 2002.

Archer-Nicholls, S., Lowe, D., Schultz, D. M., and McFiggans, G.: Aerosol–radiation–cloud interactions in a regional
5 coupled model: the effects of convective parameterisation and resolution, *Atmos. Chem. Phys.*, 16, 5573–5594, 2016.

Bangert, M., Kottmeier, C., Vogel, B., and Vogel, H.: Regional scale effects of the aerosol cloud interaction simulated with
an online coupled comprehensive chemistry model, *Atmos. Chem. Phys.*, 11, 4411–4423, 2011.

Bellouin, N., Mann, G. W., Woodhouse, M. T., Johnson, C., Carslaw, K. S., and Dalvi, M.: Impact of the modal aerosol
scheme GLOMAP-mode on aerosol forcing in the Hadley Centre Global Environmental Model, *Atmos. Chem. Phys.*, 13,
10 3027–3044, 2013.

Boucher, O., Randall, D., Artaxo, P., Bretherton, C., Feingold, G., Forster, P., Kerminen, V.-M., Kondo, Y., Liao, H.,
Lohmann, U., Rasch, P., Satheesh, S. K., Sherwood, S., Stevens, B., and Zhang, X. Y.: Clouds and aerosols. In: Climate
Change 2013: The physical basis. Contribution of working group I to the Fifth Assessment Report of the
Intergovernmental Panel on Climate Change [Stocker, T., F., Qin, D., Plattner, G.-K., Tignor, M., Allen, S. K.,
15 Boschung, J., Nauels, A., Xia, Y., Bex, V., and Midgley, P. M. (eds.)], Cambridge University Press, Cambridge, United
Kingdom and New York, NY, USA, 2013.

Carslaw, K. S., Lee, L. A., Reddington, C. L., Pringle, K. J., Rap, A., Forster, P. M., Mann, G. W., Spracklen, D. V.,
Woodhouse, M. T., Regayre, L. A., and Pierce, J. R.: Large contribution of natural aerosols to uncertainty in indirect
forcing, *Nature*, 503, 67–71, 2013.

20 Cui, Z., Davies, S., Carslaw, K. S., and Blyth, A. M.: The response of precipitation to aerosol through riming and melting in
deep convective clouds, *Atmos. Chem. Phys.*, 11, 3495–3510, 2011.

Devine, G. M., Carslaw, K. S., Parker, D. J., and Petch, J. C.: The influence of subgrid surface-layer variability on vertical
transport of a chemical species in a convective environment, *Geophys. Res. Lett.*, 33, 2006.

Ekman, A., Wang, C., Wilson, J., and Ström, J.: Explicit simulations of aerosol physics in a cloud-resolving model: a
25 sensitivity study based on an observed convective cloud. *Atmos. Chem. Phys.*, 4, 773–791, 2004.

Ekman, A., Wang, C., Ström, J., and Krejci, R.: Explicit simulation of aerosol physics in a cloud-resolving model: Aerosol
transport and processing in free troposphere, *J. Atmos. Sci.*, 63, 682–695, 2006.

Forster, P., Ramaswamy, V., Artaxo, P., Berntsen, T., Betts, R., Fahey, D. W., Haywood, J., Lean, J., Lowe, D. C., Myhre,
G., Nganga, J., Prinn, R., Raga, G., Schulz, M., and Van Dorland, R.: Changes in atmospheric constituents and in
30 radiative forcing. Chapter: Climate Change 2007: The Physical Science Basis. In: Contribution of Working Group I to
Fourth Assessment Report of the Intergovernmental Panel on Climate Change Cambridge University Press, Cambridge,
UK and New York, USA, 129–234, 2007.

Ghan, S. J., Easter, R. C., Chapman, E. G., Abdul-Razzak, H., Zhang, Y., Leung, L. R., Laulainen, N. S., Saylor, R. D., and Zaveri, R. A.: A physically based estimate of radiative forcing by anthropogenic sulphate aerosol, *J. Geophys. Res.*, 106, 5279-5293, 2001.

Gong, S. L., Barrie, L. A., and Lazare, M.: Canadian Aerosol Module (CAM): A size-segregated simulation of atmospheric aerosol processes for climate and air quality models. 2. Global sea-salt aerosol and its budgets, *J. Geophys. Res.*, 107, D244779, 2002.

Gong, S. L.: A parameterization of sea-salt aerosol source function for sub- and super-micron particles, *Global Biogeochem. Cycles.*, 14, 1097-1103, 2003.

Gregory, D., and Rowntree, P. R.: A mass flux convection scheme with representation of cloud ensemble characteristics and stability-dependent closure, *Mon. Wea. Rev.*, 118, 1483-1506, 1990.

Grythe H., Ström, J., Krejci, R., Quinn, P. and Stohl, A., A review of sea-spray aerosol source functions using a large global set of sea salt aerosol concentration measurements, *Atmos. Chem. Phys.*, 14, 1277–1297, 2014.

Jones, C. D., Hughes, J. K., Bellouin, N., Hardiman, S. C., Jones, G. S., Knight, J., Liddicoat, S., O'Connor, F. M., Andres, R. J., Bell, C., Boo, K.-O., Bozzo, A., Butchart, N., Cadule, P., Corbin, K. D., Doutriaux-Boucher, M., Friedlingstein, P., Gornall, J., Gray, L., Halloran, P. R., Hurt, G., Ingram, W. J., Lamarque, J.-F., Law, R. M., Meinshausen, M., Osprey, S., Palin, E. J., Parsons Chini, L., Raddatz, T., Sanderson, M. G., Sellar, A. A., Schurer, A., Valdes, P., Woodward, N., Woodward, S., Yoshioka, M., and Zerroukat, M.: The HadGEM2-ES implementation of CMIP5 centennial simulations, *Geosci. Model Dev.*, 4, 543-570, 2011.

Kaufman, Y. J., Koren, I., Remer, L. A., Rosenfeld, D., and Rudich, Y.: The effect of smoke, dust, and pollution aerosol on shallow cloud development over the Atlantic Ocean, *Proc. Natl. Acad. Sci. USA.*, 102, 11207–11212, 2005.

Korhonen, H., Carslaw, K. S., Spracklen, D. V., Mann, G. W., and Woodhouse, M. T.: Influence of oceanic DMS emissions on CCN concentrations and seasonality over the remote Southern Hemisphere oceans: A global model study, *J. Geophys. Res.*, 113, D15204, 2008.

Lamarque, J.-F., Bond, T. C., Eyring, V., Granier, C., Heil, A., Klimont, Z., Lee, D., Liousse, C., Mieville, A., Owen, B., Schultz, M., G., Shindell, D., Smith, S., J., Stehfest, E., van Aardenne, J., Cooper, O. R., Kainuma, M., Mahowald, N., McConnell, J. R., Naik, V., Riahi, K., and van Vuuren, D. P.: Historical (1850–2000) gridded anthropogenic and biomass burning emissions of reactive gases and aerosols: methodology and application, *Atmos. Chem. Phys.*, 10, 7017-7039, 2010.

Lohmann, U., and Feichter, J.: Global indirect aerosol effects: a review, *Atmos. Chem. Phys.*, 5, 715-737, 2005.

Mann, G. W., Carslaw, K. S., Spracklen, D. V., Ridley, D. A., Manktelow, P. T., Chipperfield, M. P., Pickering, S. J., and Johnson, C. E.: Description and evaluation of GLOMAP-mode: a modal global aerosol microphysics model for the UKCA composition-climate model, *Geosci. Model Dev.*, 3, 519-551, 2010.

Mann, G. W., Carslaw, K. S., Ridley, D. A., Spracklen, D. V., Pringle, K. J., Merikanto, J., Korhonen, H., Schwarz, J. P., Lee, L. A., Manktelow, P. T., Woodhouse, M. T., Schmidt, A., Breider, T. J., Emmerson, K. M., Reddington, C. L.,

Chipperfield, M. P., and Pickering, S. J.: Inter-comparison of modal and sectional aerosol microphysics representations within the same 3-D global chemical transport model, *Atmos. Chem. Phys.*, 12, 4449-4476, 2012.

Mann, G. W., Carslaw, K. S., Reddington, C. L., Pringle, K. J., Schulz, M., Asmi, A., Spracklen, D. V., Ridley, D. A., Woodhouse, M. T., Lee, L. A., Zhang, K., Ghan, S. J., Easter, R. C., Liu, X., Stier, P., Lee, Y. H., Adams, P. J., Tost, H.,
5 Lelieveld, J., Bauer, S. E., Tsigaridis, K., Van Noije, T. P., C., Strunk, A., Vignati, E., Bellouin, N., Dalvi, M., Johnson, C. E., Bergman, T., Kokkola, H., Von Salzen, K., Yu, F., Luo, G., Petzold, A., Petzold, A., Heintzenberg, J., Clarke, A., Ogren, J. A., Gras, J., Baltensperger, U., Kaminski, U., Jennings, S. G., O'Dowd, C. D., Harrison, R. M., Beddows, D. C. S., Kulmala, M., Viisanen, Y., Ulevicius, V., Mihalopoulos, N., Zdimal, V., Fiebig, M., Hansson, H. C., Swietlicki, E., and Henzing, J. S.: Intercomparison and evaluation of global aerosol microphysical properties among AeroCom models
10 of a range of complexity, *Atmos. Chem. Phys.*, 14, 4679-4713, 2014.

Marsham, J. H., Knippertz, P., Dixon, N., Parker, D. J., and Lister, G. M. S.: The importance of the representation of deep convection for modeled dust-generating winds over West Africa during summer, *Geophys. Res. Lett.*, 38, L16803, 2011.

Marsham, J. H., Dixon, N., Garcia-Carreras, L., Lister, G. M. S., Parker, D. J., Knippertz, P., and Birch, C.E.: The role of moist convection in the West African monsoon system - insights from continental-scale convection-permitting
15 simulations, *Geophys. Res. Lett.*, 40, 1843-1849, 2013.

Monahan, E. C., Spiel, D. E., and Davidson, K. L.: A model of marine aerosol generation via whitecaps and wave disruption. Oceanic Whitecaps. Edited by EC Monahan and G MacNiochaill, pp 167-193, D Reidel, Norwell, Mass, 1986.

Morrison, H., Thompson, G., and Tatarkii, V.: Impact of cloud microphysics on the development of trailing stratiform precipitation in a simulated squall line: comparison of one- and two-moment schemes, J. Atmos. Sci., 137, 991–1007, 2009.

Myhre, G., Samset, B. H., Schulz, M., Balkanski, Y., Bauer, S., Berntsen, T. K., Bian, H., Bellouin, N., Chin, M., Diehl, T., Easter, R. C., Feichter, J., Ghan, S. J., Hauglustaine, D., Iversen, T., Kinne, S., Kirkevåg, A., Lamarque, J.-F., Lin, G., Liu, X., Lund, M. T., Luo, G., Ma, X., van Noije, T., Penner, J. E., Rasch, P. J., Ruiz, A., Seland, Ø., Skeie, R. B., Stier, P., Takemura, T., Tsigaridis, K., Wang, P., Wang, Z., Xu, L., Yu, H., Yu, F., Yoon, J.-H., Zhang, K., Zhang, H., and Zhou, C.: Radiative forcing of the direct aerosol effect from AeroCom Phase II simulations, *Atmos. Chem. Phys.*, 13, 1853-1877, 2013.

Norris, S. J., Brooks, I. M., Hill, M. K. Brooks, B. J., Smith, M. H., Sproson, D. A. J.: Eddy covariance measurements of the sea spray aerosol flux over the open ocean, J. Geophys. Res., vol. 117, doi:10.1029/2011JD016549, 2012

O'Connor, F. M., Johnson, C. E., Morgenstern, O., Abraham, N. L., Braesicke, P., Dalvi, M., Folberth, G. A., Sanderson, M. G., Telford, P. J., Young, P. J., Zeng, G., Collins, W. J., and Pyle, J. A.: Evaluation of the new UKCA climate-composition model - Part 2: The Troposphere, *Geosci. Model Dev.*, 7, 41-91, 2014.

O'Dowd, C. D., Smith, M. H., Consterdine, I. E., and Lowe, J. A.: Marine aerosol, sea salt, and the marine sulphur cycle: a short review, *Atmos. Environ.*, 31, 73-80, 1997.

O'Dowd, C. D., and de Leeuw, G.: Marine aerosol production: a review of the current knowledge, Phil. Trans. R. Soc. A, 365, 1753-1774, 2007.

5
[Planche, C., Marsham, J., Field, P., Carslaw, K., Hill, A., Mann, G., and Shipway, B.: Precipitation sensitivity to autoconversion rate in a Numerical Weather Prediction Model, Q. J. R. Meteorol. Soc., 141, 2032-2044, DOI: 10.1002/qj.2497, 2015.](#)

Pope, R. J., Marsham, J. H., Knippertz, P., Brooks, M. E., and Roberts, A. J.: Identifying errors in dust models from data assimilation, Geophys. Res. Lett., 43, doi:10.1002/2016GL070621, 2016.

[Possner A., Zubler, E. M., Lohmann, U., and Schär, C.: The resolution dependence of cloud effects and ship-induced aerosol-cloud interactions in marine stratocumulus, J. Geophys. Res. Atmos., 121, 4810–4829, 2016.](#)

10 Raes, F., Van Dingenen, R., Wilson, J., and Saltelli, A.: Cloud condensation nuclei from dimethyl sulphide in the natural marine boundary layer: Remote vs. in-situ production, in Dimethyl Sulphide: Oceans, Atmosphere and Climate, edited by G. Restelli and G. Angeletti, pp. 311-322, Kluwer, Acad., Norwell, Mass., 1993.

[Salter, M. E., Zieger, P., Acosta Navarro, J. C., Grythe, H., Kirkevåg, A., Rosati, B., Riipinen, I., and Nilsson, E. D.: An empirically derived inorganic sea spray source function incorporating sea surface temperature, Atmos. Chem. Phys., 15, 11047-11066, doi:10.5194/acp-15-11047-2015, 2015.](#)

15 Shipway, B. J., and Hill, A. A.: Diagnosis of systematic differences between multiple parameterizations of warm rain microphysics using a kinematic framework, Quart. J. Roy. Meteor. Soc., 138, 2196-2211, 2012.

Smith, M. H., Park, P. M., and Consterdine, I. E.: Marine aerosol concentrations and estimated fluxes over the sea, Q. J. R. Meteorol. Soc., 119, 809–824, 1993.

20 Spracklen, D. V., Pringle, K. J., Carslaw, K. S., Chipperfield, M. P., and Mann, G. W.: A global offline model of size-resolved aerosol microphysics: I. Model development and prediction of aerosol properties, Atmos. Chem. Phys., 5, 2227-2252, 2005.

25 Walters, D. N., Williams, K. D., Boutle, I. A., Bushell, A. C., Edwards, J. M., Field, P. R., Lock, A. P., Morcrette, C. J., Stratton, R. A., Wilkinson, J. M., Willett, M. R., Bellouin, N., Bodas-Salcedo, A., Brooks, M. E., Copsey, D., Earnshaw, P. D., Hardiman, S. C., Harris, C. M., Levine, R. C., MacLachlan, C., Manners, J. C., Martin, G. M., Milton, S. F., Palmer, M. D., Roberts, M. J., Rodríguez, J. M., Tennant, W. J., and Vidale, P. L.: The Met Office Unified Model Global Atmosphere 4.0 and JULES Global Land 4.0 configurations, Geosci. Model Dev., 7, 361-386, 2014.

Wang, M., Ghan, S., Ovchinnikov, M., Liu, X., Easter, R., Kassianov, E., Qian, Y., and Morrison, H.: Aerosol indirect effects in a multi-scale aerosol-climate model PNNL-MMF, Atmos. Chem. Phys., 11, 5431-5455, 2011.

30 [Weigum, N., Schutgens, N., and Stier, P.: Effect of aerosol subgrid variability on aerosol optical depth and cloud condensation nuclei: implications for global aerosol modelling, Atmos. Chem. Phys., 16, 13619-13639, doi:10.5194/acp-16-13619-2016, 2016.](#)

Wilkinson, J. M., Porson, A. N. F., Bornemann, F. J., Weeks, M., Field, P. R., and Lock, A. P.: Improved microphysical parametrization of drizzle and fog for operational forecasting using the Met Office Unified Model, Q. J. R. Meteorol. Soc., 139, 488–500, DOI: 10.1002/qj.1975, 2012.

Wilson, D. R., and Ballard, S. P.: A microphysically based precipitation scheme for the UK Meteorological Office Unified
5 Model. Quart. J. Roy. Meteor. Soc. 125, 1607–1636, 1999.

Woodward, S.: Modeling the atmospheric life cycle and radiative impact of mineral dust in the Hadley Centre climate model, J. Geophys. Res., 106(D16), 18115–18166, 2001.

Yang, Q., W. I. Gustafson Jr., Fast, J. D., Wang, H., Easter, R. C., Morrison, H., Lee, Y.-N., Chapman, E. G., Spak, S. N., and Mena-Carrasco, M. A.: Assessing regional scale predictions of aerosols, marine stratocumulus, and their interactions during VOCALS-REx using WRF-Chem, Atmos. Chem. Phys., 11, 11951-11975, doi:10.5194/acp-11-11951-2011, 2011.

Yang, Q., Gustafson Jr., W. I., Fast, J. D., Wang, H., Easter, R. C., Wang, M., Ghan, S. J., Berg, L. K., Leung, L. R., and Morrison, H.: Impact of natural and anthropogenic aerosols on stratocumulus and precipitation in the Southeast Pacific: a regional modelling study using WRF-Chem, Atmos. Chem. Phys., 12, 8777–8796, 2012.

15 Yin, Y., Chen, Q., Jin, L., Chen, B., Zhu, S., and Zhang, X.: The effects of deep convection on the concentration and size distribution of aerosol particles within the upper troposphere: A case study, J. Geophys. Res., 117, D22202, 2012.

Zubler, E. M., Folini, D., Lohmann, U., Lüthi, D., Schär, C., and Wild, M.: Simulation of dimming and brightening in Europe from 1958 to 2001 using a regional climate model, J. Geophys. Res., 116, D18205, 2011.

Table 1. Standard aerosol configuration for GLOMAP-mode. The size distribution is described by lognormal modes with varying geometric mean diameter D and fixed geometric standard deviation σ_g . Particle number and mass are transferred between modes when D exceeds the upper limit for the mode. Names are given in function of the aerosols mode ('nuc', 'Ait', 'acc' and 'coa' are for 'nucleation', 'Aitken', 'accumulation' and 'coarse') and their solubility properties ('sol' and 'ins' mean the aerosols are soluble or insoluble). The aerosols can be composed of sulphate (SU), primary organic matter (POM), black carbon (BC), or sea-salt (SS).

Index	Name	Size range	Composition	Soluble	σ_g
1	nucsol	$D < 10 \text{ nm}$	SU, POM	yes	1.59
2	Aitsol	$10 \text{ nm} < D < 100 \text{ nm}$	SU, BC, POM	yes	1.59
3	accsol	$100 \text{ nm} < D < 1 \mu\text{m}$	SU, BC, POM, SS	yes	1.59
4	coasol	$D > 1 \mu\text{m}$	SU, BC, POM, SS	yes	2.00
5	Aitins	$10 \text{ nm} < D < 100 \text{ nm}$	BC, POM	no	1.59

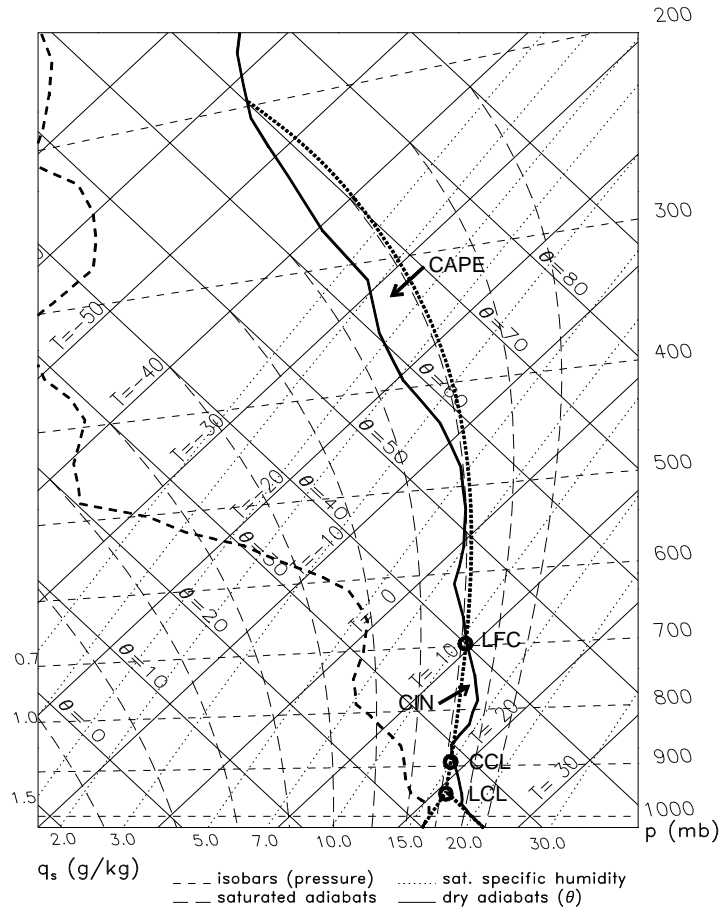


Figure 1. Tephigram representing the vertical profile of the initial dew point temperature (dashed line) and the temperature (solid line). The thick dotted line represents the adiabatic parcel ascent and the circles indicate the specific levels of the parcel such as the Lifted Condensation Level (LCL), the Convective Condensation Level (CCL) and the Level of Free Convection (LFC).

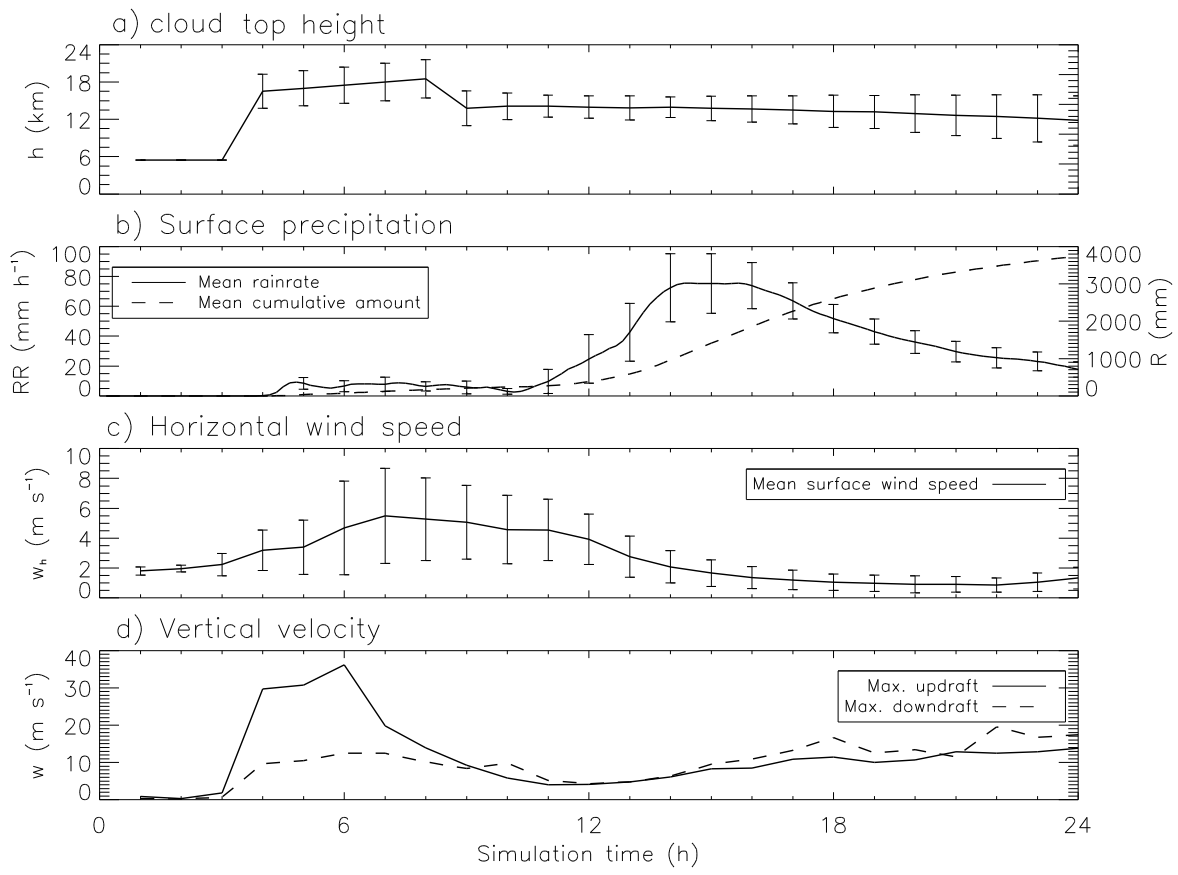


Figure 2. Temporal evolution of (a) the mean ~~total~~^{top}-cloud ~~top~~ height, (b) the mean accumulated rain accumulation and rain rate at the surface, (c) the mean surface horizontal wind speed and (d) the maximum of the updrafts and downdrafts. The averages are obtained over the entire grid points of the domain and given with \pm one standard deviation.

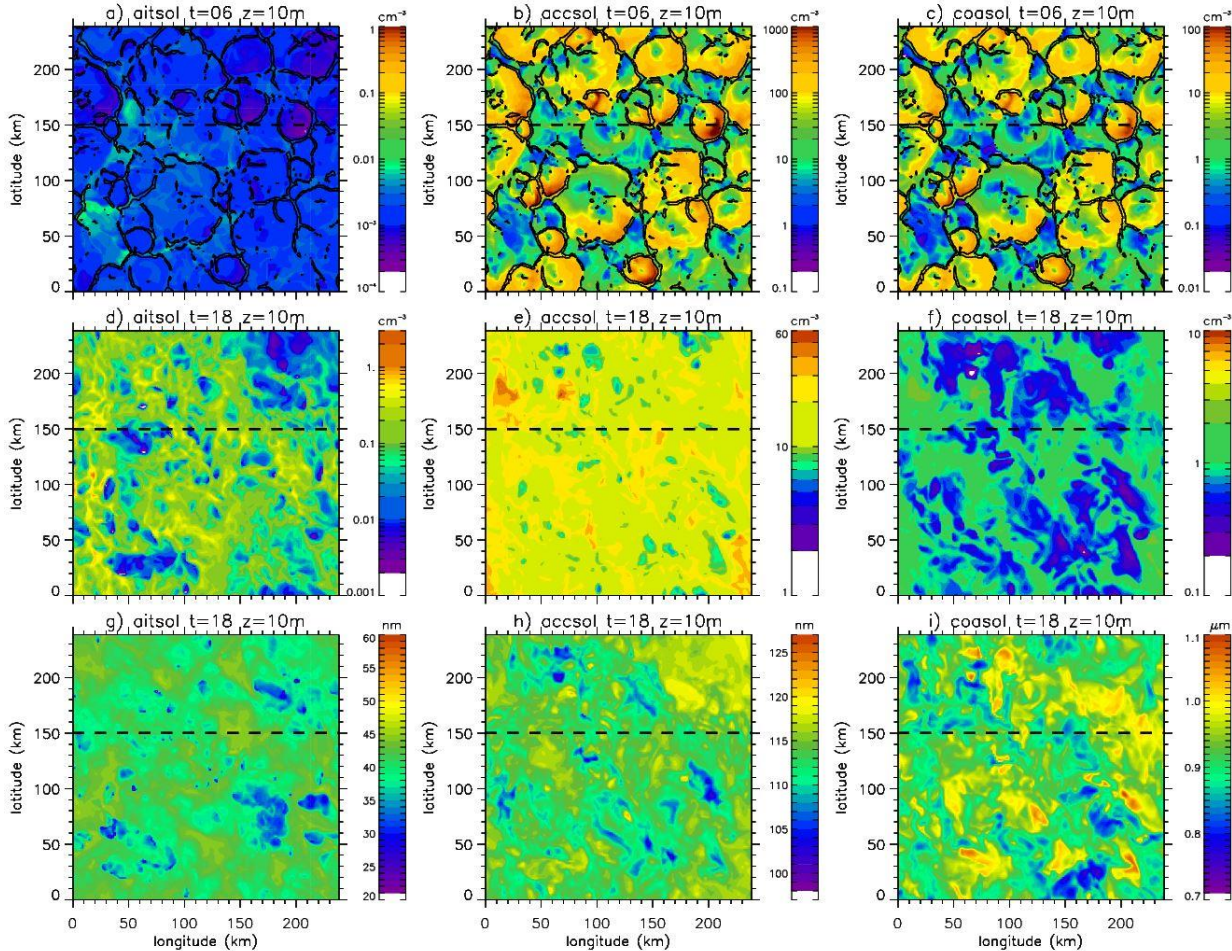


Figure 3. Snapshot spatial variations in the number concentrations (a-f) and geometric-mean radius (g-i) of the aerosol particles in the Aitken (aitsol; a, d, g), accumulation (accsol; b, e, h) and coarse (coasol; c, f, i) soluble modes after 6 h (in model spin-up) (a-c) and 18 h (d-i) of integration. The black solid lines represent the surface vertical wind speed ($w = 5 \text{ m s}^{-1}$). Note that the colour scales are different. The dashed lines correspond to the transects shown in Figures 5 and 9.

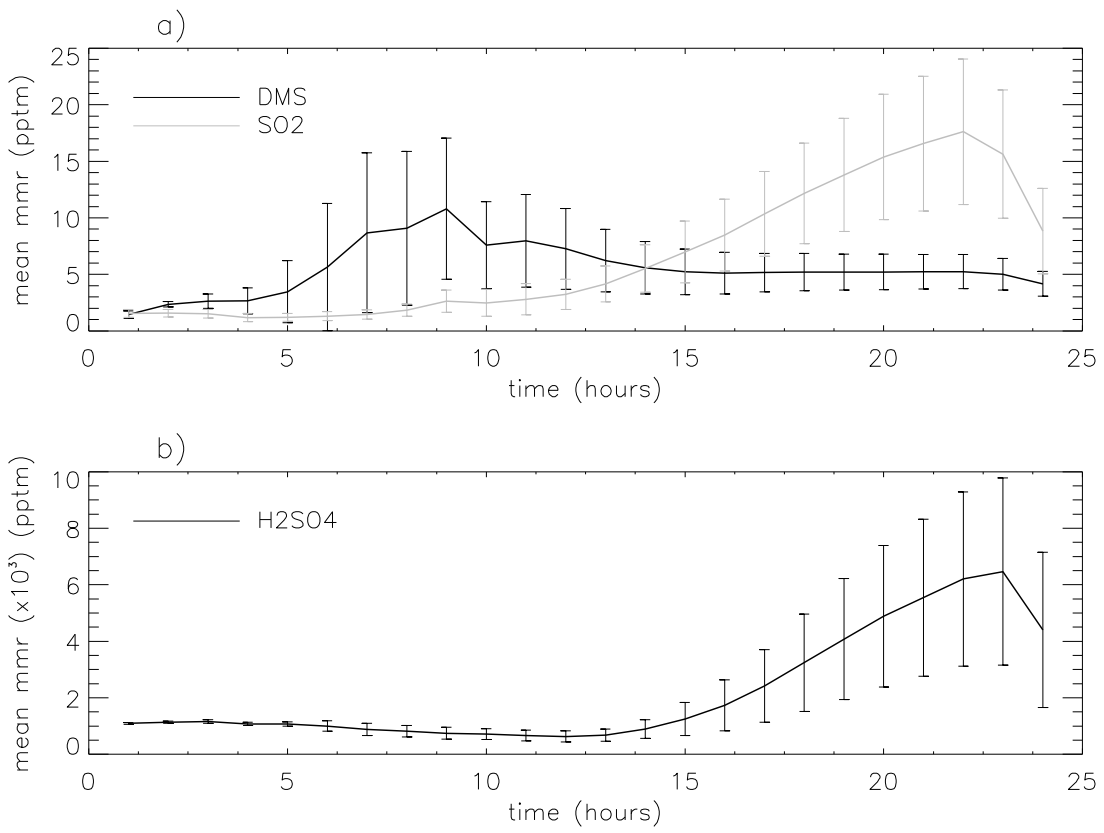


Figure 4. Temporal evolution of the mean mass mixing ratios of the gas precursors to aerosols. The DMS, SO₂ and H₂SO₄ mass concentrations are in pptm (part per trillion in mass). The error bars correspond to \pm one standard deviation.

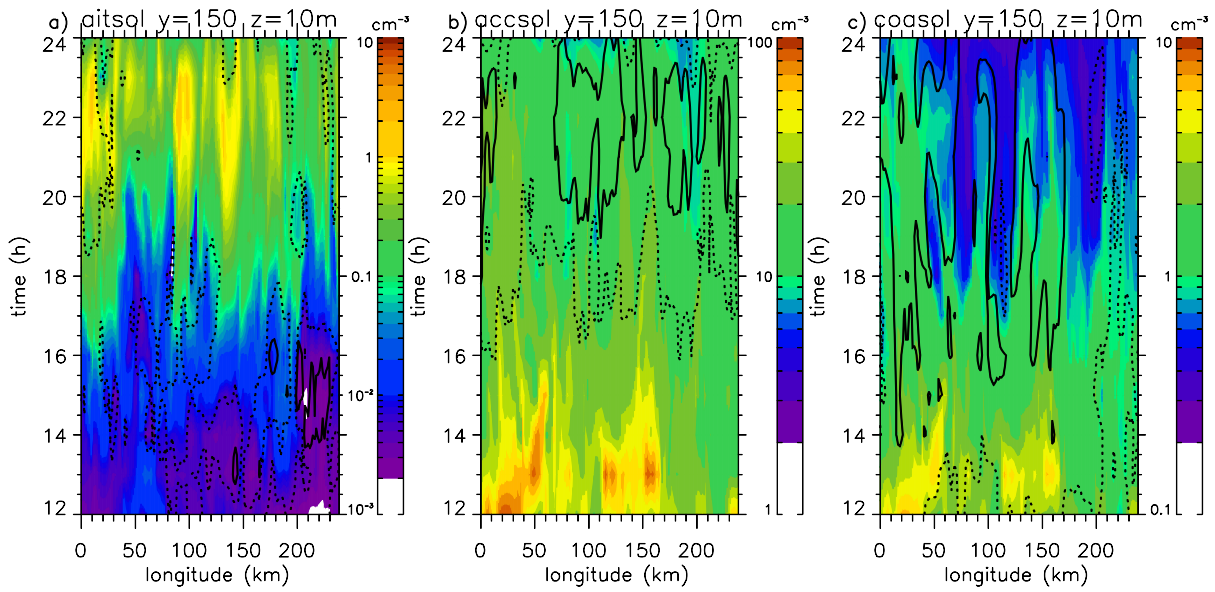


Figure 5. Temporal evolution of the aerosol concentration from the Aitken (a), accumulation (b) and coarse (c) soluble mode after the model spin-up. Temporal evolution of the aerosol dry radius is also illustrated for the 3 modes: 30 (dashed line) and 35 nm (solid line) for the Aiken soluble mode, 110 (solid line) and 115 nm (dashed line) for the accumulation soluble mode; 5 and 0.96 (solid line) and 1.0 μm (dashed lines) for coarse soluble mode. Note that the colour scales are different.

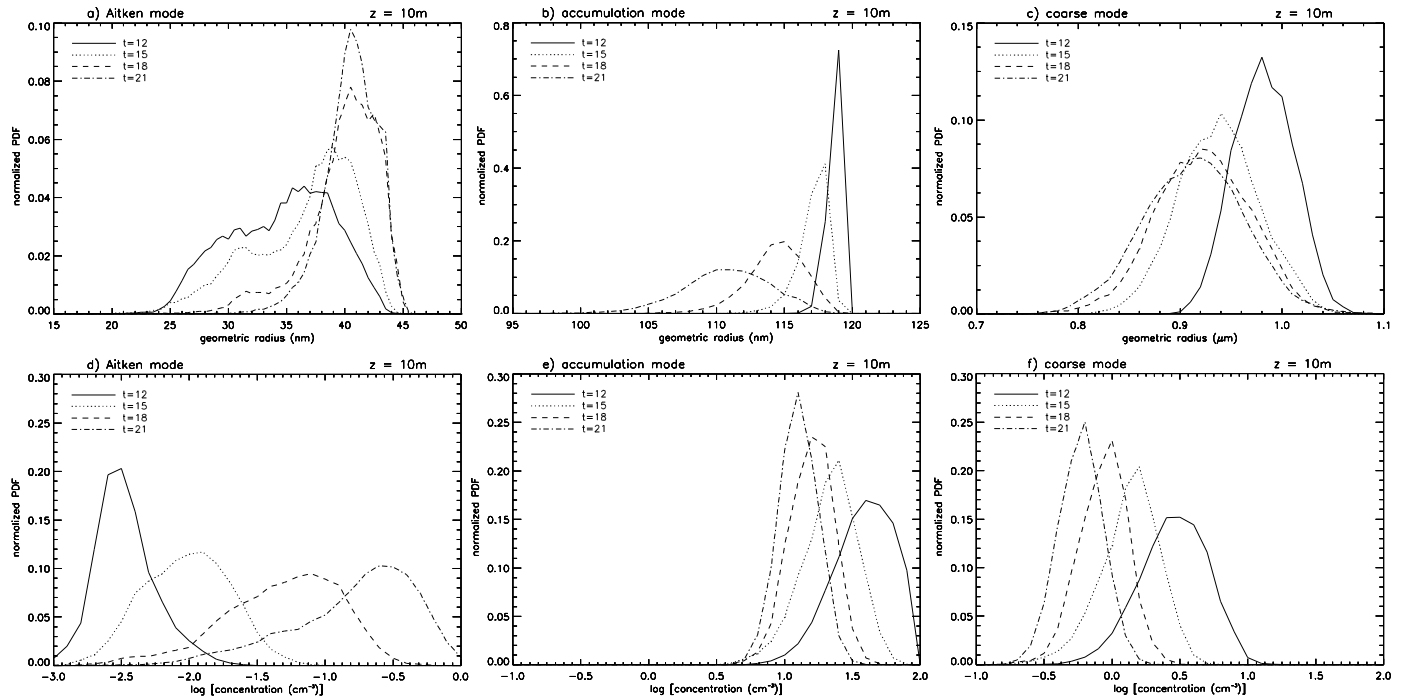


Figure 6. Normalized Probability Density Function (PDF) of the geometric radius (a, b, c) and the logarithm of the concentration (d, e, f) of the surface aerosols from the Aitken (a, d), accumulation (b, e) and coarse (c, f) soluble modes obtained at different integration time.

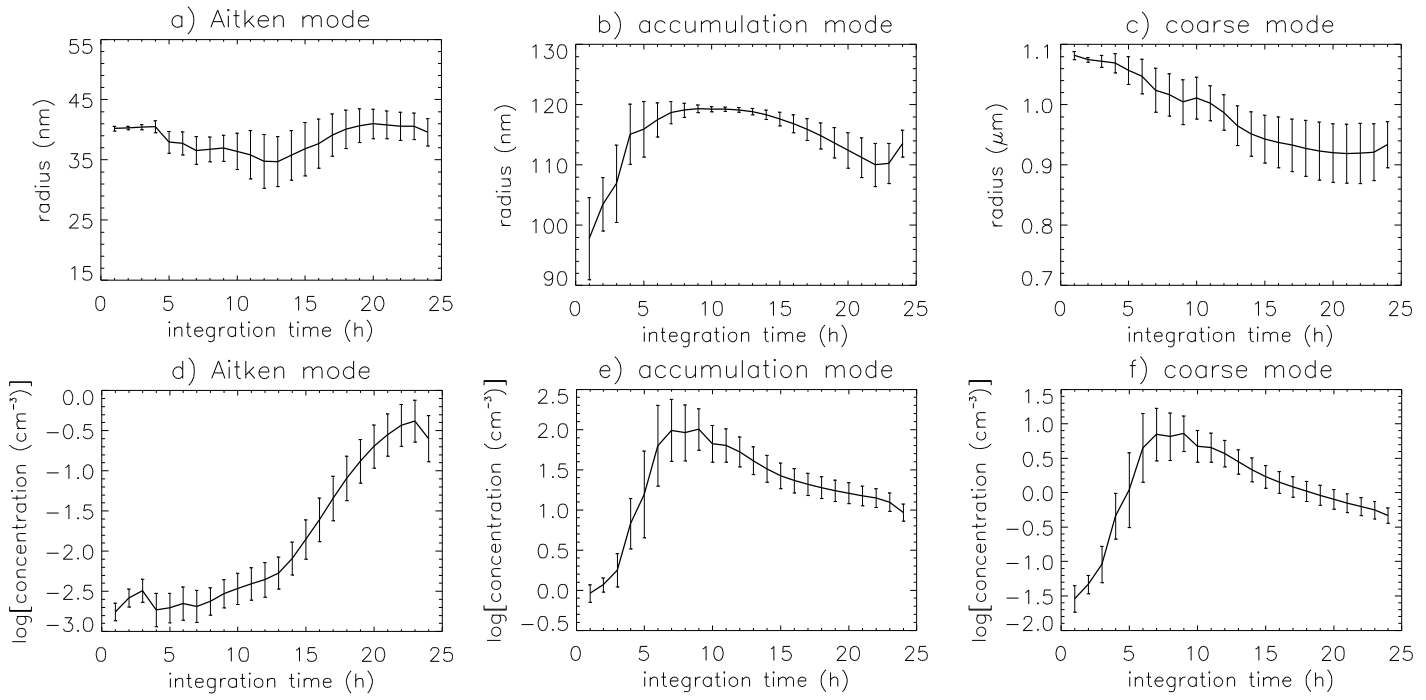


Figure 7. Time series of the mean \pm one standard deviation of the geometric radius (a, b, c) and the logarithm of the concentration (d, e, f) of the surface aerosols from the Aitken (a, d), accumulation (b, e) and coarse (c, f) soluble modes.

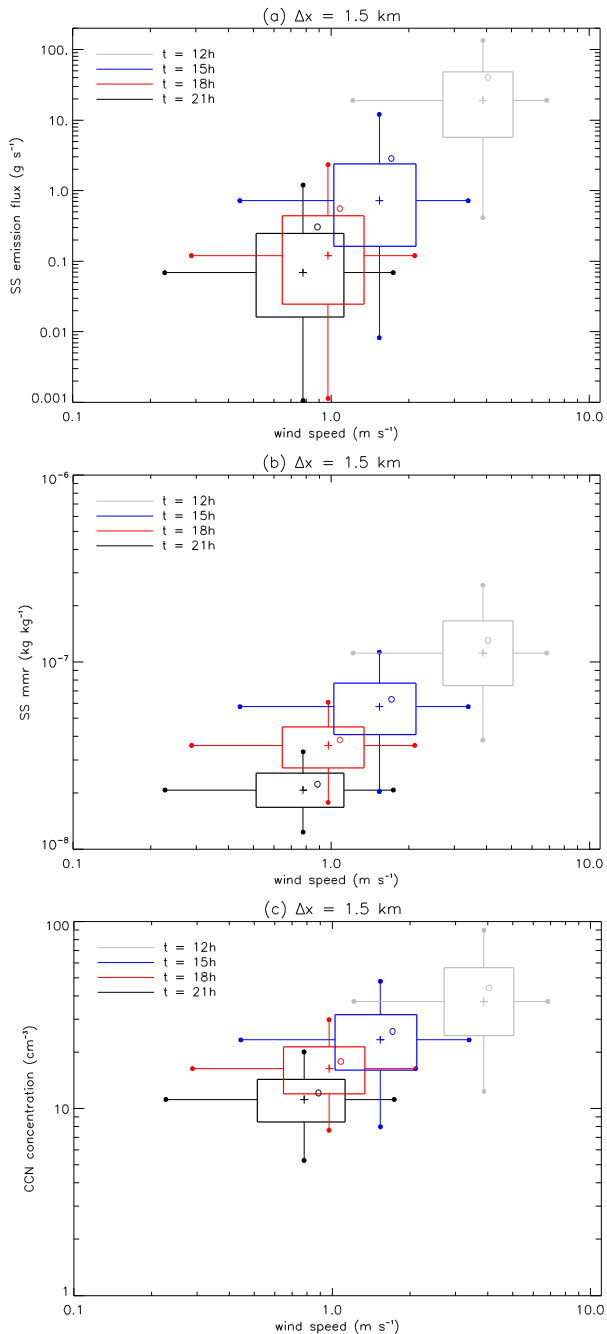


Figure 8. 2D-distribution of the surface sea-salt emission flux (a), sea-salt mass mixing ratio (mmr) (b) and CCN concentration (c) as a function of the surface horizontal wind for 4 different integration times ($t = 12, 15, 18$ or 21h). The hinges of the box-plots represent the 25th and 75th percentiles and the ends of the whiskers (full circles) represent the 5th and 95th percentiles. The ‘plus’ symbols represent the median values. The empty circles show the mean values over the domain.

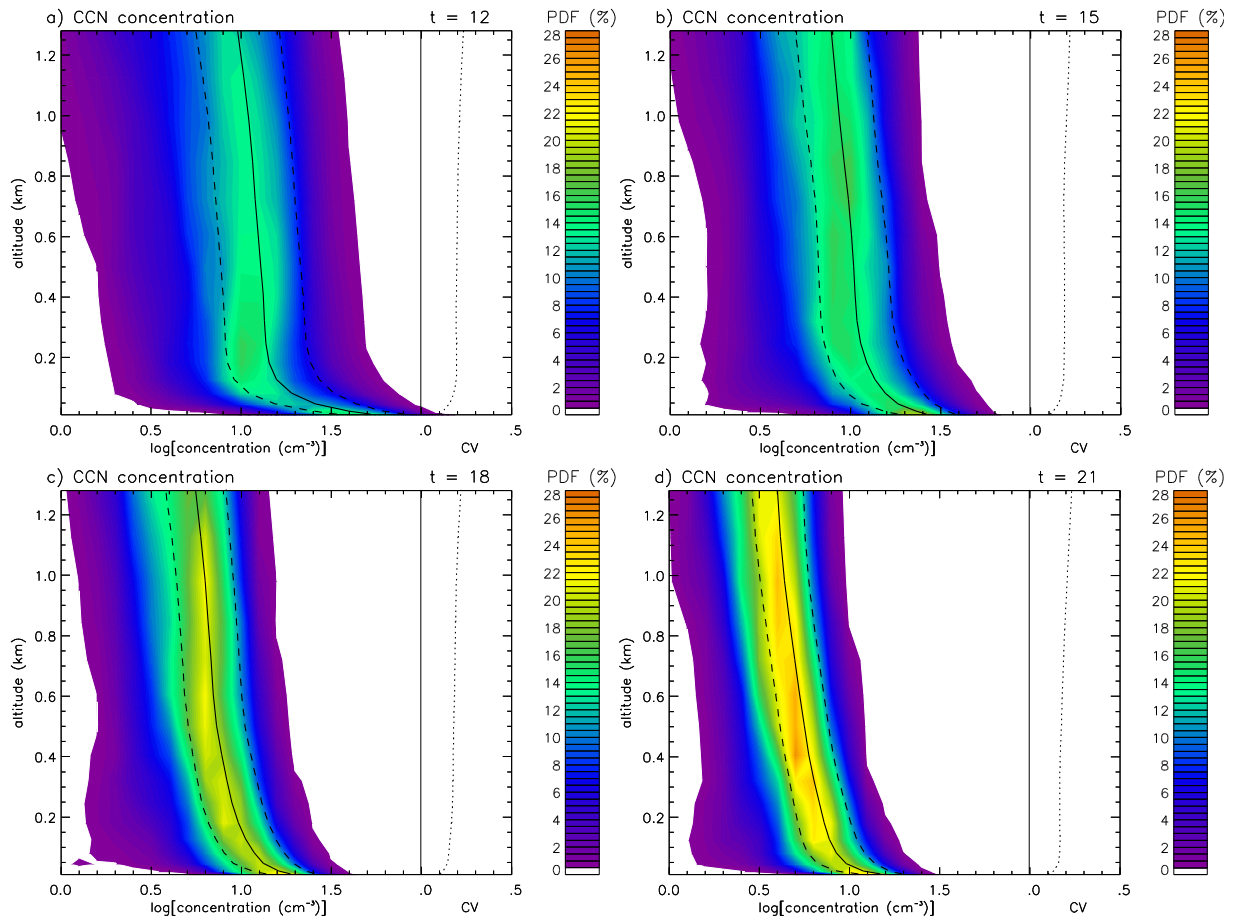


Figure 9. Altitude-dependent Probability Density Function (a-PDF) in percent of the CCN concentration at different integration times. The a-PDF are obtained calculating the PDF for each different level. A resolution of 0.1 is used for quantifying the logarithm of the concentration. The lines represent the mean (solid lines) \pm one standard deviation (dashed lines) 5 of the CCN concentration. The dotted lines represent the coefficient of variation (CV) which is defined as the ratio of the standard deviation to the mean of the CCN concentration.

Spatial and temporal CCN variations in convection-permitting aerosol microphysics simulations in an idealised marine tropical domain

Céline Planche^{1,*}, Graham W. Mann^{1,2}, Kenneth S. Carslaw¹, Mohit Dalvi³, John H. Marsham^{1,2}, and

5 Paul R. Field^{1,3}

¹ School of Earth and Environment, University of Leeds, Leeds, United Kingdom

² National Centre for Atmospheric Science, United Kingdom

³ Met Office, Exeter, United Kingdom

*Now at: Université Clermont Auvergne, Laboratoire de Météorologie Physique, OPGC/CNRS UMR 6016, Clermont-10 Ferrand, France

Correspondence to: Céline Planche (C.Planche@opgc.univ-bpclermont.fr) and Graham Mann (G.W.Mann@leeds.ac.uk)

Abstract. A convection-permitting limited area model with periodic lateral boundary conditions and prognostic aerosol

microphysics is applied to investigate how concentrations of cloud condensation nuclei (CCN) in the marine boundary layer are affected by high resolution dynamical and thermodynamic fields. The high-resolution aerosol microphysics–dynamics

15 model, which resolves differential particle growth and aerosol composition across the particle size range, is applied on a domain designed to match approximately a single grid square of a climate model. We find that, during strongly convective

conditions with intense wind-speed conditions, CCN concentrations vary by more than a factor of 8 across the domain (5th-95th percentile range), and a factor of ~3 at more moderate wind-speed conditions. One reason for these large sub-climate-

grid-scale variations in CCN is that emissions of sea-salt and DMS are much higher when spatial and temporal wind speed

20 fluctuations become resolved at this convection-permitting resolution (making peak wind speeds higher). By analysing how the model evolves during spin-up, we gain new insight into the way primary sea-salt and secondary sulphate particles contribute to the overall CCN variance in these realistic conditions, and find a marked difference in the variability of super-

micron and sub-micron CCN. Whereas the super-micron CCN are highly variable, being dominated by strongly fluctuating emitted sea-spray, the sub-micron CCN tend to be steadier, being mainly produced on longer timescales following growth

25 after new particle formation in the free troposphere, with fluctuations inherently buffered by the fact that coagulation is faster at higher particle concentrations. We also find that sub-micron CCN are less variable in particle size, the accumulation mode mean size varying by ~20% (0.101 to 0.123 µm diameter) compared to ~35% (0.75 to 1.10 µm diameter) for coarse mode particles at this resolution. We explore how the CCN variability changes in the vertical, and at different points in the

spin-up, showing how CCN concentrations are introduced both by the emissions close to the surface, and at higher altitudes

30 during strongly convective wind-speed conditions associated to the intense convective period. We also explore how the non-linear variation of sea-salt emissions with wind speed propagates into variations in sea-salt mass mixing ratio and CCN

concentrations, finding less variation in the latter two quantities due to the longer transport timescales inherent with finer CCN, which sediment more slowly. The complex mix of sources and diverse community of processes involved makes sub-grid parameterization of CCN variations difficult. However, the results presented here illustrate the limitations of predictions with large-scale models and the high-resolution aerosol-dynamics modelling system shows promise for future studies where
5 the aerosol variations will propagate through to modified cloud microphysical evolution.

Keywords. Aerosol particles, CCN variability, UKCA, GLOMAP-mode, sub-climate scale, idealised marine tropical case.

1 Introduction

Aerosol particles affect the Earth's climate system directly by scattering and absorbing short-wave and long-wave radiation and indirectly by influencing the albedo and lifetime of clouds (e.g. Lohmann and Feichter, 2005). Successive IPCC climate
10 assessment reports (e.g. Forster et al., 2007; Myhre et al., 2013) have identified the radiative forcing due to aerosol-climate interactions as having a high level of uncertainty that needs to be better constrained for improved prediction of anthropogenic climate change.

Atmospheric aerosols, whether natural or anthropogenic, originate from two different pathways: directly emitted “primary particles” (e.g. sea-spray, in marine environments) and secondary particles, which are formed by nucleation, often first
15 requiring oxidation of gaseous precursors such as dimethyl sulphide (DMS). In general, the primary particle population can be straightforwardly classified into natural (dust, sea-spray, primary biogenic) or anthropogenic (e.g. carbonaceous particles from fossil-fuel combustion sources). However, this classification is not possible for secondary particles because of the complex interactions and influences of gases with both natural and anthropogenic sources (such as sulphur dioxide) and the moderating influence of additional semi-volatile species such as ammonia and nitric acid. In the marine boundary layer
20 however, the dominant two sources of cloud condensation nuclei (CCN) are DMS and sea-spray (e.g. Raes et al., 1993; O'Dowd and de Leeuw, 2007; Boucher et al., 2013) and the relative simplicity of this particular compartment of the atmosphere allows the systematic assessment of how two types of natural particles: primary sea-spray and secondary sulphate particles from DMS, influence aerosol-cloud interactions. Carslaw et al. (2013) highlight the importance of quantifying such natural aerosols in order to accurately characterise the anthropogenic radiative forcing via aerosol-cloud
25 interactions.

Until recently, computational costs have tended to constrain most climate models participating in international climate assessment reports to treat aerosol-cloud interactions in a simplified way, with only the mass of several aerosol types transported. With this conventional approach, CCN (number) concentrations are derived from the transported masses based on an assumed size distribution for each type, often taken to be globally uniform (e.g. Jones et al., 2011). The need to
30 represent aerosol-cloud interactions more realistically has been a major motivation for the development of a new generation of composition-climate models with interactive aerosol microphysics. The models transport both particle number

concentrations and component masses (e.g. sulphate, black carbon) in multiple size classes (e.g. Mann et al., 2014), and allow to represent sources of primary and secondary CCN explicitly. For example, the UK's Earth System Model for CMIP6 (Coupled Model Intercomparison Project phase 6) includes the GLOMAP (Global Model of Aerosol Processes) aerosol microphysics module (Mann et al., 2010; 2012), which resolves differential particle growth and aerosol composition across 5 the particle size range including internal mixtures via the computationally efficient modal aerosol dynamics approach.

In order to understand how aerosols and clouds interact, it is important to assess how aerosol properties vary at finer spatial scales than are resolved in climate models, where both convective-dynamical and aerosol microphysical effects are likely to cause non-linear CCN variations. Whereas many modelling studies have assessed the main features of global variations in the aerosol particle size distribution (e.g. Ghan et al., 2001; Adams and Seinfeld, 2002; Spracklen et al., 2005) and several 10 have explored aerosol-cloud interactions in regional scale models (e.g. Bangert et al., 2011; [Zubler et al., 2011](#); Yang et al., 2012) only a few studies (Ekman et al., 2004; 2006; Wang et al., 2011; Archer-Nicholls et al., 2016; [Possner et al., 2016](#); [Weigum et al., 2016](#)) have explored the microphysical properties of aerosols, and their potential interactions with clouds, at resolutions of ~1km where convection is resolved.

It is known that deep convection can lead to transport of aerosols (e.g. Yin et al., 2012). In arid environments, cold-pool 15 outflows from convection can be a major source of dust uplift, which is missed by large-scale models that parameterise moist convection (Marsham et al., 2011; 2013; Pope et al., 2016). Similarly, it has been shown that over oceans such convectively generated flows can both increase gaseous DMS emission and transport, since the convection generates locally strong winds leading to high emissions that are then preferentially transported by the convection (Devine et al., 2006). There are, however, 20 few model studies of aerosols in ocean environments with deep convection (e.g. Cui et al., 2011) or shallow convection (e.g. Kaufman et al., 2005).

The main objective of the current study is to assess spatial and temporal variations in aerosol properties in a convection-permitting resolution model (grid-spacing ~1 km), in particular investigating the concentration range of different sized CCN, considering potential implications for aerosol-cloud interactions simulated by current composition-climate models. In order 25 to well-characterize the influence of both the dynamics and aerosol microphysic~~sal influences~~ on cloud-relevant aerosol properties, the GLOMAP aerosol microphysics scheme is applied at high resolution over an idealised three-dimensional tropical marine domain. The convection-permitting aerosol microphysics simulations represent a highly realistic representation of CCN variations ([e.g. Yang et al., 2011](#)), providing a ground-breaking research tool for investigating aerosol-cloud interactions. The model includes interactive emissions of DMS and sea-spray and an online tropospheric chemistry scheme, ensuring the simulations include a comprehensive treatment of the combined effects from dynamical, 30 chemical and aerosol-microphysics processes occurring in the marine boundary layer. The paper is organised as follows: after a description of the UKCA (UK Chemistry and Aerosol) model and its high resolution configuration in Section 2, simulation results are described in Section 3. Section 4 summarizes, concludes and discusses the findings.

2 Model description

2.1 The UK Chemistry and Aerosol model (UKCA)

The UKCA sub-model of the UK Met Office Unified Model (MetUM) is used (hereafter UM-UKCA), including the GLOMAP-mode aerosol microphysics scheme (Mann et al., 2010) which calculates the evolution of aerosol mass and number in several log-normal size modes. The scheme represents each size mode as an internal mixture, with several aerosol components able to be simulated including sulphate (SU), sea-salt (SS), dust (DU), black carbon (BC), and particulate organic matter (POM) (including primary and biogenic secondary POM). Any number of modes (with fixed standard deviation) and possible components can be tracked, but the simulations here apply the “standard” configuration used in UM-UKCA (e.g. as in Bellouin et al., 2013) with 4 components (SU, SS, BC, POM) in 5 modes (Table 1) and dust transported separately in the existing 6-bin MetUM scheme (Woodward, 2001). The aerosol processes are simulated in a size-resolved manner and include primary emissions, secondary particle formation by binary homogeneous nucleation of sulphuric acid and water, growth by coagulation, hygroscopic growth, ageing, condensation and cloud-processing and removal by dry deposition, nucleation scavenging, impaction scavenging and sedimentation. All the details about the description of the different aerosol processes and the size distributions in UKCA are available in Mann et al. (2010; 2012).

The standard tropospheric chemistry configuration of UM-UKCA is used (O'Connor et al., 2014) which includes $O_x\text{-}HO_x\text{-}NO_y$ chemistry with degradation of methane, ethane and propane. The implementation here also includes the extension for aerosol precursor chemistry (as in Bellouin et al., 2013) for the oxidation of sulphur precursors DMS and SO_2 , and produces secondary organic aerosols via gas-phase oxidation of a biogenic monoterpene tracer.

2.2 High-resolution configuration of UM-UKCA

The simulations are carried out with UM-UKCA applied in a high resolution limited area model with periodic lateral boundary conditions, specifically applying the Numerical Weather Prediction configuration of MetUM GA4.0 (Walters et al., 2014). MetUM GA4.0 provides tracer transport, boundary-layer mixing, large-scale cloud and precipitation, with UKCA simulating atmospheric chemistry and aerosol processes. The limited area domain is centred close to the equator (1.32° , 1.08°) and set to 240 km x 240 km with 1.5 km horizontal grid-spacing. At this resolution, much of the convective-scale dynamics is resolved, and the MetUM convection parameterization (Gregory and Rowntree, 1990) is not applied. Cloud microphysics is represented using a single moment scheme (Wilson and Ballard, 1999). Even if the representation of some microphysical processes may not be well captured compared to multi-moment microphysics schemes (Morrison et al., 2009), the operational Numerical Weather Prediction (NWP) models, such as the MetUM (Wilkinson et al., 2012; Planche et al., 2015), generally use single-moment microphysics schemes. In these idealised simulations the radiation scheme was switched off, with the model therefore evolving without a diurnal cycle introduced by the daily variation in solar insolation or in variations in long wave cooling. The prognostic aerosols analysed here therefore also do not affect clear sky interact radiatively transfer. The interactive We analyse CCN concentrations, defined as soluble particles with $D_p > 50$ nm

(supersaturation of 0.35%), the size taken as representative for activating nuclei in marine stratocumulus regions (e.g. O'Dowd et al., 1997). Note however that, as well as being radiatively non-interactive, the CCN variations simulated by the model also do not feed through to modified cloud physics, with the investigation here exploring only variations in aerosol properties. A 73-level vertical grid is used up to a model top of 80 km, with 50 levels in the troposphere, 21 of which span the lowest 2 km of the atmosphere. Only a short demonstration. The simulation analysed here is here carried out with just over 24 hours integration time from an initial time of 09:00 UTC on May 24, 2002. Emissions are calculated on the simulation timestep of 30 s with UKCA chemistry and aerosol processes integrated every 10 timesteps, i.e. every 5 min.

Emissions of DMS and sea spray are interactive in the model, with their flux into the atmosphere primarily driven by variations in the model wind speed (using the same approaches described in Bellouin et al., 2013). Anthropogenic emissions of SO₂ and BC/OC are taken from the corresponding relevant grid-cell of from the IPCC AR5 global emission data (Lamarque et al., 2010), with monoterpane and biomass BC/OC emissions from the GEIA¹ and GFEDv2² databases respectively, but sources from these sectors are not significant in this domain. At the initial time, the chemistry tracers and the aerosol precursor gas phase tracers are respectively set to 1 pptv and 0.001 pptv whereas the aerosol concentrations are spun up from an entirely clean environment.

The thermodynamic (temperature and humidity) and dynamic (horizontal wind) variables are initialised from a single model profile (Figure 1) taken from a global aqua-planet configuration of a MetUM operational run (where all land points are removed). The profiles are deliberately chosen to be strongly unstable so that the model will experience a sudden deep convective instability in the early phase of its evolution. The convective perturbation can clearly be seen in Figure 2, with deep convective clouds forming after a few hours, reaching up to a cloud top height of approximately 18 km (Figure 2a). The precipitation onset is system becomes precipitating after ~5 hours of simulation (Figure 2b), with the surface rain rate becoming more intensifies after 12 h of simulation and building up to reaches a maximum of approximately 80 mm h⁻¹ between 14 and 16 h of simulation. The mean horizontal surface wind speeds over the domain increase only slightly from 2 up to around 4 m s⁻¹ as the storm develops (Figure 2c), but variations within the domain are large with a maximum one standard deviation range of 3 to 9 m s⁻¹ and strong wind speeds occurring consistently between 6 h and 10 h of simulation (15:00 and 19:00 UTC). Between 3 and 6 h of integration (12:00 to 15:00 UTC), intense vertical wind speeds occur (Figure 2d) and those upward movements will transport DMS into the free troposphere where, after oxidation, it is known to cause new aerosol particle formation (e.g. Raes et al., 1993), with subsequent growth and re-entrainment into the boundary layer of the resulting secondary particles constituting a major source of marine CCN on the global scale (e.g. Korhonen et al., 2008). The sharp variations in horizontal wind speeds will also induce strong variations in the emission of sea-spray particles, since their source function has a cubic dependence on horizontal wind speed (e.g. Gong et al., 2002). Other influences such as changes in sea surface wave state will also influence sea spray emissions (e.g. Grythe et al., 2014), but these effects are not

¹ Global Emissions Inventory Activity: www.geiacenter.org

² Global Fire Emissions Database, Version2: www.globalfiredata.org

resolved in this study. The Gong-Monahan parameterization used here is based on sea spray flux measurements made over a longer time period than the model timestep (30s), and observing capabilities now include eddy covariance sea-spray flux measurements (e.g. Norris et al., 2012), we expect our approach will resolve the dominant sources of sea spray emissions flux variability. Figures 3a-c present the variation in aerosol particle concentrations across the domain at the time of maximum convective instability, i.e. intense updrafts and horizontal wind speeds, with squall lines and associated cold pooling clearly apparent, with very strong particle concentration gradients across the gust fronts, and the gravity currents inducing regions of greatly enhanced sea-spray emission. The strong convective event causes a rapid spin-up of the atmospheric composition in the model, giving an opportunity to assess the variation in aerosol properties across a range of wind speeds during the decay after the storm has subsided. In the next section, these high-resolution spatial variations in size-resolved aerosol properties are explored, examining how the different aerosol sources and processes represented in the simulations influence fluctuations in marine boundary layer CCN concentrations at this convection-permitting resolution.

3 Results

3.1 Gas-to-particle conversion

To aid interpretation and inference from the assessment of aerosol properties in subsequent sections, in this first part of the results we explore how the substantial emission of DMS during the intense storm period propagates through to simulated concentrations of its oxidised forms sulphur dioxide (SO_2) and sulphuric acid (H_2SO_4). Emissions of DMS vary strongly with wind speed and emissions fluxes will therefore be highest between 7 h and 9 h when the peak of the wind speed fluctuations is at maximum. The high emissions lead to a peak in the domain-mean DMS concentration with maximum of ~10 pptm after 9 h of simulations (i.e. at 18:00 UTC). DMS is oxidised by OH during the daytime and by NO_3 at night, both reactions producing SO_2 which, in the gas phase, goes on to form H_2SO_4 vapour following further reaction with OH. Figure 4 illustrates the timescales associated with these processes. The domain-averaged surface SO_2 and H_2SO_4 concentrations are peaking much later than DMS (22 h of simulation, 07:00 UTC, day +1) at respectively ~18 and 6.5×10^{-3} pptm. Given the photochemistry involved, the peak concentration at 07:00 UTC is surprising, but illustrates how atmospheric composition at the surface is strongly influenced by dynamical effects, not just atmospheric chemistry. That the model was still spinning up at this time is greatly beneficial as it helps identify which processes cause the CCN variations and allows to better understand the temporal signatures of the different processes involved. The gas phase H_2SO_4 produced from the emitted DMS is a prerequisite for effective new particle formation and also causes growth of existing particles following vapour condensation, both effects being important sources of marine cloud condensation nuclei (e.g. Korhonen et al., 2008). Although BC and POM are resolved in the model, and UKCA chemistry includes the oxidation of monoterpenes, their emission in this marine domain is negligible. Rather sea spray and DMS-derived sulphate particles are the only two significant particle sources in these simulations.

Hereafter, the analysis focuses on assessing separately the aerosol particles in the different size modes, investigating how the identified driver sources and processes are influencing simulated CCN variations at this convection permitting resolution. The analysis is restricted to the last 12 h of simulation with an emphasis on the results obtained after 18 h of integration, by which time the model has fully spun-up.Indeed, according to the extreme convective instability that induces intense updrafts
5 the spin-up time lasts approximately 6 h.

3.2 Properties of the aerosol fields

In this section, the focus is on quantifying variations in aerosol properties in the three different particle size ranges: Aitken, accumulation and coarse modes. The analysis begins (Figure 3) with instantaneous snapshots of surface aerosol particle concentration and size at two different times in the simulation. Figures 3a-c present a snapshot of spatial variability at 6 h of
10 integration, when ~~an dynamics~~ intense storm period was occurring. Figures 3d-i show the snapshot spatial variation at 18 h of integration, in more modest and representative wind speed conditions but with intense rain rates. The coarse mode consists entirely of sea-spray particles, so highest particle concentrations are expected to generally be indicating regions where simulated horizontal wind speeds are highest. However, during the initial storm period, and at this high spatial
15 resolution, there are also regions of intense localised precipitation (greater than 10 mm h⁻¹) and powerful vertical wind speeds, which will also strongly influence aerosol properties due to removal and transport effects. At 6 h of simulation, Figures 3a-c show that particle concentrations in the two largest modes (accumulation and coarse) are indeed extremely variable over the entire domain. For example, particle concentrations vary from 1 to 1,000 cm⁻³ for the accumulation mode and from 0.1 to 100 cm⁻³ for the coarse mode. Note however that this very high aerosol variability is unrealistically large, being mostly due to the model being initialised with a “warm bubble” to ensure model spin-up proceeds rapidly. However,
20 the period from 12 to 24 hours of integration can be considered to span representative range of wind speed conditions, and we focus on this 2nd half of the day in the rest of the results sections.

Despite the fact that particles in Aitken mode can be affected by the emission of sea spray (e.g., Salter et al., 2015), In this remote marine domain, particles in the Aitken mode are almost exclusively secondary in nature, being originally formed via nucleation in the free troposphere. Over the initial 12 hours, free troposphere concentrations of the driver gas for nucleation,
25 H₂SO₄ are not yet high enough to initiate significant particle formation, with low simulated concentrations of its precursor species SO₂ (see Figure 4) and timescales for oxidation and transport being relative long. After 18 h of simulations, the strongly convective episode has passed, and coarse mode particle concentrations (Figure 3f), although still quite variable,
have more moderate peak concentrations, lower by around a factor of 10 than during the intense storm period (Figures 3c, f).
Accumulation mode particle concentrations at 18 h (Figure 3e) are also much less variable than at 6 h, with highest
30 concentration in the same regions that coarse mode particle concentrations were highest, likely indicating where sea spray emissions are highest (horizontal wind speeds are strongest). Patches of low concentrations are also found where the precipitation is most intense, with the washout rate (impaction scavenging efficiency) tied to rainfall rates. In the Aitken

mode (Figure 3d), particle concentrations have become significant by 18 h, although still an order of magnitude lower than in the accumulation mode. Spatial variations in the size of the aerosol particles ~~are~~ is also highest for the coarse mode (Figure 3i), ~~with regions of highest particle concentration generally corresponding to smaller particles,~~ likely reflecting the nature of the sea spray source function. The general spatial patterns of size variation seen for the coarse mode are also seen for the accumulation mode (Figure 3h) but the accumulation mode has additional regions of lower particle size where Aitken mode particle concentrations are highest (Figure 3d). This co-variation is expected, since the accumulation mode mean radius will be lower, on average, when there are a significant number of smaller particles being chemically cloud processed or mode-merged in from the Aitken mode. Over the domain, mean particle size variations are largest for the Aitken mode at 118% min-to-max ratio (geometric mean radius from 22 to 48 nm), compared to ~20% for the accumulation mode (101 to 123 nm) and ~35% for the coarse mode (0.75 to 1.10 μm).

In Figure 5 we show Hovmöller diagrams to further explore the temporal evolution in surface concentrations of Aitken, accumulation and coarse mode particles during the last 12 h of integration (at $y = 150$ km). Highest particle concentrations from accumulation and coarse modes are apparent between 12 and 15 h of integrations, whereas Aitken mode particle concentrations evolve with quite different time-variation. The convective storm period in the first 12 hours causes very strong wind speeds and the decay of the coarse mode particles concentrations over this second half of the day reflects the progression to calmer conditions, with consequently reduced sea spray emissions but also the intensification of the precipitation (Figure 2) increasing the scavenging process efficiency. By contrast, Aitken particle concentrations are steadily increasing to a maximum of around 1-2 particles per cm^3 after 22 h, matching that seen for SO_2 and gas phase H_2SO_4 (Figure 4), consistent with the timescales of the two oxidation steps required to convert enough of the emitted DMS into sulphuric acid vapour to trigger new particle formation. For particles to reach Aitken sizes, growth by condensation and coagulation is also required, and since nucleation will mostly tend to occur in the free troposphere, any transition to a statically stable boundary layer during late evening would likely also be important, influencing particle entrainment and the timing of the increase in Aitken particle concentrations at the surface. In these idealised simulations however, the short wave and long wave radiation schemes are switched off, there then being no solar-induced diurnal variations in boundary layer entrainment (but photochemical variations proceeding in the model based on local time).

Assessing how each of the size modes is spinning up reveals how temporal variations in marine CCN concentrations are actually reflecting the very different time-profiles of the two dominant CCN production pathways: primary emissions of sea-spray particles and entrainment of DMS-derived secondary particles formed in the free troposphere. The analysis illustrates the way a diverse community of processes (dynamical, chemical and microphysical) together determine CCN variations in the marine boundary layer. Figure 5a shows an Aitken mode emerging after 17 h of integration which also explains the dip in accumulation mode size (contour lines), as a substantial number of smaller secondary particles is being “mode-merged in” from the Aitken mode at that time. For the coarse mode, as particle concentrations decrease, there is also a progression to smaller particles, which can be explained by that fact that, in the model, sedimentation (the dominant removal process for

this mode) removes both number and mass, enabling the simulation to reflect the fact that larger particles fall faster even when they are in the same mode.

A more quantitative analysis of the simulated aerosol properties is presented hereafter, with Figure 6 showing probability density functions (PDFs) of the geometric dry radius (a-c) and particle concentrations (d-f) for the Aitken, accumulation and coarse modes at different times in the 2nd twelve hours of the integration. The analysis shows that, for the accumulation and coarse modes, as seen in Figure 5, as time progresses, the particle size PDFs shift to smaller sizes, with the accumulation mode PDFs becoming much wider in the evening as the source of smaller particles from the Aitken mode becomes significant. By contrast, as Aitken mode concentrations increase, the particles are clearly also larger, reflecting that growth

processes are acting on the particles with this size-increase ceasing at about 18 h of integration, while particle concentrations continue to increase (likely due to entrainment). For the accumulation and coarse mode particles, this quantitative approach is consistent with sedimentation causing the shift in size distribution as the larger particles sediment out faster than the smaller ones. Figure 7 shows the temporal evolution of the mean and standard deviation of the geometric mean radius values and number concentration (over grid boxes in the domain) for Aitken, accumulation and coarse modes at the surface. The accumulation and coarse mode concentration and radius fields have largest spatial variations between 5 and 8 h as the model

adjusts to the very strong sea-salt emission and quite efficient wet removal induced by the precipitation onset during the peak convective activity, whereas Aitken mode concentrations, and their variations, stay approximately constant through that period. During the simulations, the mean radius and particle concentration values from the coarse mode are, on average, decreasing (Figures 7c, f), but the mean size variations show the opposite evolution, with greater variability in the calmer 2nd half of the day, reflecting the strengthening influence of sedimentation as sea-spray emissions decrease. For the accumulation mode, the mean particle size displays remarkably little variation over the domain between 9 and 14 h of simulation (as seen in Figure 6a), with the variation increasing as the source of secondary CCN from the Aitken mode becomes significant later in the day.

3.3 CCN spatial and temporal features

In this marine domain, sea-salt particles represent a major component of the CCN population (e.g. O'Dowd et al., 1997; O'Dowd and de Leeuw, 2007). Models parameterize sea-spray emission fluxes as a function of the 10 m wind speed (u_{10}), with some source functions linked directly to field measurements of the particle concentrations (e.g. Smith et al., 1993) while others (e.g. Monahan et al., 1986) reflect also the processes that form ocean whitecaps, and laboratory experiments on particle emissions. In the simulations presented here, the model uses the sea spray source function of Gong (2003) which applies the approach of Monahan et al. (1986), and its $u^{3.41}$ 10 m-wind-speed dependence, with a refined formulation with an additional parameter determining emission of ultra-fine sea-spray particles, as constrained by field measurements from O'Dowd et al. (1997).

In light of the inference of sea-spray emissions fluxes from measurements of particle concentrations, Figure 8 presents several snapshot variation box-plots for simulated sea-salt emission flux, sea-salt mass mixing ratio (mmr) and the CCN number concentration as a function of the u_{10} (called hereafter surface wind speed) at different integration times. At this convection-permitting resolution, the sea-salt emission fields are highly heterogeneous at each integration time with the 5 emission flux median highest at 12 h of integration then decreasing towards the end of the simulations, consistent with the mean wind speed evolution (Figure 2c). After their emission into the atmosphere, sea-salt aerosols are transported vertically by turbulence, with larger particles also being influenced by sedimentation. As expected, near the surface, the higher are the sea-salt emission fluxes, the higher are the sea-salt mmr, but, as we show below, the co-variation of the sea-salt mmr field with wind speed (Figure 8b) is fundamentally different than it is for sea-salt emission (Figure 8a). Sea-spray particles are 10 highly soluble and are, in most cases, directly emitted at sizes where they are effective CCN, but, as discussed earlier, in marine regions, the CCN population also has a substantial contribution from nucleated sulphate particles which have grown large enough to be CCN-active. Figure 8c shows the variation of CCN concentrations in this marine domain at different integration times and permits to explore how its variation compares to that seen for sea-spray mmr and emissions flux. By 15 sampling the four periods at 12, 15, 18 and 21 h of integration, it is possible to assess the spatial variability in sea-salt emissions, sea-salt concentrations, and CCN concentrations at a range of wind speed conditions; the earliest period 20 representing a strong convective period (i.e. intense wind speeds) when sea-spray would be dominant, and through the progression to calmer conditions later in the simulation. First, the relative change in the median between each period (12-15, 15-18 and 18-21 h) is assessed. As expected, the median sea-salt emission flux (Figure 8a) decreases linearly on the log-log plot over the period, reflecting the 3.41 exponent in the wind-speed-dependence for the sea-spray source function. The relative decrease in sea spray emissions between 12 h and 15 h is reflected also between 15 h and 18 h, and between 18 h and 21 h. By contrast, the median sea-salt mixing ratio (Figure 8b) decreases much more steeply over the 18-21 h period 25 than in the 12-15 h period, despite strong decreases in wind speed. This effect is likely a result of the timescale for the decay from the excited state acquired during the strong convection period (the strong turbulence and direct transport having lifted particles much higher) the atmosphere still “catching up”, with the adjustment to the new calmer conditions only being visible after 18 h of integration. The equivalent temporal decay for CCN concentrations is also curved (Figure 8c), but part 30 of the signal of steeper decline between 18 and 21 h (from the decreased sea-salt) is “straightened out” by the compensating emergence of the secondary nucleated particles making an important contribution to CCN in this later period (as we showed in Figure 7). In the calm conditions, wind speeds across the domain vary (5th to 95th percentile) from ~0.21 to 1.6 m s⁻¹, around a factor of 8, with the CCN concentration range from around 6 to 20 particles per cubic centimetre (a factor of 3). In contrast, during the strongly convective 12-15 h period (i.e. with intense wind speeds and moderate rain rates), the CCN variation is much larger, between 12 and 95 particles per cubic centimetre (a factor of 8).

Figure 9 presents the vertical variation of the simulated CCN concentration using an altitude PDF profile (a-PDF) for the same periods as mentioned above. As expected, on average, the CCN concentration drops-off with increasing altitude

reflecting a balance between turbulence and convection lifting the particles vertically and gravitational settling transporting larger particles back towards the surface. In the atmospheric surface layer (lowest 100 metres or so) the profile of mean CCN follows a power-law profile but the spatial CCN variance (standard deviation over grid boxes in the domain) decreases much less rapidly with altitude. As a consequence, the coefficient of variation increases with increasing altitude from approx. 11% at the surface to approx. 22.5% at 1.3 km height. The CCN concentration fields close to the surface are mainly influenced by the emissions whereas at higher altitudes they are mostly influenced by the transport. This explains why, after 12 h of simulation, the coefficient of variation is slightly higher than at the others times. Note that the emergence of the secondary nucleated particles is also visible in the CCN concentration vertical properties on the 18-21 h period.

4 Conclusions and Discussions

We have analysed spatial and temporal sea-spray and CCN variations in a convection-permitting model with interactive sea-spray emissions, sulphur chemistry and aerosol microphysics over an idealised marine tropical domain. In this marine atmosphere the two dominant CCN sources are both natural: ~~the cloud nuclei population comprising two elements~~ primary sea-spray particles and secondary sulphate particles. However, even in this relatively simple two-component CCN system, our analysis has revealed that there is a diverse community of processes: dynamical, chemical, and microphysical, that together combine to determine the number of particles which can activate to cloud droplets.

First, the dynamics strongly influences the sea-spray emissions since highest particle concentrations occur where wind speeds are highest, and there is a cubic wind speed dependence for sea-salt emission. The emitted sea-spray particles have a range of sizes, being directly emitted in both the accumulation (sub-micron) and coarse (super-micron) modes. After their emission into the atmosphere, sea-salt aerosols are transported vertically by turbulent diffusion and convective updrafts, with larger particles also being influenced by sedimentation. We show that the co-variation of sea-salt mass mixing ratio with wind speed is fundamentally different than that for sea-salt emission, with implications for derivations that treat the two synonymously. In particular, since sub-micron sea-spray has much longer atmospheric residence time (days) than super-micron sea-spray (hours), care must be taken when relating measured sea-spray concentrations to emissions. Intense localised precipitation during strong convection also impacts aerosol concentrations at the climate grid-scale with removal effects introducing strong variations (e.g. via the impaction scavenging process). The combination of these processes impacts the particle concentration properties, which become extremely variable in space (about a factor of 8 over the entire domain, one climate model grid square) and time.

Moreover, the emissions of DMS strongly vary spatially and temporally according to wind speeds conditions and become substantial during intense storm period (as in Devine et al., 2006). There is a requirement for gas phase species SO₂ and H₂SO₄ vapour to be sufficiently produced following oxidation of DMS before new sulphate particle formation in the free troposphere can occur, and the latter species also cause enhanced growth of existing particles following condensation. The combination of the two oxidation steps being required to convert emitted DMS into sulphuric acid vapour, with also the

timescales inherent in particle growth processes (e.g. coagulation and condensation), explain why here is a quite different time-variation for the Aitken mode particle concentrations. Provided the airmass has had sufficient time, a significant proportion of these small secondary particles grow large enough to be cloud processed or mode-merged from the Aitken mode to the accumulation mode. The effects of these processes is illuminated by assessing how each of the particle modes is 5 spinning up, revealing the way they influence spatial- and temporal CCN variations in the marine boundary layer.

Sea-spray particles are highly soluble and, in most cases, are directly emitted at sizes where they are already effective CCN. In contrast, a different component of the CCN population comprises nucleated sulphate particles which need more time to grow large enough to be CCN-active. The variations in the CCN concentrations are strong and can attain a factor of 8 in strongly convective conditions, mostly reflecting the properties of larger CCN. Smaller (sub-micron) CCN, from the 10 accumulation mode, tend to have less variation, which in part is due to their source having a significant contribution from the steady formation of secondary sulphate particles in the free troposphere. We have seen how dynamics and microphysical processes also affect CCN, in particular with a 2nd CCN peak at the top of the boundary layer during the strongly convective period before the secondary particles emerged. These effects combine to determine how the coefficient of variation in CCN concentration changes with altitude, our results suggesting an increase from around 10% at the surface to more than 20% at 15 the top of the marine boundary layer. Whereas CCN concentration fields close to the surface are mainly influenced by the emissions, at higher altitudes they are in general older, and inheriting influences propagated via transport.

We also examine spatial and temporal variations in aerosol particle size, finding that the geometric radius of the Aitken and coarse modes are particularly variable, which will introduce further variability in cloud droplet number concentrations and 20 cloud brightness. The different influences on the two CCN types (primary and secondary), and the diverse community of processes involved (microphysical, chemical and dynamical) makes sub-grid parameterization of the CCN variations difficult. This study provides valuable results on e.g. the impact of the local dynamics and aerosol sources on the CCN population and then on the aerosol-cloud interactions occurring at these fine spatial scales. Work to apply the UM-UKCA model for non-idealised case-studies with a nesting procedure to retain the larger scale influences has now been developed, 25 as is the capability to allow these aerosol variations to couple with a new cloud microphysics scheme in MetUM (Shipway and Hill, 2012).

Acknowledgement. This project was made possible through the financial support of the Leeds-Met Office Academic Partnership (ASCI project). The authors acknowledge use of the MONSooN system, a collaborative facility supplied under the Joint Weather and Climate Research Programme, which is a strategic partnership between the Met Office and the Natural 30 Environment Research Council. The lead author wishes to thank Douglas Parker for useful discussions. G. W. Mann is funded by the UK National Centre for Atmospheric Science, one of the UK Natural Environment Research Council (NERC) research centres. J. Marsham acknowledges funding from the SAMMBA project (NE/J009822/1).

References

Adams, P. J., and Seinfeld, J. H.: Predicting global aerosol size distributions in general circulation models, *J. Geophys. Res.*, 107, D19, 4370, 2002.

Archer-Nicholls, S., Lowe, D., Schultz, D. M., and McFiggans, G.: Aerosol–radiation–cloud interactions in a regional
5 coupled model: the effects of convective parameterisation and resolution, *Atmos. Chem. Phys.*, 16, 5573–5594, 2016.

Bangert, M., Kottmeier, C., Vogel, B., and Vogel, H.: Regional scale effects of the aerosol cloud interaction simulated with
an online coupled comprehensive chemistry model, *Atmos. Chem. Phys.*, 11, 4411–4423, 2011.

Bellouin, N., Mann, G. W., Woodhouse, M. T., Johnson, C., Carslaw, K. S., and Dalvi, M.: Impact of the modal aerosol
scheme GLOMAP-mode on aerosol forcing in the Hadley Centre Global Environmental Model, *Atmos. Chem. Phys.*, 13,

10 3027–3044, 2013.

Boucher, O., Randall, D., Artaxo, P., Bretherton, C., Feingold, G., Forster, P., Kerminen, V.-M., Kondo, Y., Liao, H.,
Lohmann, U., Rasch, P., Satheesh, S. K., Sherwood, S., Stevens, B., and Zhang, X. Y.: Clouds and aerosols. In: Climate
Change 2013: The physical basis. Contribution of working group I to the Fifth Assessment Report of the
Intergovernmental Panel on Climate Change [Stocker, T., F., Qin, D., Plattner, G.-K., Tignor, M., Allen, S. K.,
15 Boschung, J., Nauels, A., Xia, Y., Bex, V., and Midgley, P. M. (eds.)], Cambridge University Press, Cambridge, United
Kingdom and New York, NY, USA, 2013.

Carslaw, K. S., Lee, L. A., Reddington, C. L., Pringle, K. J., Rap, A., Forster, P. M., Mann, G. W., Spracklen, D. V.,
Woodhouse, M. T., Regayre, L. A., and Pierce, J. R.: Large contribution of natural aerosols to uncertainty in indirect
forcing, *Nature*, 503, 67–71, 2013.

20 Cui, Z., Davies, S., Carslaw, K. S., and Blyth, A. M.: The response of precipitation to aerosol through riming and melting in
deep convective clouds, *Atmos. Chem. Phys.*, 11, 3495–3510, 2011.

Devine, G. M., Carslaw, K. S., Parker, D. J., and Petch, J. C.: The influence of subgrid surface-layer variability on vertical
transport of a chemical species in a convective environment, *Geophys. Res. Lett.*, 33, 2006.

Ekman, A., Wang, C., Wilson, J., and Ström, J.: Explicit simulations of aerosol physics in a cloud-resolving model: a
25 sensitivity study based on an observed convective cloud. *Atmos. Chem. Phys.*, 4, 773–791, 2004.

Ekman, A., Wang, C., Ström, J., and Krejci, R.: Explicit simulation of aerosol physics in a cloud-resolving model: Aerosol
transport and processing in free troposphere, *J. Atmos. Sci.*, 63, 682–695, 2006.

Forster, P., Ramaswamy, V., Artaxo, P., Berntsen, T., Betts, R., Fahey, D. W., Haywood, J., Lean, J., Lowe, D. C., Myhre,
G., Nganga, J., Prinn, R., Raga, G., Schulz, M., and Van Dorland, R.: Changes in atmospheric constituents and in
30 radiative forcing. Chapter: Climate Change 2007: The Physical Science Basis. In: Contribution of Working Group I to
Fourth Assessment Report of the Intergovernmental Panel on Climate Change Cambridge University Press, Cambridge,
UK and New York, USA, 129–234, 2007.

Ghan, S. J., Easter, R. C., Chapman, E. G., Abdul-Razzak, H., Zhang, Y., Leung, L. R., Laulainen, N. S., Saylor, R. D., and Zaveri, R. A.: A physically based estimate of radiative forcing by anthropogenic sulphate aerosol, *J. Geophys. Res.*, 106, 5279-5293, 2001.

Gong, S. L., Barrie, L. A., and Lazare, M.: Canadian Aerosol Module (CAM): A size-segregated simulation of atmospheric aerosol processes for climate and air quality models. 2. Global sea-salt aerosol and its budgets, *J. Geophys. Res.*, 107, D244779, 2002.

Gong, S. L.: A parameterization of sea-salt aerosol source function for sub- and super-micron particles, *Global Biogeochem. Cycles.*, 14, 1097-1103, 2003.

Gregory, D., and Rowntree, P. R.: A mass flux convection scheme with representation of cloud ensemble characteristics and stability-dependent closure, *Mon. Wea. Rev.*, 118, 1483-1506, 1990.

Grythe H., Ström, J., Krejci, R., Quinn, P. and Stohl, A., A review of sea-spray aerosol source functions using a large global set of sea salt aerosol concentration measurements, *Atmos. Chem. Phys.*, 14, 1277–1297, 2014.

Jones, C. D., Hughes, J. K., Bellouin, N., Hardiman, S. C., Jones, G. S., Knight, J., Liddicoat, S., O'Connor, F. M., Andres, R. J., Bell, C., Boo, K.-O., Bozzo, A., Butchart, N., Cadule, P., Corbin, K. D., Doutriaux-Boucher, M., Friedlingstein, P., Gornall, J., Gray, L., Halloran, P. R., Hurt, G., Ingram, W. J., Lamarque, J.-F., Law, R. M., Meinshausen, M., Osprey, S., Palin, E. J., Parsons Chini, L., Raddatz, T., Sanderson, M. G., Sellar, A. A., Schurer, A., Valdes, P., Woodward, N., Woodward, S., Yoshioka, M., and Zerroukat, M.: The HadGEM2-ES implementation of CMIP5 centennial simulations, *Geosci. Model Dev.*, 4, 543-570, 2011.

Kaufman, Y. J., Koren, I., Remer, L. A., Rosenfeld, D., and Rudich, Y.: The effect of smoke, dust, and pollution aerosol on shallow cloud development over the Atlantic Ocean, *Proc. Natl. Acad. Sci. USA.*, 102, 11207–11212, 2005.

Korhonen, H., Carslaw, K. S., Spracklen, D. V., Mann, G. W., and Woodhouse, M. T.: Influence of oceanic DMS emissions on CCN concentrations and seasonality over the remote Southern Hemisphere oceans: A global model study, *J. Geophys. Res.*, 113, D15204, 2008.

Lamarque, J.-F., Bond, T. C., Eyring, V., Granier, C., Heil, A., Klimont, Z., Lee, D., Liousse, C., Mieville, A., Owen, B., Schultz, M., G., Shindell, D., Smith, S., J., Stehfest, E., van Aardenne, J., Cooper, O. R., Kainuma, M., Mahowald, N., McConnell, J. R., Naik, V., Riahi, K., and van Vuuren, D. P.: Historical (1850–2000) gridded anthropogenic and biomass burning emissions of reactive gases and aerosols: methodology and application, *Atmos. Chem. Phys.*, 10, 7017-7039, 2010.

Lohmann, U., and Feichter, J.: Global indirect aerosol effects: a review, *Atmos. Chem. Phys.*, 5, 715-737, 2005.

Mann, G. W., Carslaw, K. S., Spracklen, D. V., Ridley, D. A., Manktelow, P. T., Chipperfield, M. P., Pickering, S. J., and Johnson, C. E.: Description and evaluation of GLOMAP-mode: a modal global aerosol microphysics model for the UKCA composition-climate model, *Geosci. Model Dev.*, 3, 519-551, 2010.

Mann, G. W., Carslaw, K. S., Ridley, D. A., Spracklen, D. V., Pringle, K. J., Merikanto, J., Korhonen, H., Schwarz, J. P., Lee, L. A., Manktelow, P. T., Woodhouse, M. T., Schmidt, A., Breider, T. J., Emmerson, K. M., Reddington, C. L.,

Chipperfield, M. P., and Pickering, S. J.: Inter-comparison of modal and sectional aerosol microphysics representations within the same 3-D global chemical transport model, *Atmos. Chem. Phys.*, 12, 4449-4476, 2012.

Mann, G. W., Carslaw, K. S., Reddington, C. L., Pringle, K. J., Schulz, M., Asmi, A., Spracklen, D. V., Ridley, D. A., Woodhouse, M. T., Lee, L. A., Zhang, K., Ghan, S. J., Easter, R. C., Liu, X., Stier, P., Lee, Y. H., Adams, P. J., Tost, H.,
5 Lelieveld, J., Bauer, S. E., Tsigaridis, K., Van Noije, T. P., C., Strunk, A., Vignati, E., Bellouin, N., Dalvi, M., Johnson, C. E., Bergman, T., Kokkola, H., Von Salzen, K., Yu, F., Luo, G., Petzold, A., Petzold, A., Heintzenberg, J., Clarke, A., Ogren, J. A., Gras, J., Baltensperger, U., Kaminski, U., Jennings, S. G., O'Dowd, C. D., Harrison, R. M., Beddows, D. C. S., Kulmala, M., Viisanen, Y., Ulevicius, V., Mihalopoulos, N., Zdimal, V., Fiebig, M., Hansson, H. C., Swietlicki, E., and Henzing, J. S.: Intercomparison and evaluation of global aerosol microphysical properties among AeroCom models
10 of a range of complexity, *Atmos. Chem. Phys.*, 14, 4679-4713, 2014.

Marsham, J. H., Knippertz, P., Dixon, N., Parker, D. J., and Lister, G. M. S.: The importance of the representation of deep convection for modeled dust-generating winds over West Africa during summer, *Geophys. Res. Lett.*, 38, L16803, 2011.

Marsham, J. H., Dixon, N., Garcia-Carreras, L., Lister, G. M. S., Parker, D. J., Knippertz, P., and Birch, C.E.: The role of moist convection in the West African monsoon system - insights from continental-scale convection-permitting
15 simulations, *Geophys. Res. Lett.*, 40, 1843-1849, 2013.

Monahan, E. C., Spiel, D. E., and Davidson, K. L.: A model of marine aerosol generation via whitecaps and wave disruption. Oceanic Whitecaps. Edited by EC Monahan and G MacNiochaill, pp 167-193, D Reidel, Norwell, Mass, 1986.

Morrison, H., Thompson, G., and Tatarkii, V.: Impact of cloud microphysics on the development of trailing stratiform precipitation in a simulated squall line: comparison of one- and two-moment schemes, J. Atmos. Sci., 137, 991–1007, 2009.

Myhre, G., Samset, B. H., Schulz, M., Balkanski, Y., Bauer, S., Berntsen, T. K., Bian, H., Bellouin, N., Chin, M., Diehl, T., Easter, R. C., Feichter, J., Ghan, S. J., Hauglustaine, D., Iversen, T., Kinne, S., Kirkevåg, A., Lamarque, J.-F., Lin, G., Liu, X., Lund, M. T., Luo, G., Ma, X., van Noije, T., Penner, J. E., Rasch, P. J., Ruiz, A., Seland, Ø., Skeie, R. B., Stier, P., Takemura, T., Tsigaridis, K., Wang, P., Wang, Z., Xu, L., Yu, H., Yu, F., Yoon, J.-H., Zhang, K., Zhang, H., and Zhou, C.: Radiative forcing of the direct aerosol effect from AeroCom Phase II simulations, *Atmos. Chem. Phys.*, 13, 1853-1877, 2013.

Norris, S. J., Brooks, I. M., Hill, M. K. Brooks, B. J., Smith, M. H., Sproson, D. A. J.: Eddy covariance measurements of the sea spray aerosol flux over the open ocean, J. Geophys. Res., vol. 117, doi:10.1029/2011JD016549, 2012

O'Connor, F. M., Johnson, C. E., Morgenstern, O., Abraham, N. L., Braesicke, P., Dalvi, M., Folberth, G. A., Sanderson, M. G., Telford, P. J., Young, P. J., Zeng, G., Collins, W. J., and Pyle, J. A.: Evaluation of the new UKCA climate-composition model - Part 2: The Troposphere, *Geosci. Model Dev.*, 7, 41-91, 2014.

O'Dowd, C. D., Smith, M. H., Consterdine, I. E., and Lowe, J. A.: Marine aerosol, sea salt, and the marine sulphur cycle: a short review, *Atmos. Environ.*, 31, 73-80, 1997.

O'Dowd, C. D., and de Leeuw, G.: Marine aerosol production: a review of the current knowledge, Phil. Trans. R. Soc. A, 365, 1753-1774, 2007.

5
[Planche, C., Marsham, J., Field, P., Carslaw, K., Hill, A., Mann, G., and Shipway, B.: Precipitation sensitivity to autoconversion rate in a Numerical Weather Prediction Model, Q. J. R. Meteorol. Soc., 141, 2032-2044, DOI: 10.1002/qj.2497, 2015.](#)

Pope, R. J., Marsham, J. H., Knippertz, P., Brooks, M. E., and Roberts, A. J.: Identifying errors in dust models from data assimilation, Geophys. Res. Lett., 43, doi:10.1002/2016GL070621, 2016.

[Possner A., Zubler, E. M., Lohmann, U., and Schär, C.: The resolution dependence of cloud effects and ship-induced aerosol-cloud interactions in marine stratocumulus, J. Geophys. Res. Atmos., 121, 4810–4829, 2016.](#)

10 Raes, F., Van Dingenen, R., Wilson, J., and Saltelli, A.: Cloud condensation nuclei from dimethyl sulphide in the natural marine boundary layer: Remote vs. in-situ production, in Dimethyl Sulphide: Oceans, Atmosphere and Climate, edited by G. Restelli and G. Angeletti, pp. 311-322, Kluwer, Acad., Norwell, Mass., 1993.

[Salter, M. E., Zieger, P., Acosta Navarro, J. C., Grythe, H., Kirkevåg, A., Rosati, B., Riipinen, I., and Nilsson, E. D.: An empirically derived inorganic sea spray source function incorporating sea surface temperature, Atmos. Chem. Phys., 15, 11047-11066, doi:10.5194/acp-15-11047-2015, 2015.](#)

15 Shipway, B. J., and Hill, A. A.: Diagnosis of systematic differences between multiple parameterizations of warm rain microphysics using a kinematic framework, Quart. J. Roy. Meteor. Soc., 138, 2196-2211, 2012.

Smith, M. H., Park, P. M., and Consterdine, I. E.: Marine aerosol concentrations and estimated fluxes over the sea, Q. J. R. Meteorol. Soc., 119, 809–824, 1993.

20 Spracklen, D. V., Pringle, K. J., Carslaw, K. S., Chipperfield, M. P., and Mann, G. W.: A global offline model of size-resolved aerosol microphysics: I. Model development and prediction of aerosol properties, Atmos. Chem. Phys., 5, 2227-2252, 2005.

25 Walters, D. N., Williams, K. D., Boutle, I. A., Bushell, A. C., Edwards, J. M., Field, P. R., Lock, A. P., Morcrette, C. J., Stratton, R. A., Wilkinson, J. M., Willett, M. R., Bellouin, N., Bodas-Salcedo, A., Brooks, M. E., Copsey, D., Earnshaw, P. D., Hardiman, S. C., Harris, C. M., Levine, R. C., MacLachlan, C., Manners, J. C., Martin, G. M., Milton, S. F., Palmer, M. D., Roberts, M. J., Rodríguez, J. M., Tennant, W. J., and Vidale, P. L.: The Met Office Unified Model Global Atmosphere 4.0 and JULES Global Land 4.0 configurations, Geosci. Model Dev., 7, 361-386, 2014.

Wang, M., Ghan, S., Ovchinnikov, M., Liu, X., Easter, R., Kassianov, E., Qian, Y., and Morrison, H.: Aerosol indirect effects in a multi-scale aerosol-climate model PNNL-MMF, Atmos. Chem. Phys., 11, 5431-5455, 2011.

30 [Weigum, N., Schutgens, N., and Stier, P.: Effect of aerosol subgrid variability on aerosol optical depth and cloud condensation nuclei: implications for global aerosol modelling, Atmos. Chem. Phys., 16, 13619-13639, doi:10.5194/acp-16-13619-2016, 2016.](#)

Wilkinson, J. M., Porson, A. N. F., Bornemann, F. J., Weeks, M., Field, P. R., and Lock, A. P.: Improved microphysical parametrization of drizzle and fog for operational forecasting using the Met Office Unified Model, Q. J. R. Meteorol. Soc., 139, 488–500, DOI: 10.1002/qj.1975, 2012.

Wilson, D. R., and Ballard, S. P.: A microphysically based precipitation scheme for the UK Meteorological Office Unified
5 Model. Quart. J. Roy. Meteor. Soc. 125, 1607–1636, 1999.

Woodward, S.: Modeling the atmospheric life cycle and radiative impact of mineral dust in the Hadley Centre climate model, J. Geophys. Res., 106(D16), 18115–18166, 2001.

Yang, Q., W. I. Gustafson Jr., Fast, J. D., Wang, H., Easter, R. C., Morrison, H., Lee, Y.-N., Chapman, E. G., Spak, S. N., and Mena-Carrasco, M. A.: Assessing regional scale predictions of aerosols, marine stratocumulus, and their interactions during VOCALS-REx using WRF-Chem, Atmos. Chem. Phys., 11, 11951-11975, doi:10.5194/acp-11-11951-2011, 2011.

Yang, Q., Gustafson Jr., W. I., Fast, J. D., Wang, H., Easter, R. C., Wang, M., Ghan, S. J., Berg, L. K., Leung, L. R., and Morrison, H.: Impact of natural and anthropogenic aerosols on stratocumulus and precipitation in the Southeast Pacific: a regional modelling study using WRF-Chem, Atmos. Chem. Phys., 12, 8777–8796, 2012.

15 Yin, Y., Chen, Q., Jin, L., Chen, B., Zhu, S., and Zhang, X.: The effects of deep convection on the concentration and size distribution of aerosol particles within the upper troposphere: A case study, J. Geophys. Res., 117, D22202, 2012.

Zubler, E. M., Folini, D., Lohmann, U., Lüthi, D., Schär, C., and Wild, M.: Simulation of dimming and brightening in Europe from 1958 to 2001 using a regional climate model, J. Geophys. Res., 116, D18205, 2011.

Table 1. Standard aerosol configuration for GLOMAP-mode. The size distribution is described by lognormal modes with varying geometric mean diameter D and fixed geometric standard deviation σ_g . Particle number and mass are transferred between modes when D exceeds the upper limit for the mode. Names are given in function of the aerosols mode ('nuc', 'Ait', 'acc' and 'coa' are for 'nucleation', 'Aitken', 'accumulation' and 'coarse') and their solubility properties ('sol' and 'ins' mean the aerosols are soluble or insoluble). The aerosols can be composed of sulphate (SU), primary organic matter (POM), black carbon (BC), or sea-salt (SS).

Index	Name	Size range	Composition	Soluble	σ_g
1	nucsol	$D < 10 \text{ nm}$	SU, POM	yes	1.59
2	Aitsol	$10 \text{ nm} < D < 100 \text{ nm}$	SU, BC, POM	yes	1.59
3	accesol	$100 \text{ nm} < D < 1 \mu\text{m}$	SU, BC, POM, SS	yes	1.59
4	coasol	$D > 1 \mu\text{m}$	SU, BC, POM, SS	yes	2.00
5	Aitins	$10 \text{ nm} < D < 100 \text{ nm}$	BC, POM	no	1.59

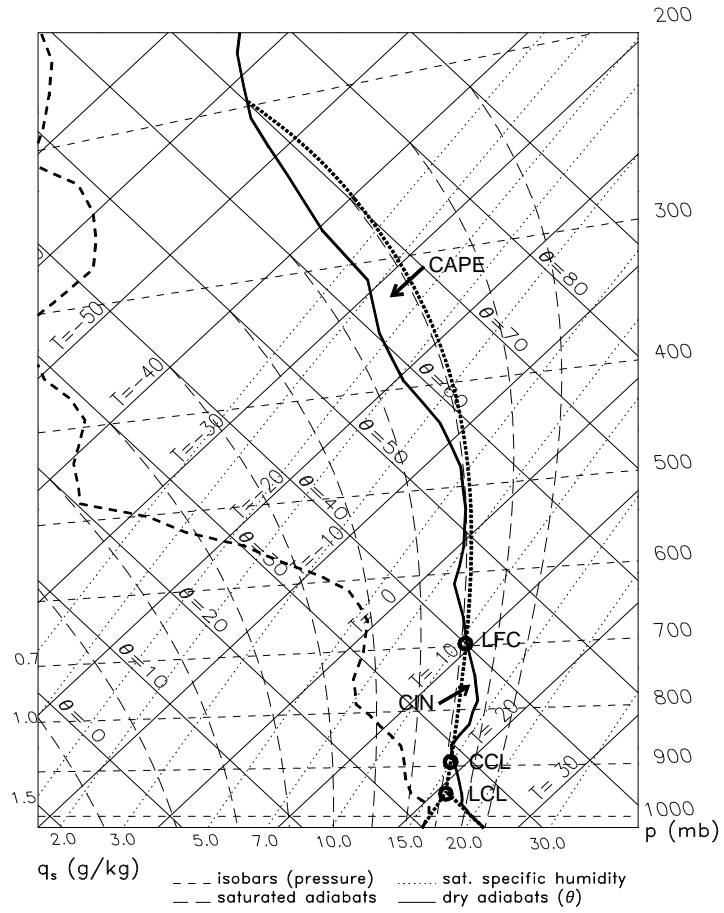


Figure 1. Tephigram representing the vertical profile of the initial dew point temperature (dashed line) and the temperature (solid line). The thick dotted line represents the adiabatic parcel ascent and the circles indicate the specific levels of the parcel such as the Lifted Condensation Level (LCL), the Convective Condensation Level (CCL) and the Level of Free Convection (LFC).

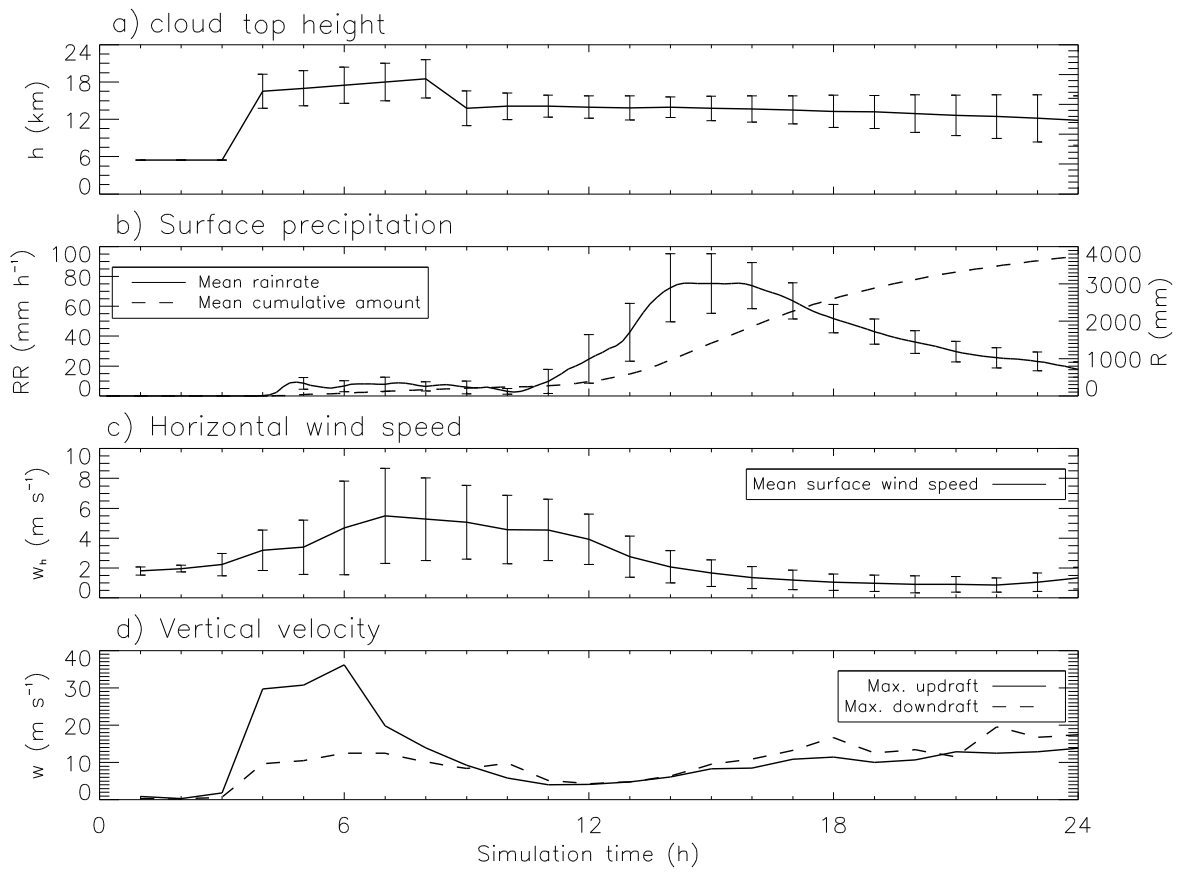


Figure 2. Temporal evolution of (a) the mean ~~total~~ top-cloud top height, (b) the mean accumulated rain accumulation and rain rate at the surface, (c) the mean surface horizontal wind speed and (d) the maximum of the updrafts and downdrafts. The averages are obtained over the entire grid points of the domain and given with \pm standard deviation.

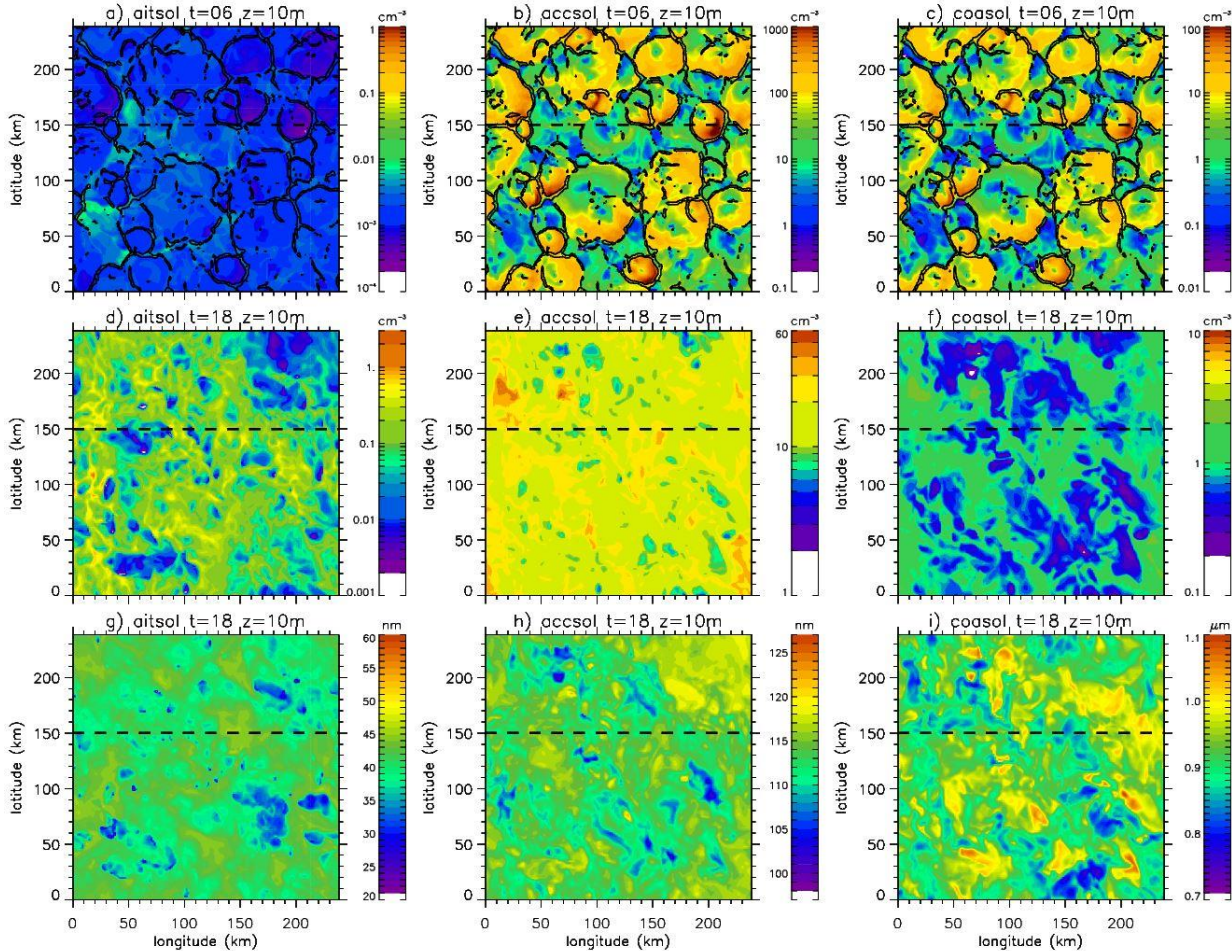


Figure 3. Snapshot spatial variations in the number concentrations (a-f) and geometric-mean radius (g-i) of the aerosol particles in the Aitken (aitsol; a, d, g), accumulation (accsol; b, e, h) and coarse (coasol; c, f, i) soluble modes after 6 h (in model spin-up) (a-c) and 18 h (d-i) of integration. The black solid lines represent the surface vertical wind speed ($w = 5 \text{ m s}^{-1}$). Note that the colour scales are different. The dashed lines correspond to the transects shown in Figures 5 and 9.

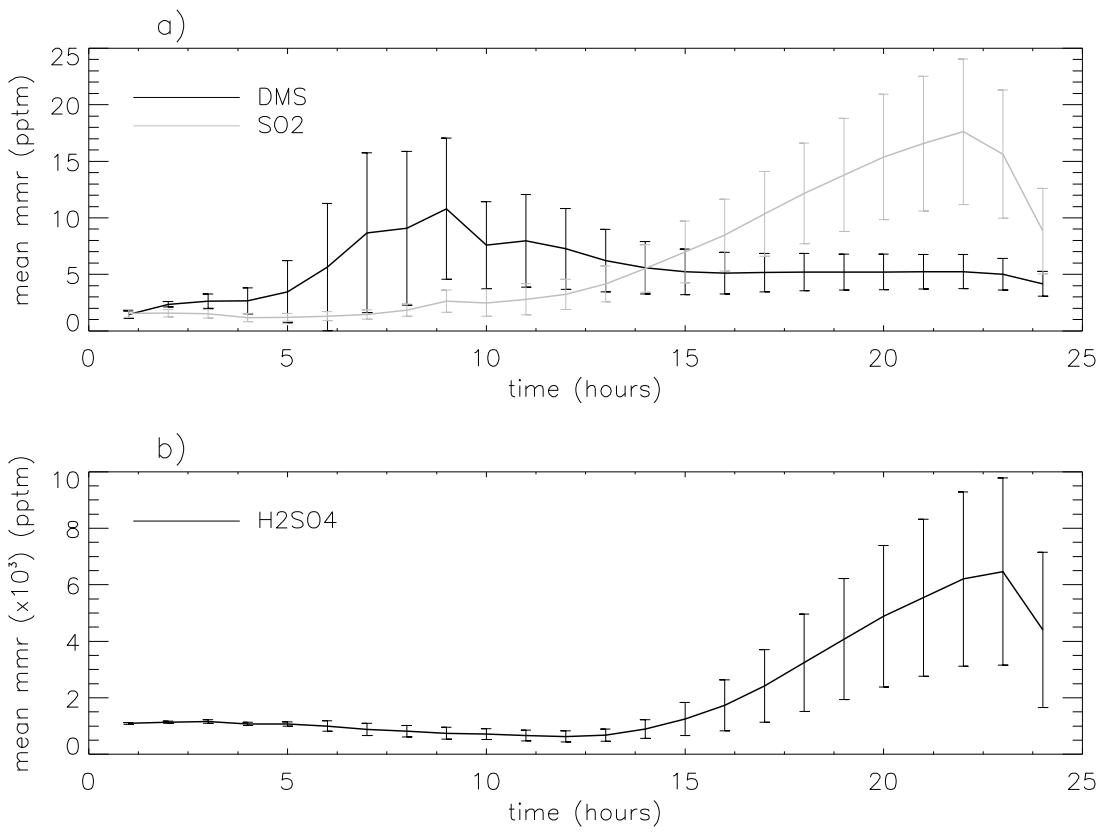


Figure 4. Temporal evolution of the mean mass mixing ratios of the gas precursors to aerosols. The DMS, SO₂ and H₂SO₄ mass concentrations are in pptm (part per trillion in mass). The error bars correspond to \pm one standard deviation.

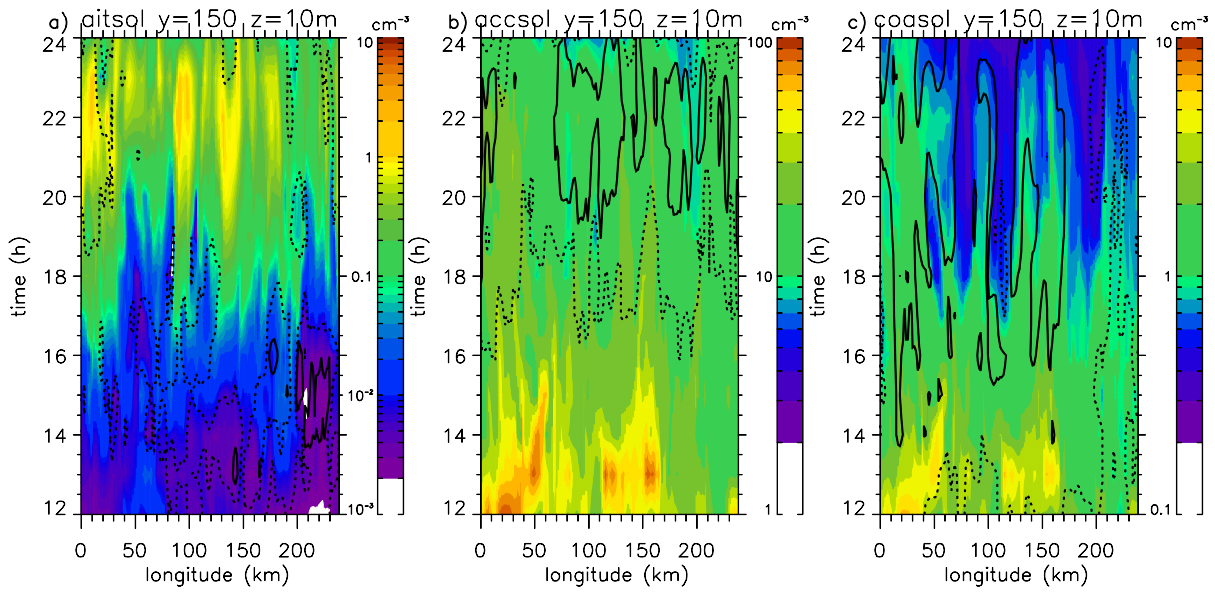


Figure 5. Temporal evolution of the aerosol concentration from the Aitken (a), accumulation (b) and coarse (c) soluble mode after the model spin-up. Temporal evolution of the aerosol dry radius is also illustrated for the 3 modes: 30 (dashed line) and 35 nm (solid line) for the Aiken soluble mode, 110 (solid line) and 115 nm (dashed line) for the accumulation soluble mode; 5 and 0.96 (solid line) and 1.0 μm (dashed lines) for coarse soluble mode. Note that the colour scales are different.

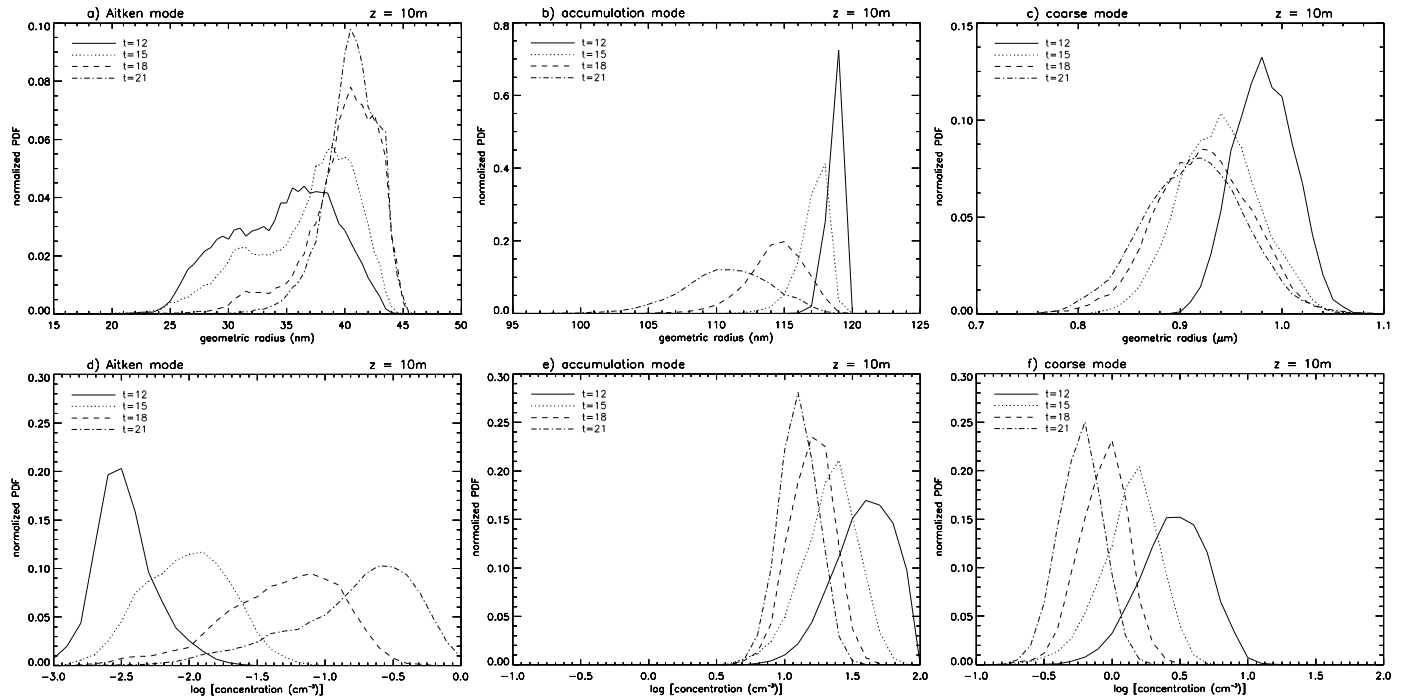


Figure 6. Normalized Probability Density Function (PDF) of the geometric radius (a, b, c) and the logarithm of the concentration (d, e, f) of the surface aerosols from the Aitken (a, d), accumulation (b, e) and coarse (c, f) soluble modes obtained at different integration time.

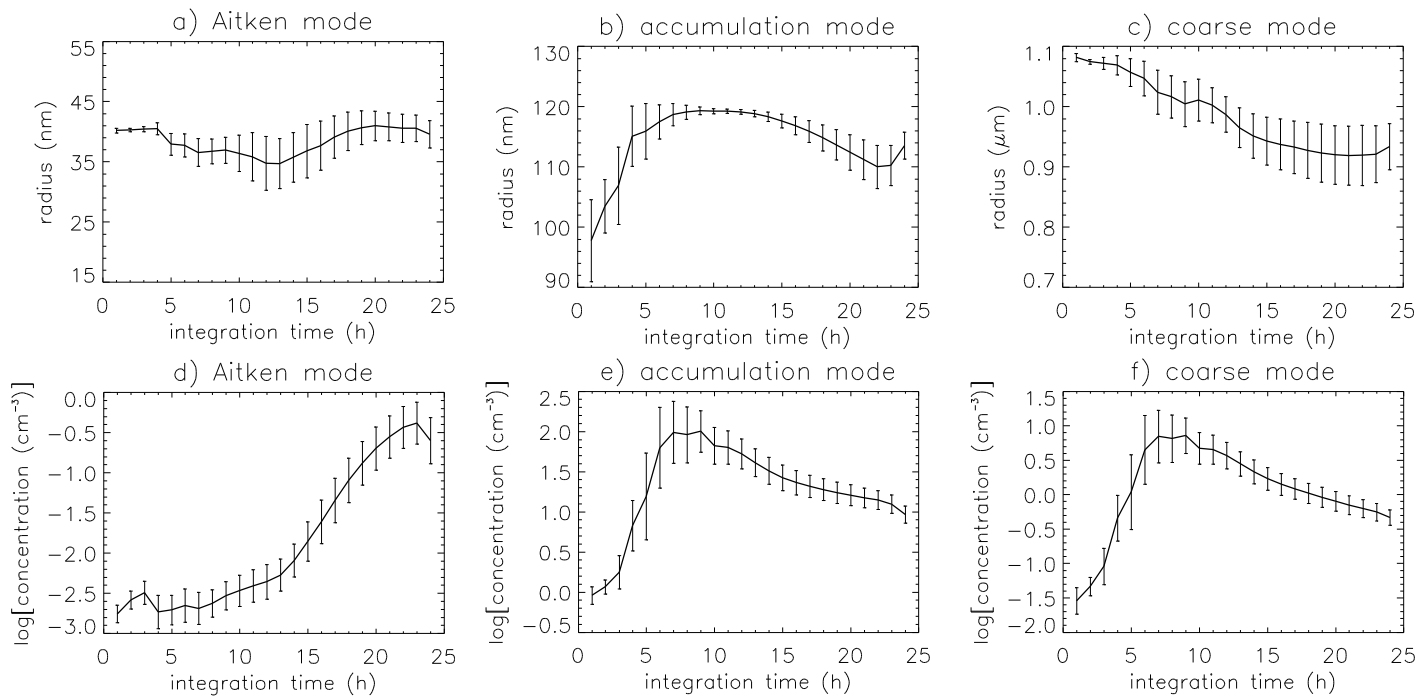


Figure 7. The series of the mean \pm one standard deviation of the geometric radius (a, b, c) and the logarithm of the concentration (d, e, f) of the surface aerosols from the Aitken (a, d), accumulation (b, e) and coarse (c, f) soluble modes.

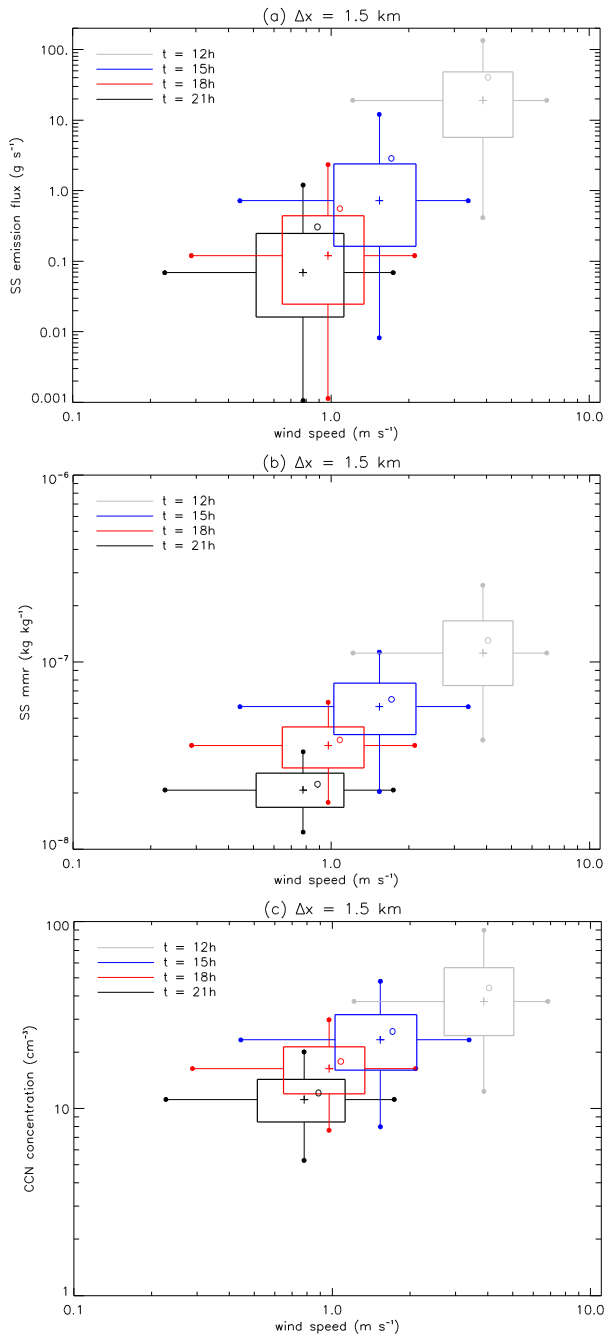


Figure 8. 2D-distribution of the surface sea-salt emission flux (a), sea-salt mass mixing ratio (mmr) (b) and CCN concentration (c) as a function of the surface horizontal wind for 4 different integration times ($t = 12, 15, 18$ or 21h). The hinges of the box-plots represent the 25th and 75th percentiles and the ends of the whiskers (full circles) represent the 5th and 95th percentiles. The ‘plus’ symbols represent the median values. The empty circles show the mean values over the domain.

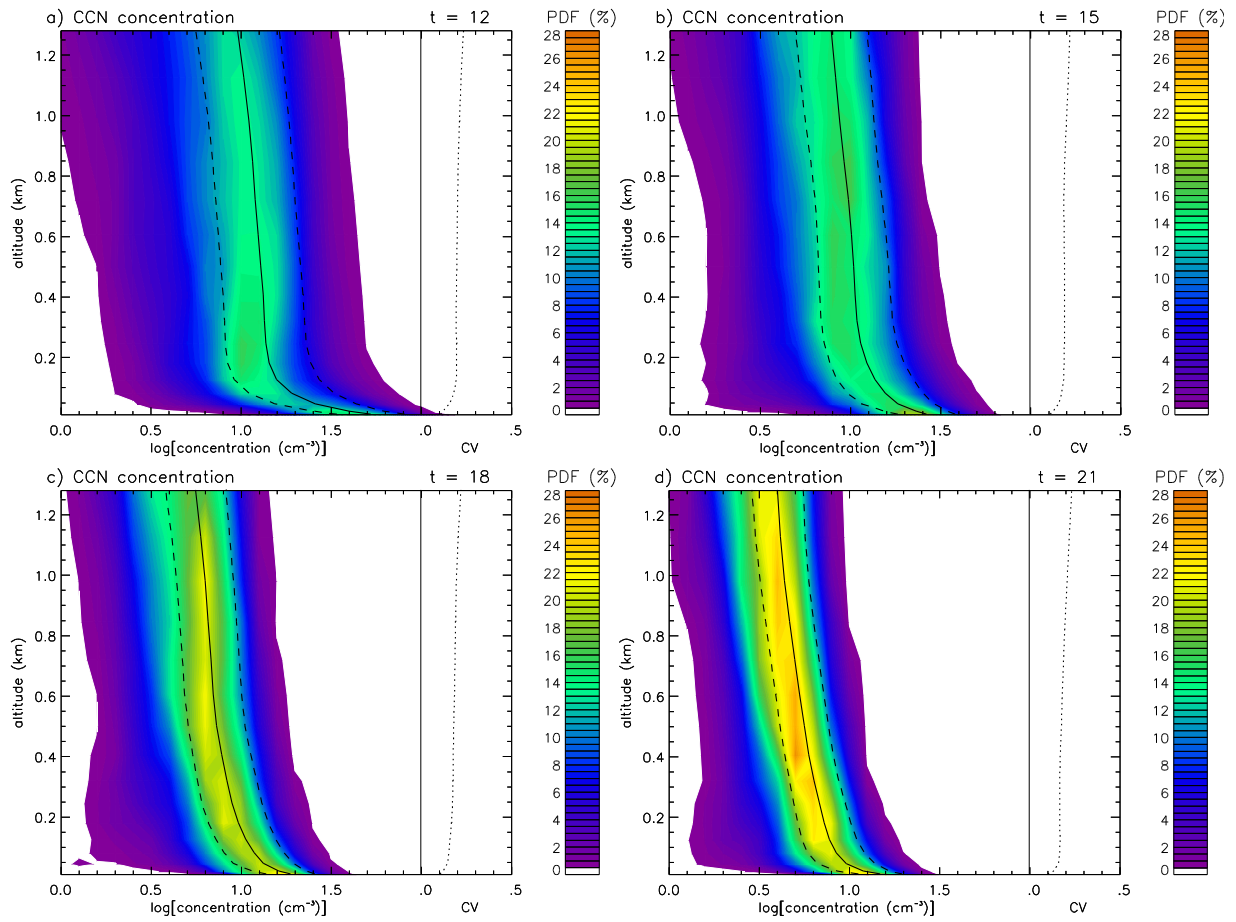


Figure 9. Altitude-dependent Probability Density Function (a-PDF) in percent of the CCN concentration at different integration times. The a-PDF are obtained calculating the PDF for each different level. A resolution of 0.1 is used for quantifying the logarithm of the concentration. The lines represent the mean (solid lines) \pm one standard deviation (dashed lines) 5 of the CCN concentration. The dotted lines represent the coefficient of variation (CV) which is defined as the ratio of the standard deviation to the mean of the CCN concentration.

Spatial and temporal CCN variations in convection-permitting aerosol microphysics simulations in an idealised marine tropical domain

Céline Planche^{1,*}, Graham W. Mann^{1,2}, Kenneth S. Carslaw¹, Mohit Dalvi³, John H. Marsham^{1,2}, and

5 Paul R. Field^{1,3}

¹ School of Earth and Environment, University of Leeds, Leeds, United Kingdom

² National Centre for Atmospheric Science, United Kingdom

³ Met Office, Exeter, United Kingdom

*Now at: Université Clermont Auvergne, Laboratoire de Météorologie Physique, OPGC/CNRS UMR 6016, Clermont-Ferrand, France

Correspondence to: Céline Planche (celine.planche@uca.fr) and Graham Mann (G.W.Mann@leeds.ac.uk)

Abstract. A convection-permitting limited area model with periodic lateral boundary conditions and prognostic aerosol microphysics is applied to investigate how concentrations of cloud condensation nuclei (CCN) in the marine boundary layer are affected by high resolution dynamical and thermodynamic fields. The high-resolution aerosol microphysics–dynamics

15 model, which resolves differential particle growth and aerosol composition across the particle size range, is applied on a domain designed to match approximately a single grid square of a climate model. We find that, during strongly convective conditions with intense wind-speed conditions, CCN concentrations vary by more than a factor of 8 across the domain (5th-

95th percentile range), and a factor of ~3 at more moderate wind-speed conditions. One reason for these large sub-climate-grid-scale variations in CCN is that emissions of sea-salt and DMS are much higher when spatial and temporal wind speed

20 fluctuations become resolved at this convection-permitting resolution (making peak wind speeds higher). By analysing how the model evolves during spin-up, we gain new insight into the way primary sea-salt and secondary sulphate particles contribute to the overall CCN variance in these realistic conditions, and find a marked difference in the variability of super-micron and sub-micron CCN. Whereas the super-micron CCN are highly variable, being dominated by strongly fluctuating emitted sea-spray, the sub-micron CCN tend to be steadier, being mainly produced on longer timescales following growth

25 after new particle formation in the free troposphere, with fluctuations inherently buffered by the fact that coagulation is faster at higher particle concentrations. We also find that sub-micron CCN are less variable in particle size, the accumulation mode mean size varying by ~20% (0.101 to 0.123 µm diameter) compared to ~35% (0.75 to 1.10 µm diameter) for coarse mode particles at this resolution. We explore how the CCN variability changes in the vertical, and at different points in the

30 spin-up, showing how CCN concentrations are introduced both by the emissions close to the surface, and at higher altitudes during strongly convective wind-speed conditions associated to the intense convective period. We also explore how the non-linear variation of sea-salt emissions with wind speed propagates into variations in sea-salt mass mixing ratio and CCN

concentrations, finding less variation in the latter two quantities due to the longer transport timescales inherent with finer CCN, which sediment more slowly. The complex mix of sources and diverse community of processes involved makes sub-grid parameterization of CCN variations difficult. However, the results presented here illustrate the limitations of predictions with large-scale models and the high-resolution aerosol-dynamics modelling system shows promise for future studies where
5 the aerosol variations will propagate through to modified cloud microphysical evolution.

Keywords. Aerosol particles, CCN variability, UKCA, GLOMAP-mode, sub-climate scale, idealised marine tropical case.

1 Introduction

Aerosol particles affect the Earth's climate system directly by scattering and absorbing short-wave and long-wave radiation and indirectly by influencing the albedo and lifetime of clouds (e.g. Lohmann and Feichter, 2005). Successive IPCC climate
10 assessment reports (e.g. Forster et al., 2007; Myhre et al., 2013) have identified the radiative forcing due to aerosol-climate interactions as having a high level of uncertainty that needs to be better constrained for improved prediction of anthropogenic climate change.

Atmospheric aerosols, whether natural or anthropogenic, originate from two different pathways: directly emitted "primary particles" (e.g. sea-spray, in marine environments) and secondary particles, which are formed by nucleation, often first
15 requiring oxidation of gaseous precursors such as dimethyl sulphide (DMS). In general, the primary particle population can be straightforwardly classified into natural (dust, sea-spray, primary biogenic) or anthropogenic (e.g. carbonaceous particles from fossil-fuel combustion sources). However, this classification is not possible for secondary particles because of the complex interactions and influences of gases with both natural and anthropogenic sources (such as sulphur dioxide) and the moderating influence of additional semi-volatile species such as ammonia and nitric acid. In the marine boundary layer
20 however, the dominant two sources of cloud condensation nuclei (CCN) are DMS and sea-spray (e.g. Raes et al., 1993; O'Dowd and de Leeuw, 2007; Boucher et al., 2013) and the relative simplicity of this particular compartment of the atmosphere allows the systematic assessment of how two types of natural particles: primary sea-spray and secondary sulphate particles from DMS, influence aerosol-cloud interactions. Carslaw et al. (2013) highlight the importance of quantifying such natural aerosols in order to accurately characterise the anthropogenic radiative forcing via aerosol-cloud
25 interactions.

Until recently, computational costs have tended to constrain most climate models participating in international climate assessment reports to treat aerosol-cloud interactions in a simplified way, with only the mass of several aerosol types transported. With this conventional approach, CCN (number) concentrations are derived from the transported masses based on an assumed size distribution for each type, often taken to be globally uniform (e.g. Jones et al., 2011). The need to
30 represent aerosol-cloud interactions more realistically has been a major motivation for the development of a new generation of composition-climate models with interactive aerosol microphysics. The models transport both particle number

concentrations and component masses (e.g. sulphate, black carbon) in multiple size classes (e.g. Mann et al., 2014), and allow to represent sources of primary and secondary CCN explicitly. For example, the UK's Earth System Model for CMIP6 (Coupled Model Intercomparison Project phase 6) includes the GLOMAP (Global Model of Aerosol Processes) aerosol microphysics module (Mann et al., 2010; 2012), which resolves differential particle growth and aerosol composition across 5 the particle size range including internal mixtures via the computationally efficient modal aerosol dynamics approach.

In order to understand how aerosols and clouds interact, it is important to assess how aerosol properties vary at finer spatial scales than are resolved in climate models, where both convective-dynamical and aerosol microphysical effects are likely to cause non-linear CCN variations. Whereas many modelling studies have assessed the main features of global variations in the aerosol particle size distribution (e.g. Ghan et al., 2001; Adams and Seinfeld, 2002; Spracklen et al., 2005) and several 10 have explored aerosol-cloud interactions in regional scale models (e.g. Bangert et al., 2011; [Zubler et al., 2011](#); Yang et al., 2012) only a few studies (Ekman et al., 2004; 2006; Wang et al., 2011; Archer-Nicholls et al., 2016; [Possner et al., 2016](#); [Weigum et al., 2016](#)) have explored the microphysical properties of aerosols, and their potential interactions with clouds, at resolutions of ~1km where convection is resolved.

It is known that deep convection can lead to transport of aerosols (e.g. Yin et al., 2012). In arid environments, cold-pool 15 outflows from convection can be a major source of dust uplift, which is missed by large-scale models that parameterise moist convection (Marsham et al., 2011; 2013; Pope et al., 2016). Similarly, it has been shown that over oceans such convectively generated flows can both increase gaseous DMS emission and transport, since the convection generates locally strong winds leading to high emissions that are then preferentially transported by the convection (Devine et al., 2006). There are, however, 20 few model studies of aerosols in ocean environments with deep convection (e.g. Cui et al., 2011) or shallow convection (e.g. Kaufman et al., 2005).

The main objective of the current study is to assess spatial and temporal variations in aerosol properties in a convection-permitting resolution model (grid-spacing ~1 km), in particular investigating the concentration range of different sized CCN, considering potential implications for aerosol-cloud interactions simulated by current composition-climate models. In order 25 to well-characterize the influence of both the dynamics and aerosol microphysic~~s~~ sal influences on cloud-relevant aerosol properties, the GLOMAP aerosol microphysics scheme is applied at high resolution over an idealised three-dimensional tropical marine domain. The convection-permitting aerosol microphysics simulations represent a highly realistic representation of CCN variations ([e.g. Yang et al., 2011](#)), providing a ground-breaking research tool for investigating aerosol-cloud interactions. The model includes interactive emissions of DMS and sea-spray and an online tropospheric chemistry scheme, ensuring the simulations include a comprehensive treatment of the combined effects from dynamical, 30 chemical and aerosol-microphysics processes occurring in the marine boundary layer. The paper is organised as follows: after a description of the UKCA (UK Chemistry and Aerosol) model and its high resolution configuration in Section 2, simulation results are described in Section 3. Section 4 summarizes, concludes and discusses the findings.

2 Model description

2.1 The UK Chemistry and Aerosol model (UKCA)

The UKCA sub-model of the UK Met Office Unified Model (MetUM) is used (hereafter UM-UKCA), including the GLOMAP-mode aerosol microphysics scheme (Mann et al., 2010) which calculates the evolution of aerosol mass and number in several log-normal size modes. The scheme represents each size mode as an internal mixture, with several aerosol components able to be simulated including sulphate (SU), sea-salt (SS), dust (DU), black carbon (BC), and particulate organic matter (POM) (including primary and biogenic secondary POM). Any number of modes (with fixed standard deviation) and possible components can be tracked, but the simulations here apply the “standard” configuration used in UM-UKCA (e.g. as in Bellouin et al., 2013) with 4 components (SU, SS, BC, POM) in 5 modes (Table 1) and dust transported separately in the existing 6-bin MetUM scheme (Woodward, 2001). The aerosol processes are simulated in a size-resolved manner and include primary emissions, secondary particle formation by binary homogeneous nucleation of sulphuric acid and water, growth by coagulation, hygroscopic growth, ageing, condensation and cloud-processing and removal by dry deposition, nucleation scavenging, impaction scavenging and sedimentation. All the details about the description of the different aerosol processes and the size distributions in UKCA are available in Mann et al. (2010; 2012).

The standard tropospheric chemistry configuration of UM-UKCA is used (O'Connor et al., 2014) which includes $O_x-HO_x-NO_y$ chemistry with degradation of methane, ethane and propane. The implementation here also includes the extension for aerosol precursor chemistry (as in Bellouin et al., 2013) for the oxidation of sulphur precursors DMS and SO_2 , and produces secondary organic aerosols via gas-phase oxidation of a biogenic monoterpene tracer.

2.2 High-resolution configuration of UM-UKCA

The simulations are carried out with UM-UKCA applied in a high resolution limited area model with periodic lateral boundary conditions, specifically applying the Numerical Weather Prediction configuration of MetUM GA4.0 (Walters et al., 2014). MetUM GA4.0 provides tracer transport, boundary-layer mixing, large-scale cloud and precipitation, with UKCA simulating atmospheric chemistry and aerosol processes. The limited area domain is centred close to the equator (1.32° , 1.08°) and set to 240 km x 240 km with 1.5 km horizontal grid-spacing. At this resolution, much of the convective-scale dynamics is resolved, and the MetUM convection parameterization (Gregory and Rowntree, 1990) is not applied. Cloud microphysics is represented using a single moment scheme (Wilson and Ballard, 1999). Even if the representation of some microphysical processes may not be well captured compared to multi-moment microphysics schemes (Morrison et al., 2009; Igel et al., 2015), the operational Numerical Weather Prediction (NWP) models, such as the MetUM (Wilkinson et al., 2012; Planche et al., 2015), generally use single-moment microphysics schemes. In these idealised simulations the radiation scheme was switched off, with the model therefore evolving without a diurnal cycle introduced by the daily variation in solar insolation or in variations in long wave cooling. The prognostic aerosols analysed here therefore also do not affect clear-sky interact radiatively transfer. The interactive We analyse CCN concentrations, defined as soluble particles with the dry

diameter $D_p > 50$ nm (supersaturation of 0.35%, assuming a pure sulphuric acid solution droplet), the size taken as representative for activating nuclei in marine stratocumulus regions (e.g. O'Dowd et al., 1997). Note however that, as well as being radiatively non-interactive, the CCN variations simulated by the model also do not feed through to modified cloud physics, with the investigation here exploring only variations in aerosol properties. A 73-level vertical grid is used up to a model top of 80 km, with 50 levels in the troposphere, 21 of which span the lowest 2 km of the atmosphere. Only a short demonstration. The simulation analysed here is here carried out with just over 24 hours integration time from an initial time of 09:00 UTC on May 24, 2002. Emissions are calculated on the simulation timestep of 30 s with UKCA chemistry and aerosol processes integrated every 10 timesteps, i.e. every 5 min.

Emissions of DMS and sea spray are interactive in the model, with their flux into the atmosphere primarily driven by variations in the model wind speed (using the same approaches described in Bellouin et al., 2013). Anthropogenic emissions of SO₂ and BC/OC are taken from the corresponding relevant grid-cell of from the IPCC AR5 global emission data (Lamarque et al., 2010), with monoterpene and biomass BC/OC emissions from the GEIA¹ and GFEDv2² databases respectively, but sources from these sectors are not significant in this domain. At the initial time, the chemistry tracers (HONO₂, O₃ and H₂O₂) and the aerosol precursor gas phase tracers (DMS, SO₂, H₂SO₄, MONOTER and SEC_ORG) are respectively set to 1 pptv and 0.001 pptv whereas the aerosol concentrations are spun up from an entirely clean environment.

The thermodynamic (temperature and humidity) and dynamic (horizontal wind) variables are initialised from a single model profile (Figure 1) taken from a global aqua-planet configuration of a MetUM operational run (where all land points are removed). The profiles are deliberately chosen to be strongly unstable so that the model will experience a sudden deep convective instability in the early phase of its evolution. The convective perturbation can clearly be seen in Figure 2, with deep convective clouds forming after a few hours, reaching up to a cloud top height of approximately 18 km (Figure 2a). The precipitation onset is system becomes precipitating after ~5 hours of simulation (Figure 2b), with the surface rain rate becoming more intensifies after 12 h of simulation and building up to reaches a maximum of approximately 80 mm h⁻¹ between 14 and 16 h of simulation. The mean horizontal surface wind speeds over the domain increase only slightly from 2 up to around 4 m s⁻¹ as the storm develops (Figure 2c), but variations within the domain are large with a maximum one standard deviation range of 3 to 9 m s⁻¹ and strong wind speeds occurring consistently between 6 h and 10 h of simulation (15:00 and 19:00 UTC). Between 3 and 6 h of integration (12:00 to 15:00 UTC), intense vertical wind speeds occur (Figure 2d) and those upward movements will transport DMS into the free troposphere where, after oxidation, it is known to cause new aerosol particle formation (e.g. Raes et al., 1993), with subsequent growth and re-entrainment into the boundary layer of the resulting secondary particles constituting a major source of marine CCN on the global scale (e.g. Korhonen et al., 2008). The sharp variations in horizontal wind speeds will also induce strong variations in the emission of sea-spray particles, since their source function has a cubic dependence on horizontal wind speed (e.g. Gong et al., 2002). Other influences such as

¹ Global Emissions Inventory Activity: www.geiacenter.org

² Global Fire Emissions Database, Version2: www.globalfiredata.org

changes in sea surface wave state will also influence sea spray emissions (e.g. Grythe et al., 2014), but these effects are not resolved in this study. The Gong-Monahan parameterization used here is based on sea spray flux measurements made over a longer time period than the model timestep (30s), and observing capabilities now include eddy covariance sea-spray flux measurements (e.g. Norris et al., 2012), we expect our approach will resolve the dominant sources of sea spray emissions flux variability. Figures 3a-c present the variation in aerosol particle concentrations across the domain at the time of maximum convective instability, i.e. intense updrafts and horizontal wind speeds, with squall lines and associated cold pooling clearly apparent, with very strong particle concentration gradients across the gust fronts, and the gravity currents inducing regions of greatly enhanced sea-spray emission. The strong convective event causes a rapid spin-up of the atmospheric composition in the model, giving an opportunity to assess the variation in aerosol properties across a range of wind speeds during the decay after the storm has subsided. In the next section, these high-resolution spatial variations in size-resolved aerosol properties are explored, examining how the different aerosol sources and processes represented in the simulations influence fluctuations in marine boundary layer CCN concentrations at this convection-permitting resolution.

3 Results

3.1 Gas-to-particle conversion

To aid interpretation and inference from the assessment of aerosol properties in subsequent sections, in this first part of the results we explore how the substantial emission of DMS during the intense storm period propagates through to simulated concentrations of its oxidised forms sulphur dioxide (SO_2) and sulphuric acid (H_2SO_4). Emissions of DMS vary strongly with wind speed and emissions fluxes will therefore be highest between 7 h and 9 h when the peak of the wind speed fluctuations is at maximum. The high emissions lead to a peak in the domain-mean DMS concentration with maximum of ~10 pptm after 9 h of simulations (i.e. at 18:00 UTC). DMS is oxidised by OH during the daytime and by NO_3 at night, both reactions producing SO_2 which, in the gas phase, goes on to form H_2SO_4 vapour following further reaction with OH. Figure 4 illustrates the timescales associated with these processes. The domain-averaged surface SO_2 and H_2SO_4 concentrations are peaking much later than DMS (22 h of simulation, 07:00 UTC, day +1) at respectively ~18 and 6.5×10^{-3} pptm. Given the photochemistry involved, the peak concentration at 07:00 UTC is surprising, but illustrates how atmospheric composition at the surface is strongly influenced by dynamical effects, not just atmospheric chemistry. That the model was still spinning up at this time is greatly beneficial as it helps The fact that the simulated sulphur gases and aerosol fields are spinning up identify helps identify which processes cause the CCN variations and allows to better understand the temporal signatures of the different processes involved. The gas phase H_2SO_4 produced from the emitted DMS is a prerequisite for effective new particle formation and also causes growth of existing particles following vapour condensation, both effects being important sources of marine cloud condensation nuclei (e.g. Korhonen et al., 2008). Although BC and POM are resolved in the model, and UKCA chemistry includes the oxidation of monoterpenes, their emission in this marine domain is negligible. Rather sea spray and DMS-derived sulphate particles are the only two significant particle sources in these simulations.

Hereafter, the analysis focuses on assessing separately the aerosol particles in the different size modes, investigating how the identified driver sources and processes are influencing simulated CCN variations at this convection permitting resolution. The analysis is restricted to the last 12 h of simulation with an emphasis on the results obtained after 18 h of integration, by which time the model has fully spun-up.Indeed, according to the extreme convective instability that induces intense updrafts
5 the spin-up time lasts approximately 6 h.

3.2 Properties of the aerosol fields

In this section, the focus is on quantifying variations in aerosol properties in the three different particle size ranges: Aitken, accumulation and coarse modes. The analysis begins (Figure 3) with instantaneous snapshots of surface aerosol particle concentration and size at two different times in the simulation. Figures 3a-c present a snapshot of spatial variability at 6 h of
10 integration, when an dynamics intense storm period was occurring. Figures 3d-i show the snapshot spatial variation at 18 h of integration, in more modest and representative wind speed conditions but with intense rain rates. The coarse mode consists entirely of sea-spray particles, so highest particle concentrations are expected to generally be indicating regions where simulated horizontal wind speeds are highest. However, during the initial storm period, and at this high spatial
15 resolution, there are also regions of intense localised precipitation (greater than 10 mm h⁻¹) and powerful vertical wind speeds, which will also strongly influence aerosol properties due to removal and transport effects. At 6 h of simulation, Figures 3a-c show that particle concentrations in the two largest modes (accumulation and coarse) are indeed extremely variable over the entire domain. For example, particle concentrations vary from 1 to 1,000 cm⁻³ for the accumulation mode and from 0.1 to 100 cm⁻³ for the coarse mode. Note however that this very high aerosol variability is unrealistically large, being mostly due to the model being initialised with a “warm bubble” to ensure model spin-up proceeds rapidly. However,
20 the period from 12 to 24 hours of integration can be considered to span representative range of wind speed conditions, and we focus on this 2nd half of the day in the rest of the results sections.

Despite the fact that particles in Aitken mode can be affected by the emission of sea spray (e.g., Salter et al., 2015), In this remote marine domain, particles in the Aitken mode are almost exclusively secondary in nature, being originally formed via nucleation in the free troposphere. Over the initial 12 hours, free troposphere concentrations of the driver gas for nucleation,
25 H₂SO₄ are not yet high enough to initiate significant particle formation, with low simulated concentrations of its precursor species SO₂ (see Figure 4) and timescales for oxidation and transport being relative long. After 18 h of simulations, the strongly convective episode has passed, and coarse mode particle concentrations (Figure 3f), although still quite variable,
have more moderate peak concentrations, lower by around a factor of 10 than during the intense storm period (Figures 3c, f).
Accumulation mode particle concentrations at 18 h (Figure 3e) are also much less variable than at 6 h, with highest
30 concentration in the same regions that coarse mode particle concentrations were highest, likely indicating where sea spray emissions are highest (horizontal wind speeds are strongest). Patches of low concentrations are also found where the precipitation is most intense, with the washout rate (impaction scavenging efficiency) tied to rainfall rates. In the Aitken

mode (Figure 3d), particle concentrations have become significant by 18 h, although still an order of magnitude lower than in the accumulation mode. Spatial variations in the size of the aerosol particles ~~are~~is also highest for the coarse mode (Figure 3i), ~~with regions of highest particle concentration generally corresponding to smaller particles,~~ likely reflecting the nature of the sea spray source function. The general spatial patterns of size variation seen for the coarse mode are also seen for the 5 accumulation mode (Figure 3h) but the accumulation mode has additional regions of lower particle size where Aitken mode particle concentrations are highest (Figure 3d). This co-variation is expected, since the accumulation mode mean radius will be lower, on average, when there are a significant number of smaller particles being chemically cloud processed or mode-merged in from the Aitken mode. Over the domain, mean particle size variations are largest for the Aitken mode at 118% min-to-max ratio (geometric mean radius from 22 to 48 nm), compared to ~20% for the accumulation mode (101 to 123 nm) 10 and ~35% for the coarse mode (0.75 to 1.10 μm).

In Figure 5 we show Hovmöller diagrams to further explore the temporal evolution in surface concentrations of Aitken, accumulation and coarse mode particles during the last 12 h of integration (at $y = 150$ km). Highest particle concentrations from accumulation and coarse modes are apparent between 12 and 15 h of integrations, whereas Aitken mode particle concentrations evolve with quite different time-variation. The convective storm period in the first 12 hours causes very 15 strong wind speeds and the decay of the coarse mode particles concentrations over this second half of the day reflects the progression to calmer conditions; with consequently reduced sea spray emissions but also the intensification of the precipitation (Figure 2) increasing the scavenging process efficiency. By contrast, Aitken particle concentrations are steadily increasing to a maximum of around 1-2 particles per cm^3 ~~after~~ 22 h, matching that seen for SO_2 and gas phase H_2SO_4 (Figure 4), consistent with the timescales of the two oxidation steps required to convert enough of the emitted DMS into sulphuric 20 acid vapour to trigger new particle formation. For particles to reach Aitken sizes, growth by condensation and coagulation is also required, and since nucleation will mostly tend to occur in the free troposphere, any transition to a statically stable boundary layer during late evening would likely also be important, influencing particle entrainment and the timing of the increase in Aitken particle concentrations at the surface. In these idealised simulations however, the short wave and long 25 wave radiation schemes are switched off, there then being no solar-induced diurnal variations in boundary layer entrainment (but photochemical variations proceeding in the model based on local time).

Assessing how each of the size modes is spinning up reveals how temporal variations in marine CCN concentrations are actually reflecting the very different time-profiles of the two dominant CCN production pathways: primary emissions of sea-spray particles and entrainment of DMS-derived secondary particles formed in the free troposphere. The analysis illustrates the way a diverse community of processes (dynamical, chemical and microphysical) together determine CCN variations in 30 the marine boundary layer. Figure 5a shows an Aitken mode emerging after 17 h of integration which also explains the dip in accumulation mode size (contour lines), as a substantial number of smaller secondary particles is being “mode-merged in” from the Aitken mode at that time. For the coarse mode, as particle concentrations decrease, there is also a progression to smaller particles, which can be explained by that fact that, in the model, sedimentation (the dominant removal process for

this mode) removes both number and mass, enabling the simulation to reflect the fact that larger particles fall faster even when they are in the same mode.

A more quantitative analysis of the simulated aerosol properties is presented hereafter, with Figure 6 showing probability density functions (PDFs) of the geometric dry radius (a-c) and particle concentrations (d-f) for the Aitken, accumulation and coarse modes at different times in the 2nd twelve hours of the integration. The analysis shows that, for the accumulation and coarse modes, as seen in Figure 5, as time progresses, the particle size PDFs shift to smaller sizes, with the accumulation mode PDFs becoming much wider in the evening as the source of smaller particles from the Aitken mode becomes significant. By contrast, as Aitken mode concentrations increase, the particles are clearly also larger, reflecting that growth

processes are acting on the particles with this size-increase ceasing at about 18 h of integration, while particle concentrations continue to increase (likely due to entrainment). For the accumulation and coarse mode particles, this quantitative approach is consistent with sedimentation causing the shift in size distribution as the larger particles sediment out faster than the smaller ones. Figure 7 shows the temporal evolution of the mean and standard deviation of the geometric mean radius values and number concentration (over grid boxes in the domain) for Aitken, accumulation and coarse modes at the surface. The accumulation and coarse mode concentration and radius fields have largest spatial variations between 5 and 8 h as the model

adjusts to the very strong sea-salt emission and quite efficient wet removal induced by the precipitation onset during the peak convective activity, whereas Aitken mode concentrations, and their variations, stay approximately constant through that period. During the simulations, the mean radius and particle concentration values from the coarse mode are, on average, decreasing (Figures 7c, f), but the mean size variations show the opposite evolution, with greater variability in the calmer 2nd half of the day, reflecting the strengthening influence of sedimentation as sea-spray emissions decrease. For the accumulation mode, the mean particle size displays remarkably little variation over the domain between 9 and 14 h of simulation (as seen in Figure 6a), with the variation increasing as the source of secondary CCN from the Aitken mode becomes significant later in the day.

3.3 CCN spatial and temporal features

In this marine domain, sea-salt particles represent a major component of the CCN population (e.g. O'Dowd et al., 1997; O'Dowd and de Leeuw, 2007). Models parameterize sea-spray emission fluxes as a function of the 10 m wind speed (u_{10}), with some source functions linked directly to field measurements of the particle concentrations (e.g. Smith et al., 1993) while others (e.g. Monahan et al., 1986) reflect also the processes that form ocean whitecaps, and laboratory experiments on particle emissions. In the simulations presented here, the model uses the sea spray source function of Gong (2003) which applies the approach of Monahan et al. (1986), and its $u^{3.41}$ 10 m-wind-speed dependence, with a refined formulation with an additional parameter determining emission of ultra-fine sea-spray particles, as constrained by field measurements from O'Dowd et al. (1997).

In light of the inference of sea-spray emissions fluxes from measurements of particle concentrations, Figure 8 presents several snapshot variation box-plots for simulated sea-salt emission flux, sea-salt mass mixing ratio (mmr) and the CCN number concentration as a function of the u_{10} (called hereafter surface wind speed) at different integration times. At this convection-permitting resolution, the sea-salt emission fields are highly heterogeneous at each integration time with the 5 emission flux median highest at 12 h of integration then decreasing towards the end of the simulations, consistent with the mean wind speed evolution (Figure 2c). After their emission into the atmosphere, sea-salt aerosols are transported vertically by turbulence, with larger particles also being influenced by sedimentation. As expected, near the surface, the higher are the sea-salt emission fluxes, the higher are the sea-salt mmr, but, as we show below, the co-variation of the sea-salt mmr field with wind speed (Figure 8b) is fundamentally different than it is for sea-salt emission (Figure 8a). Sea-spray particles are 10 highly soluble and are, in most cases, directly emitted at sizes where they are effective CCN, but, as discussed earlier, in marine regions, the CCN population also has a substantial contribution from nucleated sulphate particles which have grown large enough to be CCN-active. Figure 8c shows the variation of CCN concentrations in this marine domain at different integration times and permits to explore how its variation compares to that seen for sea-spray mmr and emissions flux. By 15 sampling the four periods at 12, 15, 18 and 21 h of integration, it is possible to assess the spatial variability in sea-salt emissions, sea-salt concentrations, and CCN concentrations at a range of wind speed conditions; the earliest period 20 representing a strong convective period (i.e. intense wind speeds) when sea-spray would be dominant, and through the progression to calmer conditions later in the simulation. First, the relative change in the median between each period (12-15, 15-18 and 18-21 h) is assessed. As expected, the median sea-salt emission flux (Figure 8a) decreases linearly on the log-log plot over the period, reflecting the 3.41 exponent in the wind-speed-dependence for the sea-spray source function. The relative decrease in sea spray emissions between 12 h and 15 h is reflected also between 15 h and 18 h, and between 18 h and 21 h. By contrast, the median sea-salt mixing ratio (Figure 8b) decreases much more steeply over the 18-21 h period than in the 12-15 h period, despite strong decreases in wind speed. This effect is likely a result of the timescale for the decay from the excited state acquired during the strong convection period (the strong turbulence and direct transport having lifted particles much higher) the atmosphere still “catching up”, with the adjustment to the new calmer conditions only being 25 visible after 18 h of integration. The equivalent temporal decay for CCN concentrations is also curved (Figure 8c), but part of the signal of steeper decline between 18 and 21 h (from the decreased sea-salt) is “straightened out” by the compensating emergence of the secondary nucleated particles making an important contribution to CCN in this later period (as we showed in Figure 7). In the calm conditions, wind speeds across the domain vary (5^{th} to 95^{th} percentile) from ~ 0.21 to 1.6 m s^{-1} , around a factor of 8, with the CCN concentration range from around 6 to 20 particles per cubic centimetre (a factor of 3). In 30 contrast, during the strongly convective 12-15 h period (i.e. with intense wind speeds and moderate rain rates), the CCN variation is much larger, between 12 and 95 particles per cubic centimetre (a factor of 8).

Figure 9 presents the vertical variation of the simulated CCN concentration using an altitude PDF profile (a-PDF) for the same periods as mentioned above. As expected, on average, the CCN concentration drops-off with increasing altitude

reflecting a balance between turbulence and convection lifting the particles vertically and gravitational settling transporting larger particles back towards the surface. In the atmospheric surface layer (lowest 100 metres or so) the profile of mean CCN follows a power-law profile but the spatial CCN variance (standard deviation over grid boxes in the domain) decreases much less rapidly with altitude. As a consequence, the coefficient of variation increases with increasing altitude from approx. 11% at the surface to approx. 22.5% at 1.3 km height. The CCN concentration fields close to the surface are mainly influenced by the emissions whereas at higher altitudes they are mostly influenced by the transport. This explains why, after 12 h of simulation, the coefficient of variation is slightly higher than at the others times. Note that the emergence of the secondary nucleated particles is also visible in the CCN concentration vertical properties on the 18-21 h period.

4 Conclusions and Discussions

We have analysed spatial and temporal sea-spray and CCN variations in a convection-permitting model with interactive sea-spray emissions, sulphur chemistry and aerosol microphysics over an idealised marine tropical domain. In this marine atmosphere the two dominant CCN sources are both natural: ~~the cloud nuclei population comprising two elements~~ primary sea-spray particles and secondary sulphate particles. However, even in this relatively simple two-component CCN system, our analysis has revealed that there is a diverse community of processes: dynamical, chemical, and microphysical, that together combine to determine the number of particles which can activate to cloud droplets.

First, the dynamics strongly influences the sea-spray emissions since highest particle concentrations occur where wind speeds are highest, and there is a cubic wind speed dependence for sea-salt emission. The emitted sea-spray particles have a range of sizes, being directly emitted in both the accumulation (sub-micron) and coarse (super-micron) modes. After their emission into the atmosphere, sea-salt aerosols are transported vertically by turbulent diffusion and convective updrafts, with larger particles also being influenced by sedimentation. We show that the co-variation of sea-salt mass mixing ratio with wind speed is fundamentally different than that for sea-salt emission, with implications for derivations that treat the two synonymously. In particular, since sub-micron sea-spray has much longer atmospheric residence time (days) than super-micron sea-spray (hours), care must be taken when relating measured sea-spray concentrations to emissions. Intense localised precipitation during strong convection also impacts aerosol concentrations at the climate grid-scale with removal effects introducing strong variations (e.g. via the impaction scavenging process). The combination of these processes impacts the particle concentration properties, which become extremely variable in space (about a factor of 8 over the entire domain, one climate model grid square) and time. We acknowledge that if the aerosol was initialized with a background profile, the variability described here might have been lower.

Moreover, the emissions of DMS strongly vary spatially and temporally according to wind speeds conditions and become substantial during intense storm period (as in Devine et al., 2006). There is a requirement for gas phase species SO₂ and H₂SO₄ vapour to be sufficiently produced following oxidation of DMS before new sulphate particle formation in the free troposphere can occur, and the latter species also cause enhanced growth of existing particles following condensation. The

combination of the two oxidation steps being required to convert emitted DMS into sulphuric acid vapour, with also the timescales inherent in particle growth processes (e.g. coagulation and condensation), explain why here is a quite different time-variation for the Aitken mode particle concentrations. Provided the airmass has had sufficient time, a significant proportion of these small secondary particles grow large enough to be cloud processed or mode-merged from the Aitken mode to the accumulation mode. The effects of these processes is illuminated by assessing how each of the particle modes is spinning up, revealing the way they influence spatial- and temporal CCN variations in the marine boundary layer.

5 Sea-spray particles are highly soluble and, in most cases, are directly emitted at sizes where they are already effective CCN. In contrast, a different component of the CCN population comprises nucleated sulphate particles which need more time to grow large enough to be CCN-active. The variations in the CCN concentrations are strong and can attain a factor of 8 in
10 strongly convective conditions, mostly reflecting the properties of larger CCN. Smaller (sub-micron) CCN, from the accumulation mode, tend to have less variation, which in part is due to their source having a significant contribution from the steady formation of secondary sulphate particles in the free troposphere. We have seen how dynamics and microphysical processes also affect CCN, in particular with a 2nd CCN peak at the top of the boundary layer during the strongly convective period before the secondary particles emerged. These effects combine to determine how the coefficient of variation in CCN
15 concentration changes with altitude, our results suggesting an increase from around 10% at the surface to more than 20% at the top of the marine boundary layer. Whereas CCN concentration fields close to the surface are mainly influenced by the emissions, at higher altitudes they are in general older, and inheriting influences propagated via transport.

We also examine spatial and temporal variations in aerosol particle size, finding that the geometric radius of the Aitken and coarse modes are particularly variable, which will introduce further variability in cloud droplet number concentrations and
20 cloud brightness. The different influences on the two CCN types (primary and secondary), and the diverse community of processes involved (microphysical, chemical and dynamical) makes sub-grid parameterization of the CCN variations difficult. This study provides valuable results on e.g. the impact of the local dynamics and aerosol sources on the CCN population and then on the aerosol-cloud interactions occurring at these fine spatial scales. Work to apply the UM-UKCA model for non-idealised case-studies with a nesting procedure to retain the larger scale influences has now been developed,
25 as is the capability to allow these aerosol variations to couple with a new cloud microphysics scheme in MetUM (Shipway and Hill, 2012).

Acknowledgement. This project was made possible through the financial support of the Leeds-Met Office Academic Partnership (ASCI project). The authors acknowledge use of the MONSooN system, a collaborative facility supplied under
30 the Joint Weather and Climate Research Programme, which is a strategic partnership between the Met Office and the Natural Environment Research Council. The lead author wishes to thank Douglas Parker for useful discussions. G. W. Mann is funded by the UK National Centre for Atmospheric Science, one of the UK Natural Environment Research Council (NERC) research centres. J. Marsham acknowledges funding from the SAMMBA project (NE/J009822/1).

References

Adams, P. J., and Seinfeld, J. H.: Predicting global aerosol size distributions in general circulation models, *J. Geophys. Res.*, 107, D19, 4370, 2002.

Archer-Nicholls, S., Lowe, D., Schultz, D. M., and McFiggans, G.: Aerosol–radiation–cloud interactions in a regional
5 coupled model: the effects of convective parameterisation and resolution, *Atmos. Chem. Phys.*, 16, 5573–5594, 2016.

Bangert, M., Kottmeier, C., Vogel, B., and Vogel, H.: Regional scale effects of the aerosol cloud interaction simulated with
an online coupled comprehensive chemistry model, *Atmos. Chem. Phys.*, 11, 4411–4423, 2011.

Bellouin, N., Mann, G. W., Woodhouse, M. T., Johnson, C., Carslaw, K. S., and Dalvi, M.: Impact of the modal aerosol
scheme GLOMAP-mode on aerosol forcing in the Hadley Centre Global Environmental Model, *Atmos. Chem. Phys.*, 13,

10 3027–3044, 2013.

Boucher, O., Randall, D., Artaxo, P., Bretherton, C., Feingold, G., Forster, P., Kerminen, V.-M., Kondo, Y., Liao, H.,
Lohmann, U., Rasch, P., Satheesh, S. K., Sherwood, S., Stevens, B., and Zhang, X. Y.: Clouds and aerosols. In: Climate
Change 2013: The physical basis. Contribution of working group I to the Fifth Assessment Report of the
Intergovernmental Panel on Climate Change [Stocker, T., F., Qin, D., Plattner, G.-K., Tignor, M., Allen, S. K.,
15 Boschung, J., Nauels, A., Xia, Y., Bex, V., and Midgley, P. M. (eds.)], Cambridge University Press, Cambridge, United
Kingdom and New York, NY, USA, 2013.

Carslaw, K. S., Lee, L. A., Reddington, C. L., Pringle, K. J., Rap, A., Forster, P. M., Mann, G. W., Spracklen, D. V.,
Woodhouse, M. T., Regayre, L. A., and Pierce, J. R.: Large contribution of natural aerosols to uncertainty in indirect
forcing, *Nature*, 503, 67–71, 2013.

20 Cui, Z., Davies, S., Carslaw, K. S., and Blyth, A. M.: The response of precipitation to aerosol through riming and melting in
deep convective clouds, *Atmos. Chem. Phys.*, 11, 3495–3510, 2011.

Devine, G. M., Carslaw, K. S., Parker, D. J., and Petch, J. C.: The influence of subgrid surface-layer variability on vertical
transport of a chemical species in a convective environment, *Geophys. Res. Lett.*, 33, 2006.

Ekman, A., Wang, C., Wilson, J., and Ström, J.: Explicit simulations of aerosol physics in a cloud-resolving model: a
25 sensitivity study based on an observed convective cloud. *Atmos. Chem. Phys.*, 4, 773–791, 2004.

Ekman, A., Wang, C., Ström, J., and Krejci, R.: Explicit simulation of aerosol physics in a cloud-resolving model: Aerosol
transport and processing in free troposphere, *J. Atmos. Sci.*, 63, 682–695, 2006.

Forster, P., Ramaswamy, V., Artaxo, P., Berntsen, T., Betts, R., Fahey, D. W., Haywood, J., Lean, J., Lowe, D. C., Myhre,
G., Nganga, J., Prinn, R., Raga, G., Schulz, M., and Van Dorland, R.: Changes in atmospheric constituents and in
30 radiative forcing. Chapter: Climate Change 2007: The Physical Science Basis. In: Contribution of Working Group I to
Fourth Assessment Report of the Intergovernmental Panel on Climate Change Cambridge University Press, Cambridge,
UK and New York, USA, 129–234, 2007.

Ghan, S. J., Easter, R. C., Chapman, E. G., Abdul-Razzak, H., Zhang, Y., Leung, L. R., Laulainen, N. S., Saylor, R. D., and Zaveri, R. A.: A physically based estimate of radiative forcing by anthropogenic sulphate aerosol, *J. Geophys. Res.*, 106, 5279-5293, 2001.

5 Gong, S. L., Barrie, L. A., and Lazare, M.: Canadian Aerosol Module (CAM): A size-segregated simulation of atmospheric aerosol processes for climate and air quality models. 2. Global sea-salt aerosol and its budgets, *J. Geophys. Res.*, 107, D244779, 2002.

Gong, S. L.: A parameterization of sea-salt aerosol source function for sub- and super-micron particles, *Global Biogeochem. Cycles.*, 14, 1097-1103, 2003.

10 Gregory, D., and Rowntree, P. R.: A mass flux convection scheme with representation of cloud ensemble characteristics and stability-dependent closure, *Mon. Wea. Rev.*, 118, 1483-1506, 1990.

Grythe H., Ström, J., Krejci, R., Quinn, P. and Stohl, A., A review of sea-spray aerosol source functions using a large global set of sea salt aerosol concentration measurements, *Atmos. Chem. Phys.*, 14, 1277–1297, 2014.

Igel, A., Igel, M., and van den Heever S.: Make It a Double? Sobering Results from Simulations Using Single-Moment Microphysics Schemes. *J. Atmos. Sci.*, 72, 910–925, 2015, doi: 10.1175/JAS-D-14-0107.1.

15 Jones, C. D., Hughes, J. K., Bellouin, N., Hardiman, S. C., Jones, G. S., Knight, J., Liddicoat, S., O'Connor, F. M., Andres, R. J., Bell, C., Boo, K.-O., Bozzo, A., Butchart, N., Cadule, P., Corbin, K. D., Doutriaux-Boucher, M., Friedlingstein, P., Gornall, J., Gray, L., Halloran, P. R., Hurt, G., Ingram, W. J., Lamarque, J.-F., Law, R. M., Meinshausen, M., Osprey, S., Palin, E. J., Parsons Chini, L., Raddatz, T., Sanderson, M. G., Sellar, A. A., Schurer, A., Valdes, P., Wood, N., Woodward, S., Yoshioka, M., and Zerroukat, M.: The HadGEM2-ES implementation of CMIP5 centennial simulations, 20 Geosci. Model Dev., 4, 543-570, 2011.

Kaufman, Y. J., Koren, I., Remer, L. A., Rosenfeld, D., and Rudich, Y.: The effect of smoke, dust, and pollution aerosol on shallow cloud development over the Atlantic Ocean, *Proc. Natl. Acad. Sci. USA.*, 102, 11207–11212, 2005.

25 Korhonen, H., Carslaw, K. S., Spracklen, D. V., Mann, G. W., and Woodhouse, M. T.: Influence of oceanic DMS emissions on CCN concentrations and seasonality over the remote Southern Hemisphere oceans: A global model study, *J. Geophys. Res.*, 113, D15204, 2008.

Lamarque, J.-F., Bond, T. C., Eyring, V., Granier, C., Heil, A., Klimont, Z., Lee, D., Liousse, C., Mieville, A., Owen, B., Schultz, M., G., Shindell, D., Smith, S., J., Stehfest, E., van Aardenne, J., Cooper, O. R., Kainuma, M., Mahowald, N., McConnell, J. R., Naik, V., Riahi, K., and van Vuuren, D. P.: Historical (1850–2000) gridded anthropogenic and biomass burning emissions of reactive gases and aerosols: methodology and application, *Atmos. Chem. Phys.*, 10, 7017-7039, 30 2010.

Lohmann, U., and Feichter, J.: Global indirect aerosol effects: a review, *Atmos. Chem. Phys.*, 5, 715-737, 2005.

Mann, G. W., Carslaw, K. S., Spracklen, D. V., Ridley, D. A., Manktelow, P. T., Chipperfield, M. P., Pickering, S. J., and Johnson, C. E.: Description and evaluation of GLOMAP-mode: a modal global aerosol microphysics model for the UKCA composition-climate model, *Geosci. Model Dev.*, 3, 519-551, 2010.

- Mann, G. W., Carslaw, K. S., Ridley, D. A., Spracklen, D. V., Pringle, K. J., Merikanto, J., Korhonen, H., Schwarz, J. P., Lee, L. A., Manktelow, P. T., Woodhouse, M. T., Schmidt, A., Breider, T. J., Emmerson, K. M., Reddington, C. L., Chipperfield, M. P., and Pickering, S. J.: Inter-comparison of modal and sectional aerosol microphysics representations within the same 3-D global chemical transport model, *Atmos. Chem. Phys.*, 12, 4449-4476, 2012.
- 5 Mann, G. W., Carslaw, K. S., Reddington, C. L., Pringle, K. J., Schulz, M., Asmi, A., Spracklen, D. V., Ridley, D. A., Woodhouse, M. T., Lee, L. A., Zhang, K., Ghan, S. J., Easter, R. C., Liu, X., Stier, P., Lee, Y. H., Adams, P. J., Tost, H., Lelieveld, J., Bauer, S. E., Tsigaridis, K., Van Noije, T. P., C., Strunk, A., Vignati, E., Bellouin, N., Dalvi, M., Johnson, C. E., Bergman, T., Kokkola, H., Von Salzen, K., Yu, F., Luo, G., Petzold, A., Petzold, A., Heintzenberg, J., Clarke, A., Ogren, J. A., Gras, J., Baltensperger, U., Kaminski, U., Jennings, S. G., O'Dowd, C. D., Harrison, R. M., Beddows, D. C.
- 10 10 Kulmala, M., Viisanen, Y., Ulevicius, V., Mihalopoulos, N., Zdimal, V., Fiebig, M., Hansson, H. C., Swietlicki, E., and Henzing, J. S.: Intercomparison and evaluation of global aerosol microphysical properties among AeroCom models of a range of complexity, *Atmos. Chem. Phys.*, 14, 4679-4713, 2014.
- Marsham, J. H., Knippertz, P., Dixon, N., Parker, D. J., and Lister, G. M. S.: The importance of the representation of deep convection for modeled dust-generating winds over West Africa during summer, *Geophys. Res. Lett.*, 38, L16803, 2011.
- 15 15 Marsham, J. H., Dixon, N., Garcia-Carreras, L., Lister, G. M. S., Parker, D. J., Knippertz, P., and Birch, C.E.: The role of moist convection in the West African monsoon system - insights from continental-scale convection-permitting simulations, *Geophys. Res. Lett.*, 40, 1843-1849, 2013.
- Monahan, E. C., Spiel, D. E., and Davidson, K. L.: A model of marine aerosol generation via whitecaps and wave disruption. Oceanic Whitecaps. Edited by EC Monahan and G MacNiochaill, pp 167-193, D Reidel, Norwell, Mass, 1986.
- 20 20 Morrison, H., Thompson, G., and Tatarkii, V.: Impact of cloud microphysics on the development of trailing stratiform precipitation in a simulated squall line: comparison of one- and two-moment schemes, *J. Atmos. Sci.*, 137, 991–1007, 2009.
- Myhre, G., Samset, B. H., Schulz, M., Balkanski, Y., Bauer, S., Berntsen, T. K., Bian, H., Bellouin, N., Chin, M., Diehl, T., Easter, R. C., Feichter, J., Ghan, S. J., Hauglustaine, D., Iversen, T., Kinne, S., Kirkevåg, A., Lamarque, J.-F., Lin, G.,
- 25 25 Liu, X., Lund, M. T., Luo, G., Ma, X., van Noije, T., Penner, J. E., Rasch, P. J., Ruiz, A., Seland, Ø., Skeie, R. B., Stier, P., Takemura, T., Tsigaridis, K., Wang, P., Wang, Z., Xu, L., Yu, H., Yu, F., Yoon, J.-H., Zhang, K., Zhang, H., and Zhou, C.: Radiative forcing of the direct aerosol effect from AeroCom Phase II simulations, *Atmos. Chem. Phys.*, 13, 1853-1877, 2013.
- Norris, S. J., Brooks, I. M., Hill, M. K. Brooks, B. J., Smith, M. H., Sproson, D. A. J.: Eddy covariance measurements of the sea spray aerosol flux over the open ocean, *J. Geophys. Res.*, vol. 117, doi:10.1029/2011JD016549, 2012
- 30 30 O'Connor, F. M., Johnson, C. E., Morgenstern, O., Abraham, N. L., Braesicke, P., Dalvi, M., Folberth, G. A., Sanderson, M. G., Telford, P. J., Young, P. J., Zeng, G., Collins, W. J., and Pyle, J. A.: Evaluation of the new UKCA climate-composition model - Part 2: The Troposphere, *Geosci. Model Dev.*, 7, 41-91, 2014.

- O'Dowd, C. D., Smith, M. H., Consterdine, I. E., and Lowe, J. A.: Marine aerosol, sea salt, and the marine sulphur cycle: a short review, *Atmos. Environ.*, 31, 73-80, 1997.
- O'Dowd, C. D., and de Leeuw, G.: Marine aerosol production: a review of the current knowledge, *Phil. Trans. R. Soc. A*, 365, 1753-1774, 2007.
- 5 [Planche, C., Marsham, J., Field, P., Carslaw, K., Hill, A., Mann, G., and Shipway, B.: Precipitation sensitivity to autoconversion rate in a Numerical Weather Prediction Model, Q. J. R. Meteorol. Soc., 141, 2032-2044, DOI: 10.1002/qj.2497, 2015.](#)
- Pope, R. J., Marsham, J. H., Knippertz, P., Brooks, M. E., and Roberts, A. J.: Identifying errors in dust models from data assimilation, *Geophys. Res. Lett.*, 43, doi:10.1002/2016GL070621, 2016.
- 10 [Possner A., Zubler, E. M., Lohmann, U., and Schär, C.: The resolution dependence of cloud effects and ship-induced aerosol-cloud interactions in marine stratocumulus, J. Geophys. Res. Atmos., 121, 4810–4829, 2016.](#)
- Raes, F., Van Dingenen, R., Wilson, J., and Saltelli, A.: Cloud condensation nuclei from dimethyl sulphide in the natural marine boundary layer: Remote vs. in-situ production, in *Dimethyl Sulphide: Oceans, Atmosphere and Climate*, edited by G. Restelli and G. Angeletti, pp. 311-322, Kluwer, Acad., Norwell, Mass., 1993.
- 15 [Salter, M. E., Zieger, P., Acosta Navarro, J. C., Grythe, H., Kirkevåg, A., Rosati, B., Riipinen, I., and Nilsson, E. D.: An empirically derived inorganic sea spray source function incorporating sea surface temperature, Atmos. Chem. Phys., 15, 11047-11066, doi:10.5194/acp-15-11047-2015, 2015.](#)
- Shipway, B. J., and Hill, A. A.: Diagnosis of systematic differences between multiple parameterizations of warm rain microphysics using a kinematic framework, *Quart. J. Roy. Meteor. Soc.*, 138, 2196-2211, 2012.
- 20 Smith, M. H., Park, P. M., and Consterdine, I. E.: Marine aerosol concentrations and estimated fluxes over the sea, *Q. J. R. Meteorol. Soc.*, 119, 809–824, 1993.
- Spracklen, D. V., Pringle, K. J., Carslaw, K. S., Chipperfield, M. P., and Mann, G. W.: A global offline model of size-resolved aerosol microphysics: I. Model development and prediction of aerosol properties, *Atmos. Chem. Phys.*, 5, 2227-2252, 2005.
- 25 Walters, D. N., Williams, K. D., Boutle, I. A., Bushell, A. C., Edwards, J. M., Field, P. R., Lock, A. P., Morcrette, C. J., Stratton, R. A., Wilkinson, J. M., Willett, M. R., Bellouin, N., Bodas-Salcedo, A., Brooks, M. E., Copsey, D., Earnshaw, P. D., Hardiman, S. C., Harris, C. M., Levine, R. C., MacLachlan, C., Manners, J. C., Martin, G. M., Milton, S. F., Palmer, M. D., Roberts, M. J., Rodríguez, J. M., Tennant, W. J., and Vidale, P. L.: The Met Office Unified Model Global Atmosphere 4.0 and JULES Global Land 4.0 configurations, *Geosci. Model Dev.*, 7, 361-386, 2014.
- 30 Wang, M., Ghan, S., Ovchinnikov, M., Liu, X., Easter, R., Kassianov, E., Qian, Y., and Morrison, H.: Aerosol indirect effects in a multi-scale aerosol-climate model PNNL-MMF, *Atmos. Chem. Phys.*, 11, 5431-5455, 2011.
- [Weigum, N., Schutgens, N., and Stier, P.: Effect of aerosol subgrid variability on aerosol optical depth and cloud condensation nuclei: implications for global aerosol modelling, Atmos. Chem. Phys., 16, 13619-13639, doi:10.5194/acp-16-13619-2016, 2016.](#)

Wilkinson, J. M., Porson, A. N. F., Bornemann, F. J., Weeks, M., Field, P. R., and Lock, A. P.: Improved microphysical parametrization of drizzle and fog for operational forecasting using the Met Office Unified Model, Q. J. R. Meteorol. Soc., 139, 488–500, DOI: 10.1002/qj.1975, 2012.

Wilson, D. R., and Ballard, S. P.: A microphysically based precipitation scheme for the UK Meteorological Office Unified
5 Model. Quart. J. Roy. Meteor. Soc. 125, 1607–1636, 1999.

Woodward, S.: Modeling the atmospheric life cycle and radiative impact of mineral dust in the Hadley Centre climate
model, J. Geophys. Res., 106(D16), 18115–18166, 2001.

Yang, Q., W. I. Gustafson Jr., Fast, J. D., Wang, H., Easter, R. C., Morrison, H., Lee, Y.-N., Chapman, E. G., Spak, S. N.,
and Mena-Carrasco, M. A.: Assessing regional scale predictions of aerosols, marine stratocumulus, and their interactions
10 during VOCALS-REx using WRF-Chem, Atmos. Chem. Phys., 11, 11951–11975, doi:10.5194/acp-11-11951-2011,
2011.

Yang, Q., Gustafson Jr., W. I., Fast, J. D., Wang, H., Easter, R. C., Wang, M., Ghan, S. J., Berg, L. K., Leung, L. R., and
Morrison, H.: Impact of natural and anthropogenic aerosols on stratocumulus and precipitation in the Southeast Pacific: a
regional modelling study using WRF-Chem, Atmos. Chem. Phys., 12, 8777–8796, 2012.

15 Yin, Y., Chen, Q., Jin, L., Chen, B., Zhu, S., and Zhang, X.: The effects of deep convection on the concentration and size
distribution of aerosol particles within the upper troposphere: A case study, J. Geophys. Res., 117, D22202, 2012.

Zubler, E. M., Folini, D., Lohmann, U., Lüthi, D., Schär, C., and Wild, M.: Simulation of dimming and brightening in
Europe from 1958 to 2001 using a regional climate model, J. Geophys. Res., 116, D18205, 2011.

Table 1. Standard aerosol configuration for GLOMAP-mode. The size distribution is described by lognormal modes with varying geometric mean diameter D and fixed geometric standard deviation σ_g . Particle number and mass are transferred between modes when D exceeds the upper limit for the mode. Names are given in function of the aerosols mode ('nuc', 'Ait', 'acc' and 'coa' are for 'nucleation', 'Aitken', 'accumulation' and 'coarse') and their solubility properties ('sol' and 'ins' mean the aerosols are soluble or insoluble). The aerosols can be composed of sulphate (SU), primary organic matter (POM), black carbon (BC), or sea-salt (SS).

Index	Name	Size range	Composition	Soluble	σ_g
1	nucsol	$D < 10 \text{ nm}$	SU, POM	yes	1.59
2	Aitsol	$10 \text{ nm} < D < 100 \text{ nm}$	SU, BC, POM	yes	1.59
3	accesol	$100 \text{ nm} < D < 1 \mu\text{m}$	SU, BC, POM, SS	yes	1.59
4	coasol	$D > 1 \mu\text{m}$	SU, BC, POM, SS	yes	2.00
5	Aitins	$10 \text{ nm} < D < 100 \text{ nm}$	BC, POM	no	1.59

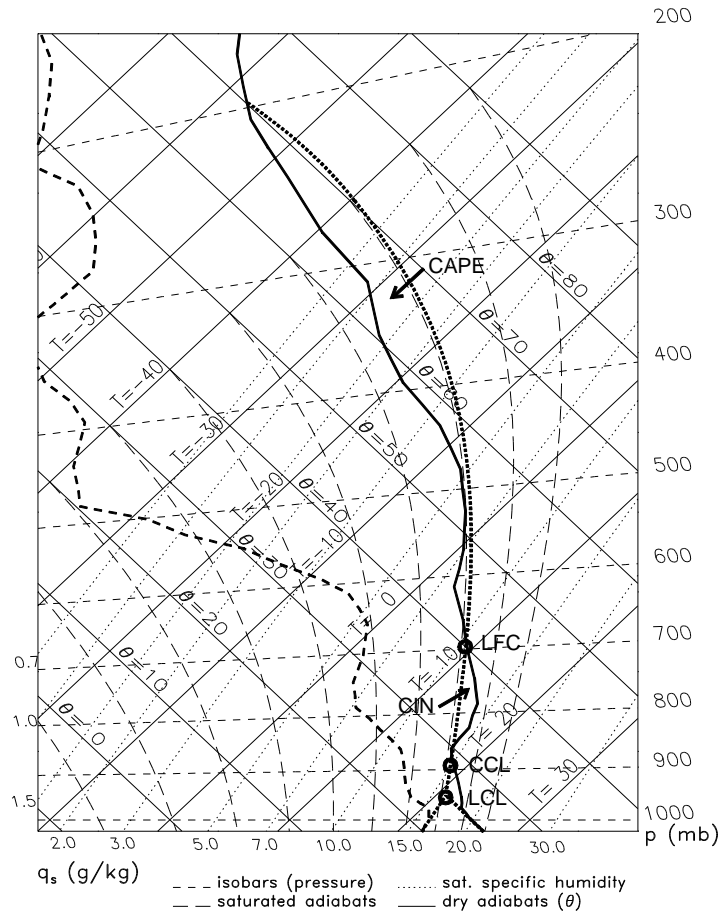


Figure 1. Tephigram representing the vertical profile of the initial dew point temperature (dashed line) and the temperature (solid line). The thick dotted line represents the adiabatic parcel ascent and the circles indicate the specific levels of the parcel such as the Lifted Condensation Level (LCL), the Convective Condensation Level (CCL) and the Level of Free Convection (LFC).

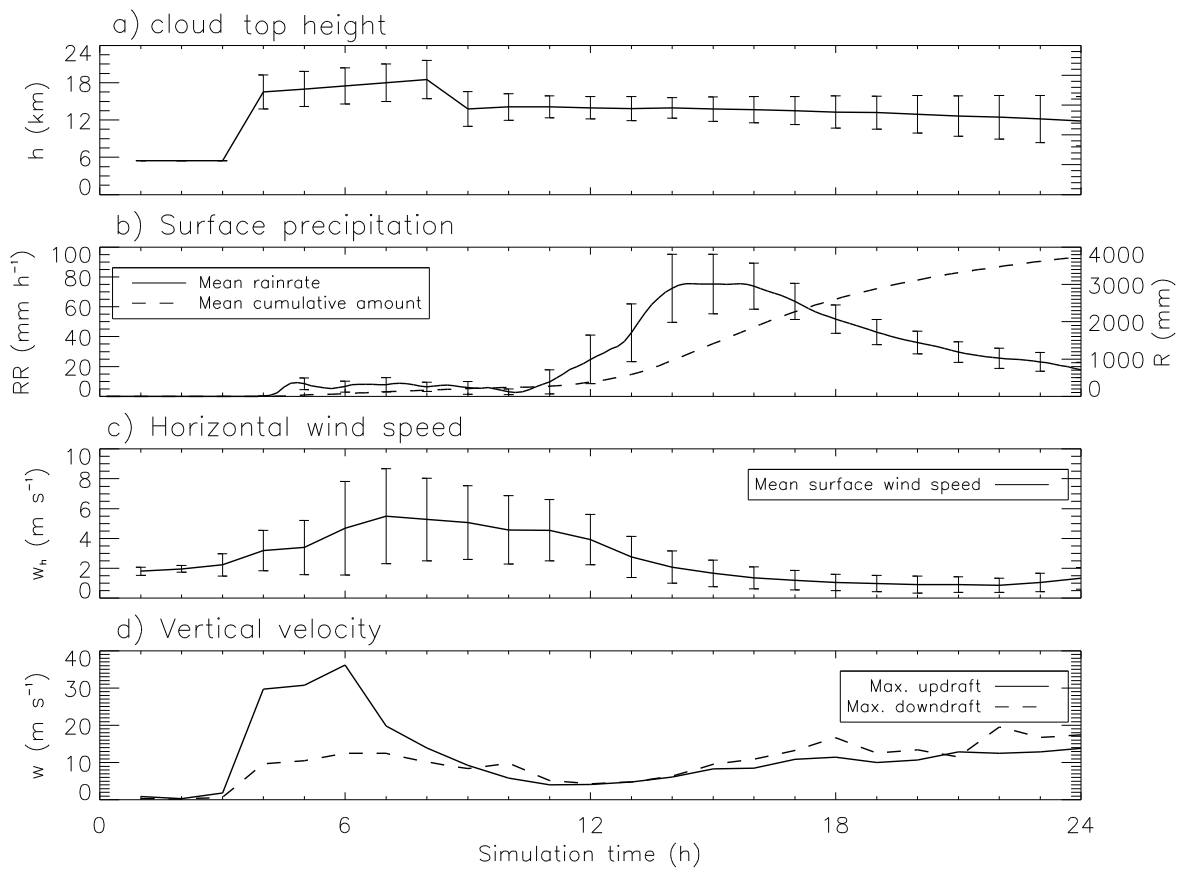


Figure 2. Temporal evolution of (a) the mean ~~total~~ ~~top~~ cloud top height, (b) the mean accumulated rain accumulation and rain rate at the surface, (c) the mean surface horizontal wind speed and (d) the maximum of the updrafts and downdrafts. The averages are obtained over the entire grid points of the domain and given with \pm one standard deviation. The initial time of the simulation is 09:00 UTC on May 24, 2002.

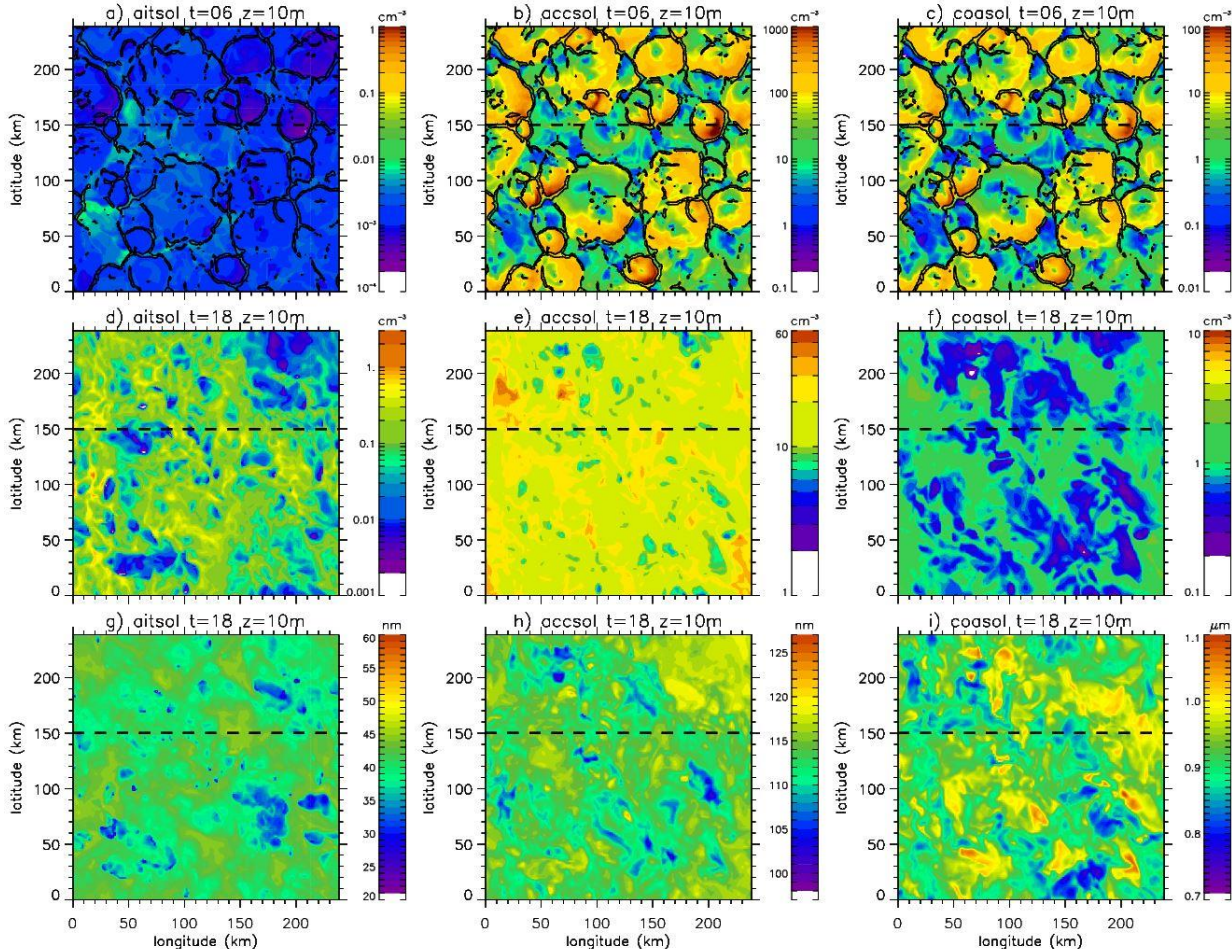


Figure 3. Snapshot spatial variations in the number concentrations (a-f) and geometric-mean radius (g-i) of the aerosol particles in the Aitken (aitsol; a, d, g), accumulation (accsol; b, e, h) and coarse (coasol; c, f, i) soluble modes after 6 h (in model spin-up) (a-c) and 18 h (d-i) of integration. The black solid lines represent the surface vertical wind speed ($w = 5 \text{ m s}^{-1}$). Note that the colour scales are different. The dashed lines correspond to the transects shown in Figures 5 and 9.

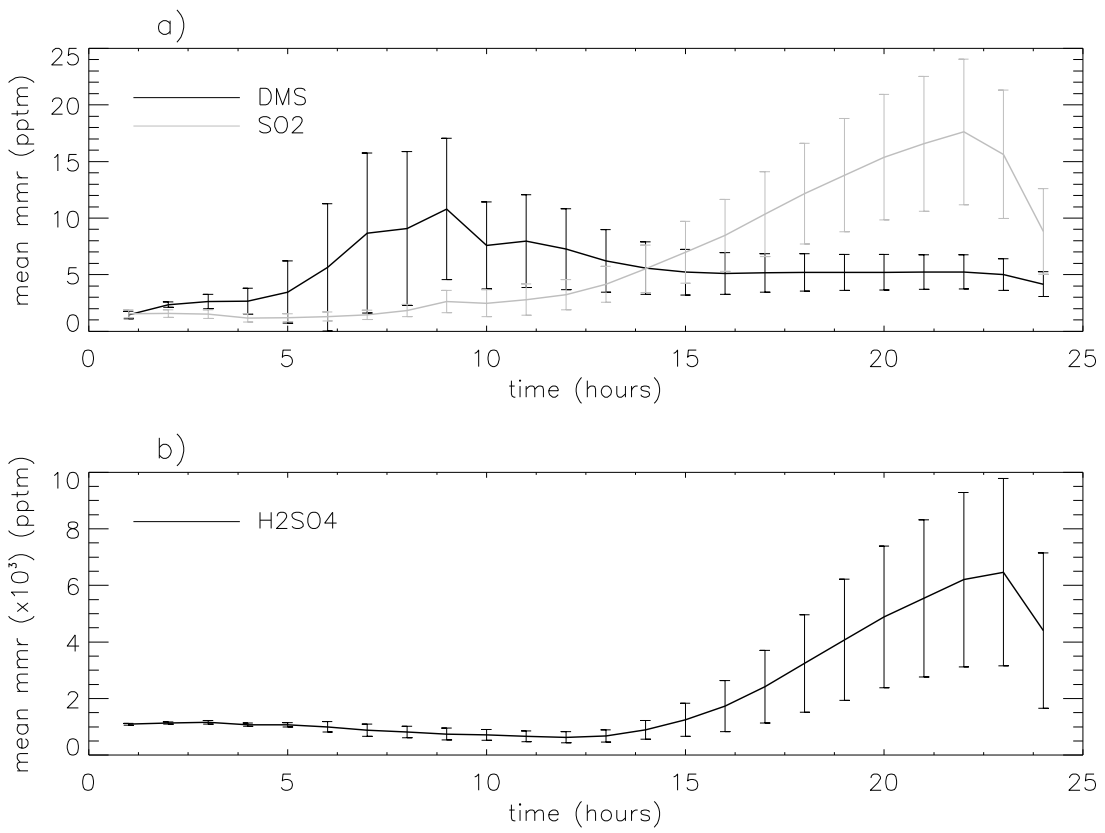


Figure 4. Temporal evolution of the mean mass mixing ratios of the gas precursors to aerosols. The DMS, SO₂ and H₂SO₄ mass concentrations are in pptm (part per trillion in mass). The error bars correspond to \pm one standard deviation.

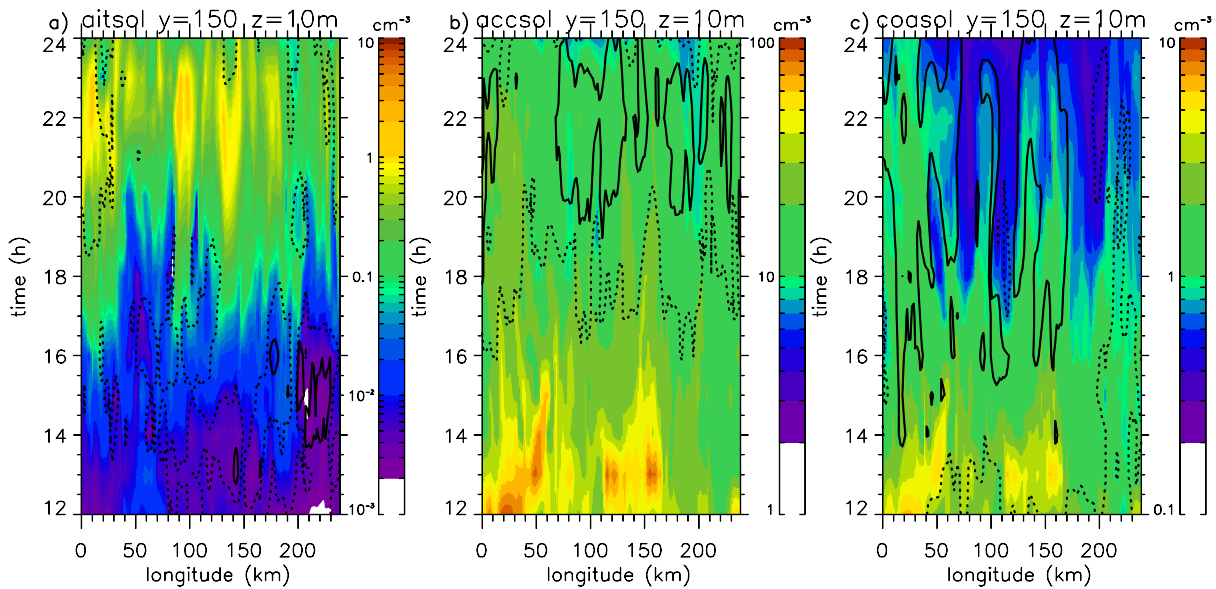


Figure 5. Temporal evolution of the aerosol concentration from the Aitken (a), accumulation (b) and coarse (c) soluble mode after the model spin-up. Temporal evolution of the aerosol dry radius is also illustrated for the 3 modes: 30 (dashed line) and 35 nm (solid line) for the Aiken soluble mode, 110 (solid line) and 115 nm (dashed line) for the accumulation soluble mode; 5 and 0.96 (solid line) and 1.0 μm (dashed lines) for coarse soluble mode. Note that the colour scales are different.

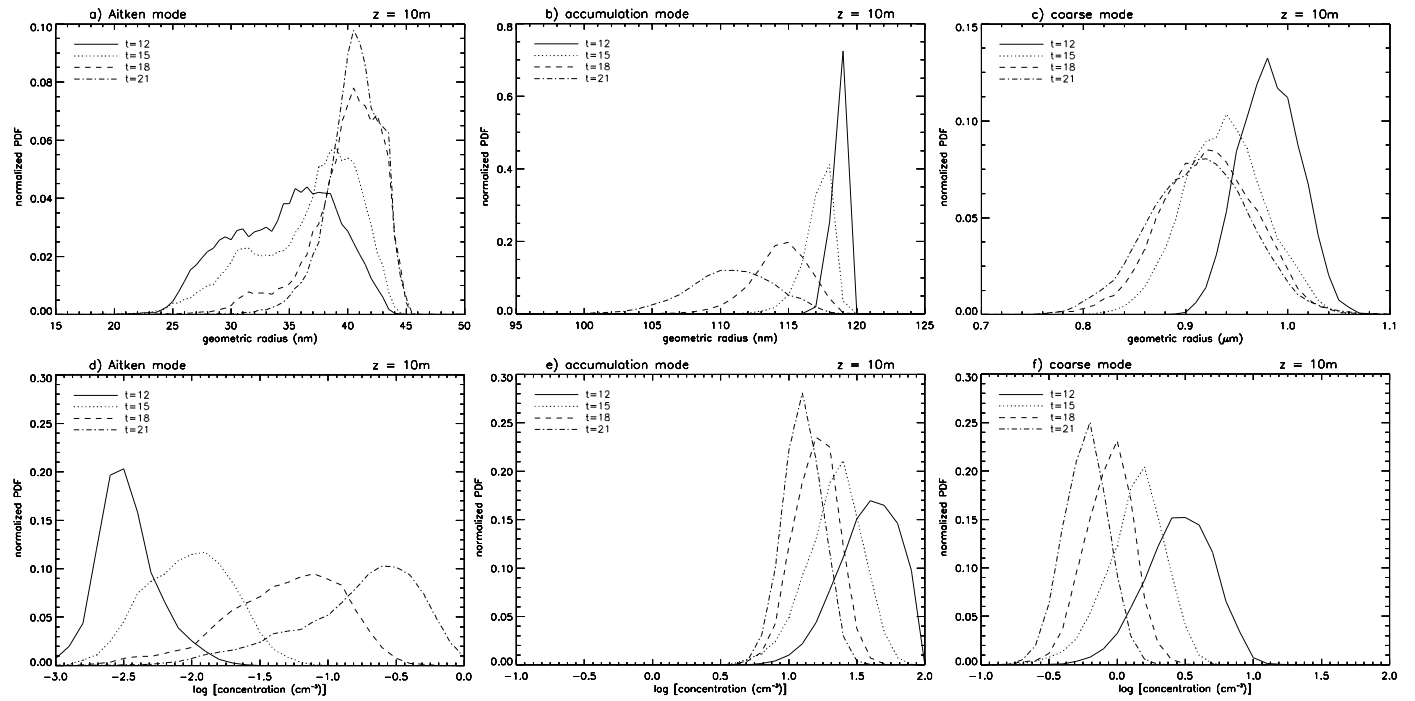


Figure 6. Normalized Probability Density Function (PDF) of the geometric radius (a, b, c) and the logarithm of the concentration (d, e, f) of the surface aerosols from the Aitken (a, d), accumulation (b, e) and coarse (c, f) soluble modes obtained at different integration time.

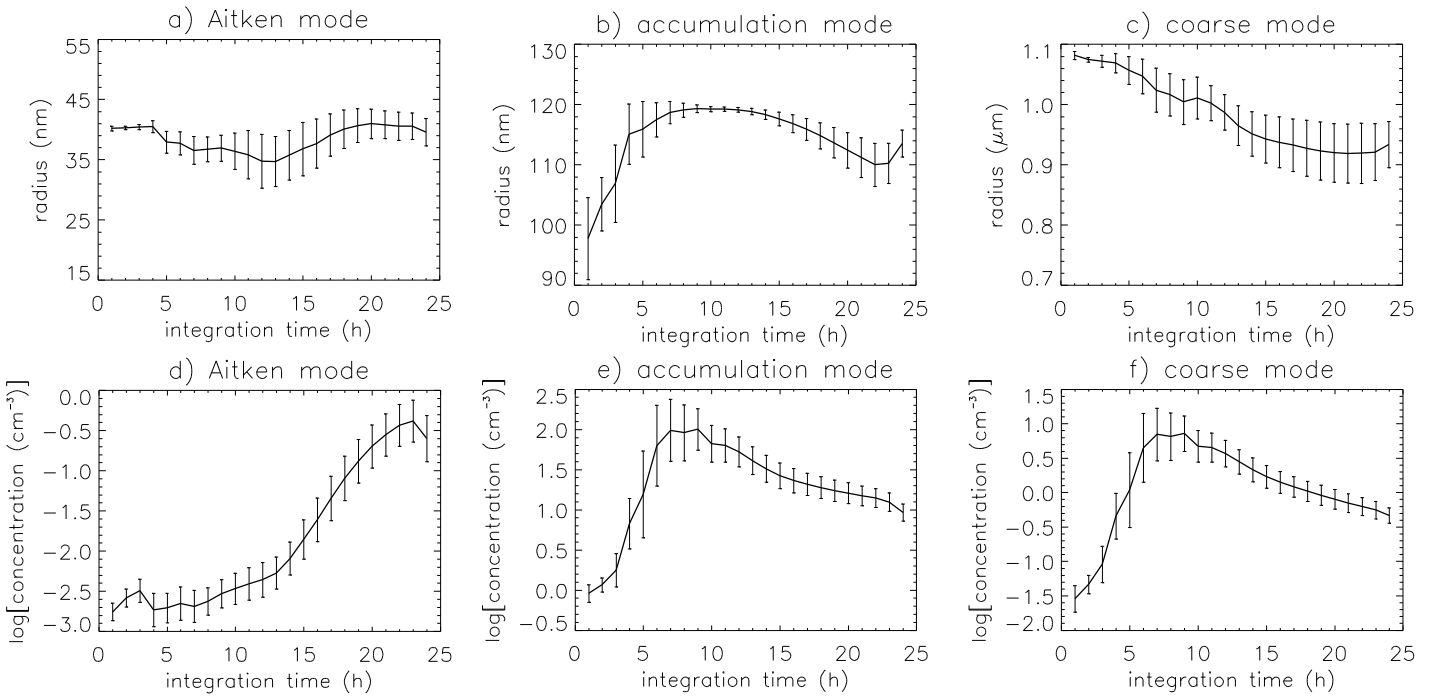


Figure 7. Time series of the mean \pm one standard deviation of the geometric radius (a, b, c) and the logarithm of the concentration (d, e, f) of the surface aerosols from the Aitken (a, d), accumulation (b, e) and coarse (c, f) soluble modes. **The initial time of the simulation is 09:00 UTC on May 24, 2002.**

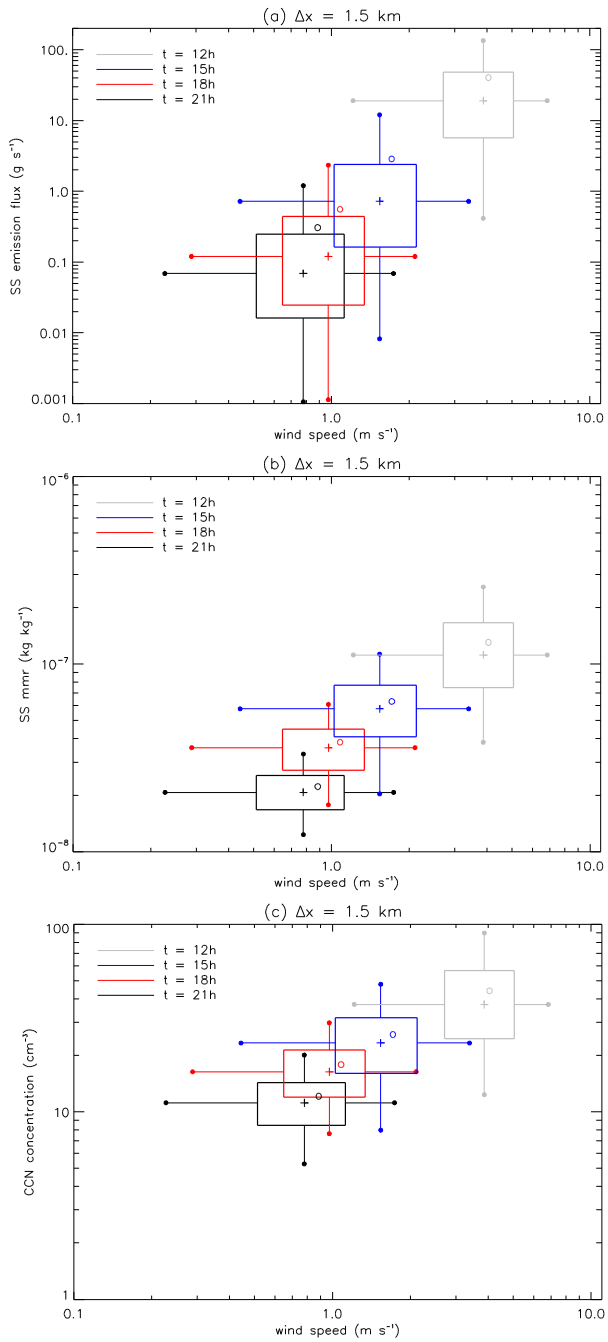


Figure 8. 2D-distribution of the surface sea-salt emission flux (a), sea-salt mass mixing ratio (mmr) (b) and CCN concentration (c) as a function of the surface horizontal wind for 4 different integration times ($t = 12, 15, 18$ or 21h). The hinges of the box-plots represent the 25th and 75th percentiles and the ends of the whiskers (full circles) represent the 5th and 95th percentiles. The ‘plus’ symbols represent the median values. The empty circles show the mean values over the domain.

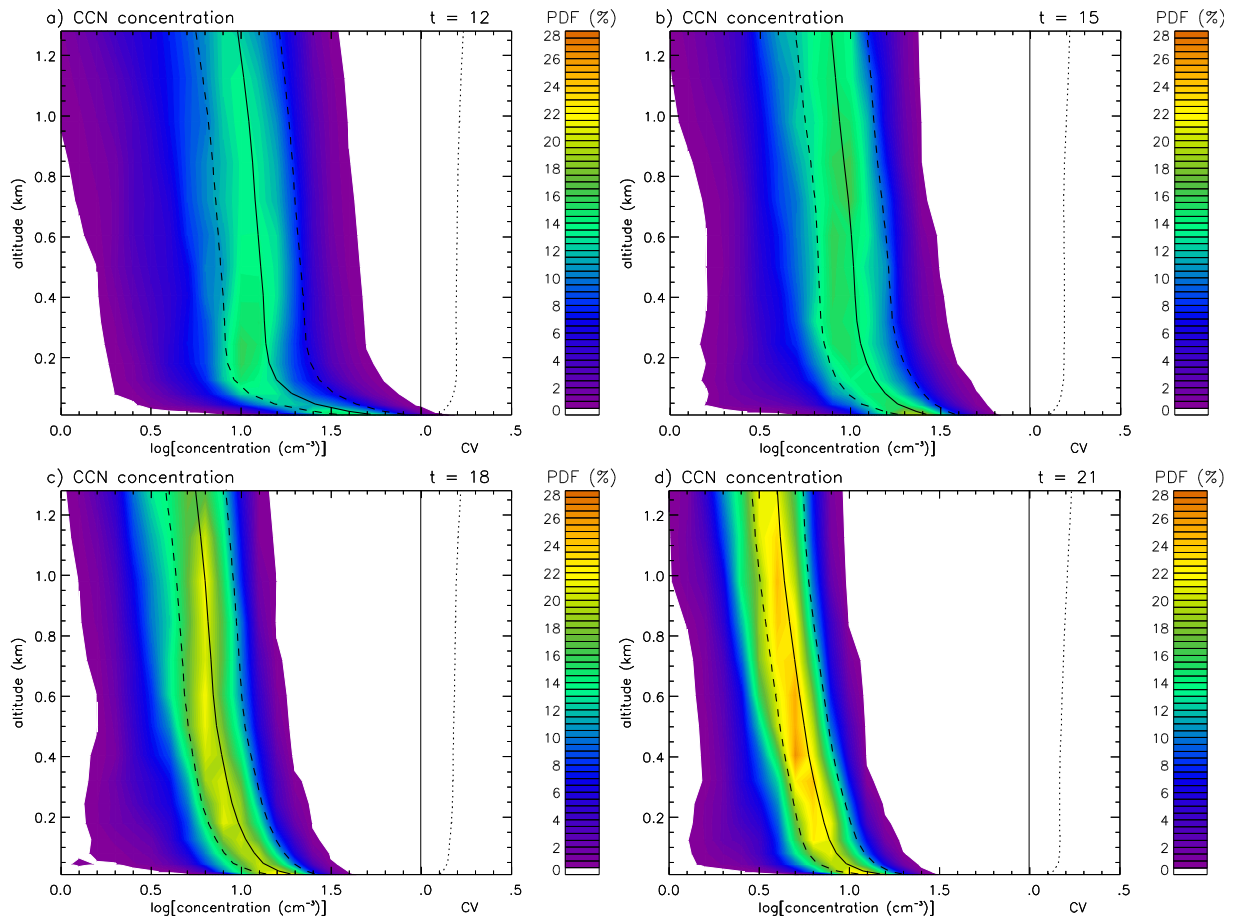


Figure 9. Altitude-dependent Probability Density Function (a-PDF) in percent of the CCN concentration at different integration times. The a-PDF are obtained calculating the PDF for each different level. A resolution of 0.1 is used for quantifying the logarithm of the concentration. The lines represent the mean (solid lines) \pm one standard deviation (dashed lines) 5 of the CCN concentration. The dotted lines represent the coefficient of variation (CV) which is defined as the ratio of the standard deviation to the mean of the CCN concentration.